Critical Survey of Data on the Spectroscopy and Kinetics of Ozone in the Mesosphere and Thermosphere

Jeffrey I. Steinfeld[a]

Department of Chemistry, Massachusetts Institute of Technology, Cambridge, Massachusetts 02139

Steven M. Adler-Golden

Spectral Sciences Inc., Burlington, Massachusetts 01803

and

Jean W. Gallagher

Atomic Collisions Data Center, Joint Institute for Laboratory Astrophysics, National Bureau of Standards and University of Colorado, Boulder, Colorado 80309-0440

Received March 3, 1987; revised manuscript received July 2, 1987

Spectroscopic data and reaction rate coefficients pertinent to ozone in the mesosphere and thermosphere (altitude > 50 km) are critically surveyed. These data should be of use in modeling atmospheric infrared luminescence, measuring atmospheric ozone concentrations by remote sensing, and designing and interpreting laboratory measurements. There is a clear need for additional data on metastable ozone electronic states, additional atmospheric ozone formation channels, collision processes involving electrons and ions, and vibrational state dependence of reaction rate coefficients.

Key words: cross sections; data; electron collisions; ion collisions; kinetics; ozone; reaction rate coefficients; spectroscopy; upper atmosphere.

Contents

[a] JILA Visiting Scientist, 1986.

List of Tables

List of Figures

1. Introduction

The reactions of ozone (O_3) in the earth's atmosphere have attracted the attention of many scientists during the last half-century and more. As the importance of ozone in controlling our planet's thermal and radiation budgets became evident, extensive efforts were undertaken in measuring its properties, modeling its behavior in the atmosphere, and systematizing an ever-increasing data base of knowledge about this deceptively simple molecule. These efforts have led to several comprehensive assessments of kinetic and photochemical data for atmospheric chemistry by the CODATA Panel,[1–3] and in a recent WMO Survey,[4] and NASA report.[5]

The purpose of the present critical review of spectroscopic and kinetic properties of ozone emphasizes several

key aspects that have not been the principal focus of the previous assessments. These include the following.

(1) Vibrationally excited ozone is a major contributor to the infrared luminosity of the upper atmosphere[6,7]; modeling atmospheric infrared emission thus requires knowledge of ozone steady-state vibrational populations and vibrational transition probabilities.

(2) Measurement of atmospheric ozone concentrations by microwave, infrared (IR), and ultraviolet (UV) remote sensing requires highly precise absorption cross sections and line positions.

(3) Interpretation of laboratory measurements of ozone formation and destruction mechanisms in the mesosphere and thermosphere[8–10] also depends on a knowledge of these spectroscopic and kinetic parameters.

The principal feature of ozone chemistry in the mesosphere and thermosphere, which has not been considered in detail in past assessments, is that the reactants and products are not in thermodynamic equilibrium. There exist instead steady-state distributions of molecular energy states which depend on local temperatures and species concentrations. Modeling such distributions requires a detailed knowledge of reactant- and product-state-specific rate coefficients. This additional complexity is partially compensated by the presence of far fewer chemical species than must be considered in stratospheric ozone photochemistry. The effects on other species that may be present and that may contribute to atmospheric luminosity, such as $OH(v)$ and $NO(v)$, also need to be considered.

The data that are critical to such modeling include detailed spectroscopic parameters for ozone electronic, vibrational, and rotational levels; infrared, visible, and ultraviolet transition stengths; electron and photon interaction cross sections; and state-to-state rate coefficients for selected species. With regard to the kinetics data, extensive reviews and surveys already exist[1–4] for reactions of stratospheric ozone. In this review, we particularize to those species most important in the mesosphere and thermosphere, i.e., at altitudes above 50 km. These species include:

$O(^3P,^1D,^1S)$,

$O_2(^3\Sigma_u^-,^1\Delta_g,^1\Sigma_g^+)$,

H, OH, HO_2, $N(^4S)$,N_2,NO,NO_2.

Reactions involving organic and/or halogenated species are not included. Wherever possible, values for the thermal rate coefficients are taken from the recommended values of the CODATA Panel[1–3] and the NASA report.[5] We also include processes involving electrons and ionic species, which may be of importance in the upper atmosphere.

In addition to the directly relevant spectroscopic and kinetic parameters, we include ancillary data on ozone that may be of use to experimentalists planning laboratory measurements, or to theoreticians attempting to model spectroscopic or kinetic behavior of the molecule. These data include molecular properties (dipole, quadrupole, and magnetic moments; potential energy surfaces), bulk properties such as vapor pressure, and laser interactions such as infrared multiple-photon excitation (IRMPE).

2. Methodology

2.1. Literature Search

This review is based on literature published through June, 1986, augmented by preprints and unpublished reports furnished by numerous investigators. A literature search was carried out using previously published surveys,[1–3] the Molecular Spectroscopy Newsletter published by the Physics and Astronomy departments of the University of California at Berkeley (1963–1986), and the Lockheed Dialog® data base system.

2.2. Units

As in earlier surveys,[11] rate data are presented in standardized units of cm^3 molecule^{-1} s^{-1}. Thermal rate coefficients are given in the Arrhenius form,

$$k(T) = A \exp(-E_{act}/T),$$

with E_{act} in units of kelvin ($=$ kcal mol^{-1}/1.986 $=$ kJ mol^{-1}/8.314). Cross sections for photon and electron interaction processes are given in units of cm^2 (10^{-16} $cm^2 = 1$ Å^2). Spectroscopic term values are given in cm^{-1} units (1 cm^{-1} corresponds to 2.997 924 58$\times 10^{10}$ Hz), and transition moments in esu cm (10^{-18} esu cm $= 1$ Debye unit $= 3.3356\times 10^{-30}$ C m).

3. Survey of Spectroscopic Data

3.1. Vibrational and Rotational Spectroscopy

This section is concerned with infrared and microwave spectroscopy of the ground electronic ($^1A_1$) state of ozone.

3.1.a. Energy Levels

3.1.a.1. Vibrational Molecular Constants

Vibrational energies are listed in Table 1 for $^{16}O_3$ and $^{18}O_3$ bands which have been studied with better than 1-cm^{-1}

TABLE 1. Vibrational energies (cm^{-1}) of $^{16}O_3$ and $^{18}O_3$

v_1	v_2	v_3	$^{16}O_3$	Reference	$^{18}O_3$	Reference
0	1	0	700.931	13,28	661.7	12
0	0	1	1042.084	43	984.6	12
1	0	0	1103.141	43	1041.9	12
0	2	0	1399.275	13,28	···	
0	1	1	1726.528	44	1631.2	12
1	1	0	1796.261	44	1695.9	12
0	0	2	2063.55	45	1945.4	12
1	0	1	2110.785	45	1995.1	12
2	0	0	2195.50	45	2079.4	12
0	2	1	2409.5	12	···	
0	1	2	2725.6	12	2579.5	12
1	1	1	2785.245	46	2634.3	12
0	0	3	3046.0	12	2883.2	12
2	0	1	3185.7	12	3012.6	12
1	0	2	3084.1	12	···	
1	2	1	3457.5	12	3271.0	12
0	1	3	3697.1	12	3501.4	12
2	1	1	3849.4	12	···	
1	0	3	4026	12	3814.1	12

TABLE 2. Vibrational harmonic frequencies, anharmonic constants, and Darling–Dennison coupling constant (cm^{-1}), from Barbe *et al.* Ref. 12

	$^{16}O_3$	$^{18}O_3$
ω_1	1134.9	1070.0
ω_2	716.0	674.7(5)
ω_3	1089.2	1026.5
x_{11}	−4.9	−4.3
x_{22}	−1.0[a]	−0.9
x_{33}	−10.6	−9.4
x_{13}	−34.8	−31.4
x_{23}	−17.0	14.8
x_{12}	−9.1	−7.7
γ	−27.0(5)	−24.2

[a] Value is −1.3 from Devi *et al.* (Ref. 13).

resolution. Nearly all of these bands were observed by Barbe *et al.*,[12] who derived from them a set of anharmonic constants, listed in Table 2. An improved value of x_{22} was obtained by Devi *et al.*[13] based on their observation of the (0 2 0) band.

A number of $^{16}O_3$ higher-lying vibrational states have been observed under lower resolution, as listed in Table 3. Here, ν_3 hot bands observed in emission from recombining ozone by Rawlins and Armstrong[9] lead to approximate values for the (0 0 4) and (0 0 5) state energies. Agreement with a calculation[14] based on the Barbe anharmonic constants[12] is within experimental uncertainty. The (0 0 5) band may also be present in a recent long-path Fourier transform infrared (FTIR) spectrum by Damon *et al.*[15]

High-lying $v_2 = 0$ "bands" having considerable ν_1 and/or ν_3 excitation have been observed under low resolution in the ultraviolet resonance Raman spectrum by Imre *et al.*[16] Their energies and assignments are reproduced in Table 3 along with calculated energies. Several authors (Levine and co-workers[17,18] and Lehmann[19]) have incorporated the Raman bands in determining new anharmonic constants appropriate for high vibrational energies. However, it should

TABLE 3. High-lying vibrational energies (cm^{-1}) for $^{16}O_3$

v_1	v_2	v_3	Observed[a]	Reference	Calculated
3	0	0	3294 ± 5	20	3291
0	0	4	3998 ± 3	9	4000
			4010 ± 5	20	
2	0	2	(4136)	16	4142
4	0	0	4370 ± 5	20	4372
0	0	5	4914 ± 6	9	4919
1	0	4	(4913)	16	4934
3	0	2	(5145)	16	5179
5	0	0	(5435)	16	5444
0	0	6	(5735)	16	5797
2	0	4	(5962)	20	5989
4	0	2	(6187)	16	6219
6	0	0	(6497)	16	6506
3	0	4	(6897)	16	6939
5	0	2	(7207)	16	7244
7	0	0	(7523)	16	7560

[a] Parentheses denote approximate center of cluster in Raman spectrum (Ref. 16).

TABLE 4. Vibrational energies of mixed ozone isotopes (cm^{-1})

v_1	v_2	v_3	$^{18}O^{16}O^{18}O$	$^{16}O^{18}O^{16}O$	$^{16}O^{16}O^{18}O$	$^{18}O^{18}O^{16}O$	Reference
0	0	1	1019.1	1008.453	1028.112	994.0	12,36,37
1	0	0		1074.308	1090.354		36,37
0	1	1	1671.2		1695.4	1656.8	12
1	0	1	2060.1	2049.3	2090.0	2027.5	12
1	1	1	2703.4	2718.1	2748.5	2680.5	12
0	0	3	2980.3		2998.8	2903.0	12

be noted that the assignment of these low-resolution Raman bands is ambiguous, as they are generally found to consist of clusters of individual vibrational bands under higher resolution.[20] These individual vibrational bands may be near-resonant mixtures of the nominal assignment ($v_2 = 0$) and nearby ν_2-excited states. In a few cases the assignment is unambiguous, as in the case of the (0 0 4) band which agrees well with the observation by Rawlins and Armstrong.[9]

Finally, mixed isotopic ozone bands have been observed by several authors, and their energies are given in Table 4. The shifts relative to the normal isotope agree well with the calculations of Bykov *et al.*[21,22]

3.1.a.2. Rotation and Vibration–Rotation Molecular Constants

Due to the large number of rotation and vibration–rotation molecular constants and their dependence on the choice of Hamiltonian, the reader should consult the individual rotational and vibrational bands listed in following subsections. Values of the rotational constants A, B, and C for various vibrational states are summarized in Table 5. Their vibrational dependence may be expressed via the α parameters, given by Barbe *et al.*[12] using rotational constants from previous microwave spectra.

3.1.b. Line and Band Intensities

3.1.b.1. Vibrational Band Intensities, Transition Dipole Moments

Because Coriolis coupling mixes rotational lines of different vibrational states, vibrational band intensities have

TABLE 5. Rotational constants A, B, C (cm^{-1}) for $^{16}O_3$ vibrational states

v_1	v_2	v_3	A	B	C	Reference
0	0	0	3.553666	0.4452832	0.3947518	26,48
0	0	0	3.553666	0.4452767	0.3947582	49
0	1	0	3.607094	0.4440219	0.3924393	48
0	1	0	3.607130	0.4440166	0.3924460	28
0	0	1	3.500553	0.4412969	0.3911578	26
1	0	0	3.556695	0.4427346	0.3924088	26
0	2	0	3.662409	0.4427449	0.3900725	13
0	2	0	3.662313	0.4427474	0.390078	28
0	1	1	3.55228	0.439895	0.388645	44
1	1	0	3.610736	0.441450	0.3901407	44
2	0	0	3.559538	0.440043	0.38948	45
1	0	1	3.501970	0.4385707	0.388543	45
0	0	2	3.449019	0.437486	0.38819	45
1	1	1	3.5520	0.43686	0.38458	46

Table 6. Vibrational band intensities [$\int\sigma(\tilde{\nu})d\tilde{\nu}$ in units of 10^{-20} cm^2 cm^{-1}] and transition dipole moment absolute values (D = 10^{-18} esu cm)

Band	Intensity[a]	Pure vibrational Transition Dipole	Reference	Intensity at 298 K	Reference
ν_2	71 ± 7	0.049	23,27	71 ± 7	23,27
ν_3	1524 ± 40	0.187	24,50	1484 ± 40	50,51
ν_1	12 ± 4	0.016	26	41 ± 4	23
$\nu_2+\nu_3$				6.0 ± 0.6	23,27
$\nu_1+\nu_2$				2.4 + 0.2	23,27
$2\nu_3$	5.8 ± 1	0.0082	24,27	...	
$\nu_1+\nu_3$	129 ± 13	0.0383	24,27	130 ± 13	23
$2\nu_1$	0.3 ± 0.01	0.0019	24,27	...	
$\nu_1+\nu_2+\nu_3$	3.3 ± 0.3	0.0053	27,46	2.7 ± 0.3	23
$3\nu_3$				12 ± 1	23,27
$2\nu_1+\nu_3$				1.3 ± 0.1	23,27

[a] Low-temperature limit.

only an approximate meaning at a nonzero temperature. Band intensities at 298 K are given in Table 6 based on low-resolution spectra, with a partitioning of intensity between Coriolis-resonating states generally consistent with McCaa and Shaw.[23] In the low-temperature limit the band intensities are pure vibrational, and are simply related to the transition dipole moments (also in Table 6) determined from detailed analysis of high-resolution spectra. The pure vibrational intensity for ν_1 has been revised downward from previous estimates (Flaud *et al.*,[24] Clough and Kneizys[25]) on the basis of a refined analysis by Pickett *et al.*[26]

Pure vibrational band intensities have also been calculated from an *ab initio* dipole moment function by Adler-Golden *et al.*,[27] who present results for many hot bands for which accurate experimental data are unavailable. Their results have been renormalized to the correct cold band intensities, and are given in Table 7.

There is some debate regarding the temperature at which the ν_2 band intensity measurement of McCaa and Shaw[23] was made. Goldman *et al.*[28] believe it to be 273 K, not 298 K, and therefore infer a slightly smaller ν_2 band strength compared to those given in Table 6.

TABLE 7. Theoretical pure vibrational hot band strengths, Boltzmann factor excluded [Reference 27 results were renormalized to agree with experimental (Table 6) cold band strengths.]

Transition	$\int\sigma(\tilde{\nu})d\tilde{\nu}\times10^{-20}$ cm^2 cm^{-1}
$2\nu_2-\nu_2$	142
$\nu_2+\nu_3-\nu_3$	69
$\nu_2+\nu_1-\nu_1$	65
$\nu_2+\nu_3-\nu_2$	1470
$2\nu_3-\nu_3$	2785
$\nu_1+\nu_3-\nu_1$	1361
$\nu_1+\nu_2-\nu_2$	8.5
$\nu_1+\nu_3-\nu_3$	8.9
$2\nu_1-\nu_1$	31
$\nu_1+\nu_2+\nu_3-\nu_2$	122
$\nu_1+2\nu_3-\nu_3$	224
$2\nu_1+\nu_3-\nu_1$	220
$2\nu_1-\nu_3$	167

3.1.b.2. Vibration–Rotation Line Intensities

Vibration–rotation line intensities are given in the references for the individual vibrational bands, which are discussed in Sec. 3.1.c.

3.1.c. Dipole Moment and Derivatives

The permanent dipole moment has been determined very accurately by Mack and Muenter[29] for the (0 0 0) and (0 1 0) states, and appears in Table 8 [a similar value for (0 0 0) was found by Meerts *et al.*[30]]. The vibrational dependence is quite close to that predicted by *ab initio* calculations (Adler-Golden *et al.*[27]).

Dipole moment derivatives with respect to internal coordinates have been calculated by Carney *et al.*[31] using vibrational band intensities which are slightly different from the values in Table 6. Somewhat improved values could be obtained by using more accurate band intensities, and by including higher-order derivatives. A fairly accurate *ab initio* dipole moment function is given by Adler-Golden *et al.*[27], who report linear and higher-order derivatives with respect to both internal and normal coordinates. Normal coordinate dipole moment expansions for different matrix element sign assumptions have also been derived by Voitsekhovskaya *et al.*[32] using perturbation theory.

3.1.d. Linewidths

Vibrational and rotational linewidths have been measured by various authors. The studies are summarized in Table 9, which lists average linewidth parameters γ for

TABLE 8. Dipole moment and derivatives

Parameter	Value	Units[a]	Reference
$\mu(000)$	0.5337	D	29
$\mu(010)$	0.5261	D	29
$\partial\mu_x/\partial r$	0.76	D/Å	31
$\partial\mu_x/\partial\theta$	0.74	D/rad	31
$\partial\mu_y/\partial r$	− 2.60	D/Å	31

[a] 1 D ≡ 10^{-18} esu cm.

TABLE 9. $^{16}O_3$ line broadening studies

Year	Reference	Comments
1986	52	γ_{N_2}, γ_{O_2} in millimeter region, $T = 195$–320 K. $\gamma_{O_2} \sim 20\%$–30% below theory, γ_{N_2} in excellent agreement
1985	33	Theoretical (QFT-ID) temperature dependence of γ_{N_2} ($\sim T^{-n}$); average $n = 0.76$ for air
1985	34	Theory (QFT-ID) in excellent agreement with observations; $\gamma_{air}/\gamma_{N_2} \sim 0.95$; γ nearly independent of vibrational quanta
1985	35	Theoretical (QFT-ID) γ_{N_2} for all rotational lines; $0.06 \lesssim \gamma \lesssim 0.08$ cm^{-1}/atm; no difference between A and B type transitions
1983–84	53,54	γ_{N_2}, γ_{O_2}, γ_{O_3} in millimeter region, $T = 245$–295 K. $\gamma \sim T^{-n}$, $n = 0.65$–1.2
1983	55	γ_{N_2} in ν_3 band for 156 lines, comparison with ATC theory
1983	56	γ_{O_2} in $\nu_1 + \nu_3$ band, $T = 171$–296 K. $\gamma \sim T^{-n}$, $n = 1.3 \pm 0.2$
1982	57	γ_{O_2} in $\nu_1 + \nu_2 + \nu_3$ and $\nu_1 + \nu_3$ bands; $\gamma_{N_2} \sim 0.07$ cm^{-1}/atm, $\gamma_{O_2}/\gamma_{N_2} \sim 0.8$ in $\nu_1 + \nu_3$ band
1982	58	Average $\gamma_{air} \sim 0.074$ cm^{-1}/atm in ν_1, ν_3
1982	59,60	Average $\gamma_{air} \sim 0.077$ cm^{-1}/atm in ν_1, ~ 0.083 cm^{-1}/atm in ν_3

broadening by N_2, O_2, air, and ozone. These average values must be used cautiously, as there is significant dependence on the J and K_a quantum numbers. The articles by Gamache and co-workers[33–35] provide an excellent survey of the measurements, as well as state-of-the-art calculations using QFT-ID (Quantum Fourier Transform with Improved Dynamics) theory, which yields $\sim 5\%$ agreement with measured N_2-broadened linewidths. They find essentially no dependence of linewidth on vibrational state or on type of vibrational transition (A or B). Measurements indicate that the temperature dependence of γ is given approximately by T^{-N}, where $0.6 < N < 1.3$.

Measurements of ozone self-broadening are relatively sparse (see Refs. 53, 54, 57, and 60).

3.1.e. Individual Vibrational Bands

High-resolution vibration–rotation spectra have been obtained and carefully analyzed for the ν_1, ν_2, ν_3, $\nu_1 + \nu_2$, $\nu_2 + \nu_3$, $\nu_1 + \nu_3$, $2\nu_3$, $2\nu_1$, and $\nu_1 + \nu_2 + \nu_3$ bands. The most recent studies are summarized in Table 10. The spectra include hot bands [especially those originating from (0 1 0)] as well as isotopic bands of ^{17}O and ^{18}O species. A number of compilations of ozone line parameters are available, including the AFGL,[61,62] JPL,[63] and GEISA[64] data bases.

3.1.f. Rotational Spectrum

The most recent high-resolution studies of the rotational (microwave–millimeter wave) spectrum are summarized in Table 11. These studies include isotopic species and excited vibrational states [(1 0 0), (0 1 0), and (0 0 1)]. Although these spectra provide the most accurate rotational constants, excellent results have also been obtained from the high-resolution vibrational spectra listed in Table 10.

TABLE 10. High-resolution vibrational band studies

Band(s)	Reference	Year	Comments
ν_1,ν_3	26	1985	Analysis of IR and microwave spectra
ν_1,ν_3	43	1981	*Analysis of atmospheric spectra*
ν_1,ν_3	65	1981	Line positions from laser heterodyne spectrum
ν_1,ν_3	66	1981	Line positions from laser heterodyne spectrum
ν_3	67	1979	Line positions from diode laser spectrum
ν_3	68	1977	Analysis of IR and microwave spectra
ν_2	28	1982	Analysis of atmospheric spectra
ν_2	48	1978	Analysis of IR and microwave spectra
$\nu_2 + \nu_3,\nu_1 + \nu_2$	44	1979	Analysis of laboratory spectra
$\nu_1 + \nu_3$	57	1982	Linewidths and absolute intensities
$2\nu_3,\nu_1 + \nu_3,2\nu_1$	45	1980	Analysis of laboratory spectra
$\nu_1 + \nu_2 + \nu_3$	46	1983	Analysis of laboratory spectra
$\nu_1 + \nu_2 + \nu_3$	57	1982	Linewidth and absolute intensities
$2\nu_2 - \nu_2$	28	1982	Analysis of atmospheric spectra
$2\nu_2 - \nu_2$	13	1979	Analysis of laser spectrum
$\nu_2 + \nu_3 - \nu_2$	43	1981	Analysis of atmospheric spectra
$\nu_2 + \nu_3 - \nu_2$	48	1978	Analysis of laboratory spectra
$\nu_3(^{18}O_{isotopes})$	47	1985	Isotopic abundance measured in atmospheric spectra
$\nu_1,\nu_3(^{18}O_{isotopes})$	36,37	1986	Analysis of laboratory spectra

An excellent compilation and analysis of ozone microwave spectra data prior to 1978 is given by Lovas.[38]

3.1.g. Stark and Zeeman Properties

Stark and Zeeman properties, including quadrupole moment components, have been determined accurately by Mack and Muenter,[29] and are given in Table 12.

3.1.h. Force Constants and Potential Energy Surface

Harmonic, cubic, and quartic force constants in both normal and internal coordinates have been derived by Barbe *et al.*[12] and Hennig and Strey[39] from the observed anharmonic constants (see Table 2) using standard second-order

TABLE 11. High-resolution pure rotational spectral analyses

Year	Wavelength region	Reference	Isotope(s) and vibrational state(s)
1985	millimeter	69	^{18}O ν_2
1985	microwave	26	$^{16}O_3$ ground, ν_1,ν_3
1984	millimeter and submillimeter	49	$^{16}O_3$ ground
1983	microwave	70	^{17}O ground
1978	microwave	38	^{18}O ground
			$^{16}O_3$ ground, ν_1,ν_2,ν_3
1978	microwave	48	$^{16}O_3$ ν_2
1977	microwave	71,72	^{18}O ground
			$^{16}O_3$ ground
1977	microwave	68	$^{16}O_3$ ν_1 and ν_3

TABLE 12. Stark and Zeeman properties, from Mack and Muenter (Ref. 29)

Property	Symbol	Value	Units[a]
Polarizability anisotropies	$\alpha_{aa}-\alpha_{bb}$	2.82(1)	Å^3
	$\alpha_{aa}-\alpha_{cc}$	2.63(4)	Å^3
Rotational magnetic moments	g_{aa}	2.989 33(8)	
	g_{bb}	−0.229 19(3)	
	g_{cc}	−0.076 23(6)	
Magnetic susceptibility anisotropies	$\chi_{aa}-\chi_{bb}$	5.91(2)	kHz/kg^2
	$\chi_{aa}-\chi_{cc}$	12.05(4)	kHz/kg^2
Quadrupole moment components	θ_{aa}	$-1.4(2)\times10^{-26}$	esu cm^2
	θ_{bb}	$-0.7(2)\times10^{-26}$	esu cm^2
	θ_{cc}	$2.1(3)\times10^{-26}$	esu cm^2

[a] 1 esu cm^2 = $3.335\,64\times10^{-14}$ C m^2.

TABLE 13. Normal coordinate force constants (cm^{-1}) for $^{16}O_3$ and $^{18}O_3$, from Hennig and Strey (Ref. 39)

	$^{16}O_3$	$^{18}O_3$
ϕ_{111}	−228.44	−264.00
ϕ_{112}	−59.02	−54.02
ϕ_{122}	−50.96	−46.64
ϕ_{133}	−452.27	−413.95
ϕ_{222}	−114.96	−105.22
ϕ_{233}	−119.04	−108.95
ϕ_{1111}	53.39	47.44
ϕ_{1122}	−6.62	−5.89
ϕ_{1133}	111.15	98.78
ϕ_{2222}	15.38	13.67
ϕ_{2233}	−22.90	−20.35
ϕ_{3333}	161.01	143.08

TABLE 14. Internal coordinate force constants

Force constant	Units	Hennig and Strey[a]
f_{rr}	mdyn Å^{-1}	61.164(3)
$f_{rr'}$	mdyn Å^{-1}	1.603(3)
$f_{r\alpha}$	mdyn	0.511(3)
$f_{\alpha\alpha}$	mdyn Å	2.102(1)
f_{rrr}	mdyn Å^{-2}	−54.924(85)
$f_{rrr'}$	mdyn Å^{-2}	2.586(56)
$f_{rr\alpha}$	mdyn Å^{-1}	−3.174(30)
$f_{rr'\alpha}$	mdyn Å^{-1}	−1.290(30)
$f_{r\alpha\alpha}$	mdyn	−3.937(24)
$f_{\alpha\alpha\alpha}$	mdyn Å	−3.794(3)
f_{rrrr}	mdyn Å^{-3}	397.0(6.1)
$f_{rrrr'}$	mdyn Å^{-3}	77.5(5.7)
$f_{rrr\alpha}$	mdyn Å^{-2}	≡0
$f_{rrr'r'}$	mdyn Å^{-3}	74.0(5.7)
$f_{rrr'\alpha}$	mdyn Å^{-2}	≡0
$f_{rr\alpha\alpha}$	mdyn Å^{-1}	−32.4(2.5)
$f_{rr'\alpha\alpha}$	mdyn Å^{-1}	−31.9(2.5)
$f_{r\alpha\alpha\alpha}$	mdyn	≡0
$f_{\alpha\alpha\alpha\alpha}$	mdyn Å	33.8(2.4)

[a] Reference 39.

perturbation theory. They obtained essentially identical results, given in Tables 13 and 14. The harmonic and cubic force constants should be very accurate. However, the quadratic force constants were derived under the standard, but somewhat arbitrary, assumption that $f_{rrr\alpha}=f_{rrr'\alpha}=f_{r\alpha\alpha\alpha}=0$.

An alternative set of force constants may be derived from a Sorbie–Murrell potential surface fitted directly to vibrational band centers; this type of surface forces the proper dissociation behavior. The most recent of these surfaces, by Carter *et al.*,[40] yields significantly different quartic force constants. Although we feel that the standard quartic force constants are preferable, the perturbation theory used to derive them has inherent problems at large vibrational amplitudes which the Sorbie–Murrell approach overcomes.

Potential energy functions are useful for dynamical studies (e.g., vibrational and rotational relaxation, reaction, formation, and dissociation), and for predicting higher-order spectroscopic constants. Sorbie–Murrell-type potential functions, as given for example by Carter *et al.*[40] and Varandas and Murrell,[41] are designed for global accuracy and behave properly towards dissociation. However, potential functions which employ the Barbe or Hennig–Strey force constants, such as those derived using Simons–Parr–Finlan or Morse oscillator expansion variables (Carney and coworkers,[27,42]) are probably more accurate at lower energies. All of these potential functions give reasonable agreement (several cm^{-1}) with observed vibrational band centers.

3.2. Electronic Spectroscopy

This section is concerned with ozone's near-infrared, visible and ultraviolet spectra; i.e., transitions between the ground vibrational, ground electronic state and an electronically excited state. Spectra involving transitions between or within excited states, i.e., IR spectra of electronically excited ozone or ultraviolet spectra of vibrationally or electronically excited ozone, are mainly dealt with in Sec. 3.3.

3.2.a. Excited Electronic States of Ozone

Vertical and adiabatic excitation energies of excited electronic states of ozone are available from a number of *ab*

TABLE 15. Energies of excited electronic states of ozone below 5 eV

State		Vertical ΔE(eV)				Adiabatic (C_{2v}) ΔE(eV)		
C_{2v}	C_s	Expt. (eV)	Calc. (eV)	Ref.	Method[a]	Calc. (eV)	Ref.	Method
1^3B_2	$1^3A'$		1.50	74	POL-CI	0.92	74	POL-CI
			1.20	73	MRD-CI	(0.62)		see text
			1.21	75	MCSCF/CI	0.74	75	MCSCF/CI
1^3A_2	$1^3A''$		2.12	74	POL-CI	1.35	74	POL-CI
			1.44	73	MRD-CI	(0.67)		see text
1^1A_2	$1^1A''$		2.34	74	POL-CI-R	1.66	74	POL-CI-R
		~1.6	1.59	73	MRD-CI	(0.91)		see text
1^3B_1	$2^3A''$		2.01	74	POL-CI-R	1.74	74	POL-CI-R
			1.59	73	MRD-CI	(1.32)		see text
1^1B_1	$2^1A''$		2.41	74	POL-CI-R	2.06	74	POL-CI-R
		2.1	1.95	73	MRD-CI	(1.60)		see text
2^3B_2	$2^3A'$		4.17	74	POL-CI-R	2.92	74	POL-CI-R
			3.27	73	MRD-CI	(2.02)		see text
2^1A_1	$2^1A'$		4.58	74	POL-CI-R	see below		
			3.60	73	MRD-CI			
1^1B_2	$3^1A'$		6.12	74	POL-CI-R	5.54	74	POL-CI-R
		4.9	4.97	73	MRD-CI	(4.39)		see text

[a] See Refs. 73–75 for details of computational methods. [Note: $^1A_1(D_{3h})$: ~0.5 eV (Ref. 83), 0.9 eV (Ref. 154), 1.1 eV (Ref. 155), 1.3 eV (Ref. 74).]

initio calculations. Table 15 summarizes the results of the most recent and reliable calculations on states below 5 eV. Experimental vertical excitation energies are available for the 1^1A_2, 1^1B_1, and 1^1B_2 states giving rise to the Wulf, Chappuis and Hartley absorption bands, and are also given in the table. They agree extremely well with the calculation of Thunemann *et al.*[73] which used energy extrapolation. The adiabatic excitation energies shown in parentheses were computed by combining Thunemann's vertical energies with the adiabatic-vertical energy difference calculated by Hay and Dunning.[74] This procedure gives good agreement with the calculation of Wilson and Hopper[75] for the 1^3B_2 adiabatic energy, as well as sensible values for the 1^1A_2, 1^1B_1, and 1^1B_2 states. Error limits on the vertical energies are probably 0.2 eV or better. Error limits on the adiabatic energies may be considerably larger where the geometry change is substantial. This is particularly true for the "ring" (D_{3h}) state, for which a reasonable selection of calculations yields the range 0.5–1.3 eV (see note at bottom of Table 15).

Equilibrium geometries and vibrational frequencies for the states enumerated in Table 15 have been predicted by Hay and Dunning[74] and, for the 1^3B_2 state, by Wilson and Hopper.[75] Unfortunately, the Chappuis and Hartley bands are continuous, precluding a definitive analysis of frequencies and geometries. The Huggins bands are discrete (although slightly diffuse), but as discussed below have not yet been fully analyzed taking into consideration recent fluorescence data (Sinha *et al.*[76]) and vibrational assignments (Katayama[77]). The new data and assignments imply a C_s equilibrium geometry for the $^1B_2$ state at an energy of 3.36 eV, in qualitative agreement with the calculations of Hay and coworkers.[74,78,79]

A crucial question for atmospheric chemistry is, which excited states of ozone are bound, and what are their adiabatic energies? It seems clear that the triplet state 1^3B_2 is bound and lies below the $O + O_2$ dissociation limit (1.1 eV). Evidence for one or more triplets is found in the electron energy loss spectra of Swanson and Celotta,[80,81] which show a blend of features near the predicted vertical excitation energies of 1^3B_2, 1^3A_2, and 1^3B_1. At the present time we know of no other direct spectroscopic evidence for the $^3B_2$ state.

A second frequently mentioned candidate for a bound excited state of ozone is the $^1A_1$ "ring" (D_{3h}) state, which correlates adiabatically with the ground state. As mentioned above, the energy of this state is highly uncertain; discussions may be found in Jones,[82] Burton[83] and the other studies mentioned in Table 15. If both the ring state and the barrier between it and the C_{2v} equilibrium geometry lie below the $O + O_2$ dissociation limit, the ring state could be an important intermediate in ozone recombination and thermal decomposition. However, the current consensus of *ab initio* theory is that the barrier lies considerably above the $O + O_2$ limit, even if one adopts a ring state energy in the low end of the range of estimates.

The adiabatic energy estimates in parentheses, which were obtained by combining the studies of Thunemann *et al.* and Hay and Dunning, suggest that two additional states, 1^3A_2 and 1^1A_2, may also be bound relative to the $O + O_2$ limit. Indeed, the 1^3A_2 state may lie quite close in energy to 1^3B_2. The 1^1A_2 state is identified with the Wulf bands, as discussed below.

Turning now to somewhat less speculative matters, the remainder of this section is organized around ozone's observed spectra.

3.2.b. Wulf Bands

Using a long ozone column, Wulf[84] in 1930 observed weak, diffuse near infrared absorption band fitting the formula $\nu\ (\mathrm{cm}^{-1}) = 10\,000 + 566.7n$, $n = 0$–9. Several of these bands also appear in Griggs' 1968 Chappuis spectrum[85] as weak oscillations on the red Chappuis wing, ex-

tending to the longest observed wavelength, 850 nm. To our knowledge Griggs' is the only published spectrum obtained by a photoelectric (as opposed to photographic) technique.

Consistent with Hay and Goddard[86] we interpret the Wulf bands as the vibrationally allowed (for asymmetric stretching motion) transition to the 1^1A_2 state. The electronic origin is probably close to 1.1 eV since the lowest energy cold band (1.24 eV) should be (0 0 1)–(0 0 0) rather than (0 0 0)–(0 0 0). The adiabatic energy of 0.9 eV estimated in Table 15 is in reasonable agreement with this interpretation. Furthermore, the observed band spacing of 566.7 cm^{-1} agrees well with Hay and Dunning's predicted bending frequency of 537 cm^{-1} (Ref. 74) and the length of the progression is consistent with their prediction of a considerable change in angle compared to the ground state.

3.2.c. Chappuis Bands

The weak, diffuse Chappuis absorption bands are centered in the red region. The most recent measurements are by Inn and Tanaka[87] tabulated elsewhere,[88] Vigroux,[89] and Griggs.[85] Inn and Tanaka's cross sections are up to 10% smaller than those of Vigroux and Griggs, which are consistent with each other and with the 577 nm mercury line measurement by Hearn.[90] Vigroux's values are reproduced in Table 16. Interestingly, according to Shaw[91] the smaller cross sections of Inn and Tanaka give better agreement between visible and ultraviolet determinations of atmospheric ozone. An explanation of this inconsistency would clearly be desirable.

The temperature dependence of the Chappuis bands shows contradictions between different studies prior to 1948, as discussed by Vassy and Vassy.[92] Later, Vigroux[89] found almost no temperature dependence of the cross section from -92 to $+80$ °C.

Theoretical calculations assign the Chappuis bands to the 1^1B_1 state, which according to Hay and Dunning[74] has a similar angle and longer bond than the ground state. The observed band spacing of ~ 1000 cm^{-1} (Ref. 84) is somewhat larger than Hay and Dunning's predicted stretching frequency of 965 cm^{-1}.

As expected for diffuse bands, dissociation appears to occur with unit efficiency, leading exclusively to ground state O and O_2 products, as found by Castellano and Schumacher[93] and more recently by Tkachenko *et al.*[94] However, McGrath *et al.*[95,96] reported an ultraviolet absorption transient following Chappuis band irradiation which they ascribe to direct formation of stable electronically excited ($^1A_2$) ozone.

More recently, Chappuis band photodissociation has been studied by Moore, Bomse and Valentini[97,98] and Fairchild *et al.*[99] using molecular beam techniques, leading to a detailed characterization of the product O_2 vibrational and rotational state distribution.

The gas phase Raman spectrum in the Chappuis region has been reported by Selig and Claassen.[100] An absolute Raman cross section at 500 nm for the ν_1 Q-branch is cited as 1.8×10^{-29} cm^2 by Cooney.[101] A resonantly enhanced coherent anti-Stokes Raman spectrum of ν_1 has also been observed.[102]

3.2.d. Huggins and Hartley Bands

3.2.d.1. Assignments and Analysis

The somewhat diffuse Huggins bands occur in the ultraviolet region around 370–300 nm. Using isotopic substi-

TABLE 16. Chappuis band cross sections from Vigroux (Ref. 89)

λ(nm)	$\sigma(10^{-22}$ $cm^2)$	λ(nm)	$\sigma(10^{-22}$ $cm^2)$	λ(nm)	$\sigma(10^{-22}$ $cm^2)$	λ(nm)	$\sigma(10^{-22}$ $cm^2)$
451.6	2.00	546.1	31.0	618.0	40.7	716.8	7.41
455.1	1.94	548.7	31.5	619.1	38.6	720.7	6.51
458.5	3.09	551.2	32.4	622.0	37.9	726.4	5.70
462.0	4.27	553.8	32.9	625.6	36.2	732.8	5.01
466.7	3.38	556.4	34.8	629.3	34.3	739.2	3.98
471.0	4.42	559.0	37.1	633.5	32.6		
473.1	4.17	561.7	41.4	634.9	31.4		
477.0	5.70	564.3	42.8	637.6	30.4		
483.1	8.91	567.0	44.4	641.8	28.4		
487.4	7.91	569.8	46.2	645.8	26.5		
488.8	8.2	573.5	47.3	648.6	24.8		
492.8	8.57	575.4	47.9	650.0	20.2		
496.9	9.34	578.3	47.1	654.4	23.0		
501.2	13.6	581.2	44.9	663.4	19.8		
506.0	17.2	584.2	43.8	668.1	18.4		
510.5	15.7	587.2	43.3	672.7	16.0		
511.8	15.4	590.3	44.1	677.7	14.4		
514.8	15.9	593.4	44.8	682.8	12.9		
519.6	17.5	596.8	47.6	687.6	11.8		
524.5	20.6	601.9	50.9	692.5	10.8		
529.6	25.7	603.6	50.0	698.1	9.51		
534.0	27.8	607.5	48.1	703.6	8.57		
536.5	27.3	610.8	45.2	708.9	7.93		
540.5	29.5	614.3	42.4	712.2	7.71		

tution, Katayama[77,103] established the definitive vibrational assignments, and inferred an origin (which is not observable) of 368.7 nm.

An interesting feature of the Huggins bands is the appearance of odd quanta in all three vibrational progressions, which is at first surprising in view of the molecule's C_{2v} symmetry which forbids odd ν_3 Franck–Condon factors. Odd ν_3 hot bands also appear with surprising strength in the room-temperature spectrum. Brand *et al.*[104] suggested vibronic coupling as the cause of ν_3 activity, and derived an upper state geometry of $R = 1.36$ Å, $\theta = 102°$ from a C_{2v} Franck–Condon analysis using the (pre-Katayama) spectrum and assignments of Simons *et al.*[105]

Brand *et al.*'s interpretation is challenged by the recent laser fluorescence spectrum of Sinha *et al.*[76] obtained in a supersonic beam, which cooled the ozone sufficiently to yield partially resolved rotational structure. Interpretation of this structure is consistent with a C_s rather than a C_{2v} upper state. Indeed, *ab initio* calculations by Hay and coworkers[74,76,79] predict that the $^1B_2$ state on which the Hartley continuum terminates has shallow C_s wells in the exit channels. The fluorescence spectrum yields upper state rotational constants of $A = 2.1 \pm 0.4\ \mathrm{cm}^{-1}$ and $\bar{B} = 0.45 \pm 0.01\ \mathrm{cm}^{-1}$, compatible with a bond angle of less than 106°. A preliminary C_s Franck–Condon analysis of the Huggins bands[106] suggests an angle of about 99°, and assigns ν_1 and ν_3 as local stretching modes of the long and short bonds, respectively.

The Huggins band structure washes out towards short wavelengths, and is replaced by the Hartley continuum, which peaks around 255 nm. Some residual structure remains at these wavelengths, which appears to be a continuation of the Huggins structure. The shape of the Hartley continuum, which arises from the $^1B_2$ state, has been modeled by Adler-Golden,[107] Hay *et al.*,[78] Sheppard and Walker,[79] and Atabek *et al.*,[108] and is shown to derive mainly from a symmetric stretching progression. The continuum nature arises from broadening of the vibrational lines via dissociation along the asymmetric stretching mode, which is a symmetric barrier. This interpretation was predicted by *ab initio* calculations (Devaquet and Ryan,[109] Hay and coworkers[74,78]) and is confirmed by the resonance Raman spectrum (Imre *et al.*[16]). A recent discussion of the Raman spectrum may be found in Atabek *et al.*[108]

3.2.d.2. Absorption Cross Sections

The Huggins and Hartley band cross sections are very important for atmospheric modeling. Among earlier studies the most reliable seems to be Inn and Tanaka's.[87,88] Although their resolution is rather low, it is sufficient for many atmospheric modeling purposes, and their cross-section values below ~250 nm have been utilized in the WMO/NASA recommendations.[5]

Recently, higher-resolution spectra have been obtained, e.g., by Bass and Paur[110–112] and Molina and Molina[114] at and below room temperature, and by Freeman *et al.*[115] at 195 K. Bass and Paur's measurements were relative, and have been provisionally placed on an absolute basis by normalizing to the 253.7-nm mercury line cross-section value measured by Hearn.[90] The resulting cross-section values have been adopted in the WMO/NASA report.[5] Freeman *et al.*'s measurements[115] have the highest resolution of all, but required normalization at several different wavelengths, which was accomplished using Hearn's mercury wavelength values.

Absolute ozone cross sections at mercury wavelengths are given in Table 17. It is seen that excellent agreement exists between the measurements of Hearn, the average values from Brion's survey[117] and recent absolute measurements by Freeman *et al.*[118] Bass and Paur's most recent relative measurements[111] are also in excellent agreement at most wavelengths, especially if one normalizes them to the 253.7-nm cross-section value obtained very recently by Mauersberger *et al.*,[113] 113.7×10^{-19} cm^2, which is 1% smaller than Hearn's. Molina and Molina's results are around 2%–4% higher than typical Table 17 values, but are in excellent relative agreement. Another recent set of measurements deserving mention are those of Brion *et al.*[116] at a more limited number of wavelengths. They appear to be 2%–3% too small, but they are in excellent relative agreement with the other measurements. In summary, it appears that both the relative and absolute ultraviolet absorption cross sections of ozone are now known to an accuracy of

TABLE 17. Room-temperature absorption cross sections at mercury wavelengths (10^{-19} cm^2)

λ(nm)	Brion *et al.*[a] survey average	Hearn[b]	Freeman *et al.*[c]	Bass and Paur,[d] normalized to Mauersberger[e]
253.7	114.3 ± 1.0	114.7 ± 2.4	···	114
289.4	14.76 ± 0.22	14.7 ± 0.3	14.9	14.8
296.7	5.92 ± 0.11	5.971 ± 0.026	5.97	5.95
302.2	2.87 ± 0.07	2.86 ± 0.011	2.91	2.87
334.2	0.0439 ± 0.0017	0.0427 ± 0.0006	0.0437	0.0437

[a] Reference 117.
[b] Reference 90.
[c] Reference 118.
[d] Reference 111.
[e] Reference 113.

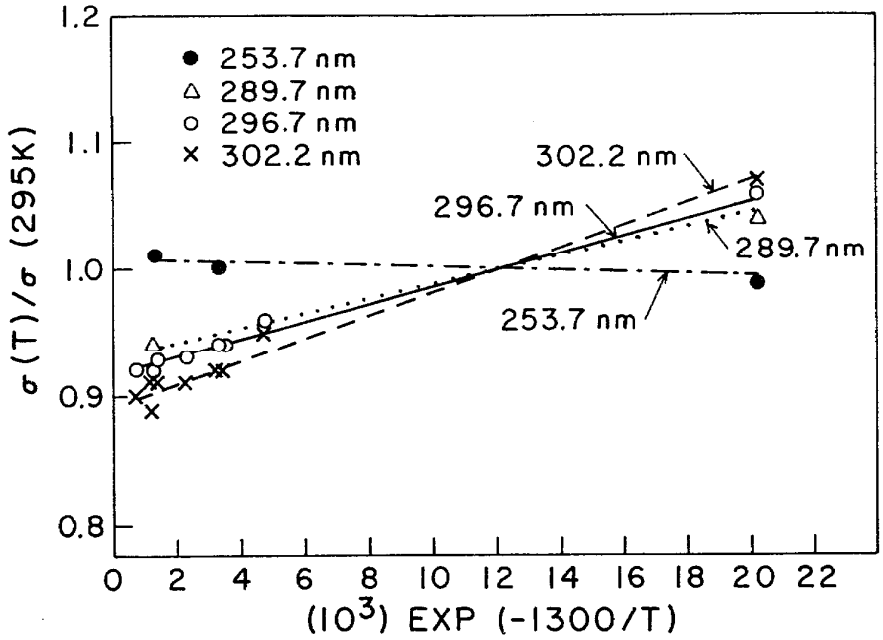

FIG. 1.Temperature dependence of mercury line cross sections.

typically ~2% or better at room temperature.

The temperature dependence of the Huggins and Hartley bands has been measured by Bass and Paur,[110–112] Simons *et al.*,[105] Brion *et al.*,[116] and Molina and Molina,[114] with very good agreement. Results at several mercury wavelengths obtained by Freeman *et al.*[115,118] also agree well with these studies. At wavelengths above ~270 nm, the cross section increases with temperature. There is now a consensus from both experiment and theory[105,107] that the cross section at 253.7 nm decreases slightly with temperature, in disagreement with the oft-cited work of Vigroux,[89] who shows an increase with temperature. As pointed out by Molina and Molina, the temperature effect at 253.7 nm should be taken into account in the normalization of the Bass and Paur relative measurements.

Parametrization of the temperature dependence may be accomplished using an empirical expression quadratic in temperature, as discussed in Refs. 111 and 114. A theoretical analysis of the Hartley band temperature dependence has been performed by Adler-Golden,[107] who proposed a semiempirical function based on Franck–Condon calculations. This function is found to yield an essentially linear dependence of cross section on $\exp(-1300/T)$, the Boltzmann factor for a vibrational frequency of 900 cm^{-1}, which is close to the average of ν_1, ν_2, and ν_3. Therefore, a plot of $\sigma(T)/\sigma(295\ K)$ vs $\exp(-1300/T)$ can facilitate interpolation of the cross section at temperatures intermediate between the low-temperature (e.g., Freeman[115]) and room-temperature data. An example of such a plot is Fig. 1. which shows the temperature dependence of mercury line cross sections. Excellent linearity as well as consistency to within 1%–2% among the measurements (taken from Bass and Paur,[111,112] Simons *et al.*,[105] Vigroux,[89] $\lambda > 290$ nm, and Freeman *et al.*[118]) is observed.

3.2.d.3. Photodissociation Products

Recent measurements have resolved the issue of the product branching ratio in the Huggins and Hartley bands. An excellent review of pre-1980 work is given by Moortgat.[119] In the Hartley continuum the major products are $O(^1D) + O_2(^1\Delta)$, with a minor contribution from ground state products $O + O_2$. A number of recent measurements of the absolute $O(^1D)$ branching ratio Φ made in the 248 to 290 nm region show excellent agreement. The detailed results are: $\Phi(248) = 0.85 \pm 0.02$ (Ref. 120), 0.91 ± 0.03 (Ref. 121), 0.94 ± 0.01 (Ref. 122); $\Phi(254) = 0.92$ (Ref. 123); $\Phi(266) = 0.88 \pm 0.02$ (Ref. 124); $\Phi(270) = 0.92 \pm 0.03$ (Ref. 125); $\Phi(290) = 0.95 \pm 0.02$ (Ref. 125). There is the suggestion of a slight increase in Φ from 270 to 300 nm (see Davenport[125] and Brock and Watson[124,126]). We recommend an average value of $\Phi = 0.92$ for $\lambda < 290$ nm.

At longer wavelengths where the "falloff" region begins, we accept the relative branching ratio measurements of Brock and Watson[126] which agree well with the measurements of Moortgat and co-workers.[127–129] Davenport's absolute measurements[125] show larger scatter but otherwise are consistent with these studies. Normalizing Brock and Watson's data to $\Phi = 0.92$ at 297.5 nm yields the value $\Phi = 0.79$ at 308 nm, in excellent agreement with Greenblatt and Wiesenfeld's accurate absolute measurement of 0.79 ± 0.02.[122] Our preferred Φ values are listed in Table 18.

The long wavelength tail seen in Brock and Watson's work, extending to around 325 nm, was not observed by Moortgat *et al.*,[127–129] perhaps due to insufficient sensitivity and the need to deconvolve the data for instrumental resolution effects. However, this tail was predicted theoretically by Adler-Golden *et al.*[130] and Hudson,[131] and has been confirmed experimentally by Martin *et al.*,[132] and Wiesenfeld

TABLE 18. Recommended values of the $O(^1D) + O_2(^1\Delta)$ branching ratio for ozone ultraviolet photolysis

λ(nm)	$T = 298$ K	$T = 230$ K
210–298	0.92	0.92
299	0.94	0.94
300	0.96	0.96
301	0.97	0.97
302	0.98	0.98
303	1.00	1.00
304	1.00	0.98
305	0.99	0.95
306	0.94	0.89
307	0.87	0.76
308	0.79	0.57
309	0.67	0.37
310	0.50	0.23
311	0.39	0.15
312	0.30	0.11
313	0.25	0.08
314	0.21	0.03
315	0.21	0.03
316	0.21	0.02
317	0.18	0.01
318.5	0.16	0.00
320	0.12	0.00
325.5	0.08	0.00
325	0.05	0.00

and Trolier.[133] It arises from vibrationally excited ozone, which has a large absorption cross section in this wavelength region.[105,107,130] Direct evidence for the efficient production of $O(^1D)$ in the falloff region by vibrationally excited ozone has been provided by Zittel and Little[134] who found a factor of ~70 enhancement in the $O(^1D)$ production cross section at 310 nm following vibrational excitation by CO_2 laser irradiation. Thus, in the upper atmosphere (~100 km), where ozone vibrational excitation exceeds thermal Boltzmann factors, the $O(^1D)$ branching ratio would be significantly enhanced in the falloff region.

Below room temperature the $O(^1D)$ falloff curve shifts to the blue as the result of the reduced ozone internal energy. The effect has been studied in detail by Moortgat *et al.*[129] The relative branching ratio values of Lin and DeMore[135] at 230 K agree very well with those of Moortgat *et al.*[129] From these data a smooth curve normalized to coincide with the 300 K data at the short wavelengths has been derived, and is given in Table 18. The effect of temperature on the branching ratio below the falloff region was studied by Davenport,[125] who found it to be negligible.

An empirical expression for Φ as a function of temperature and wavelength has been derived by Moortgat and Kudszus.[136] Except in the long wavelength tail region, it gives excellent agreement with the Table 18 values. More theoretically motivated calculations,[130,131] although less convenient, also reproduce the experimental data quite well.

Finally, state-specific product characterization has been performed in the Hartley continuum using molecular beam techniques (for details, see Fairchild *et al.*,[137] Sparks *et al.*,[138] Valentini[139]). The results have been modeled via trajectory calculations by Sheppard and Walker.[79]

In a recent followup, Valentini *et al.*[140] explain the observed propensity for even j values in the $O_2(^1\Delta)$ product in terms of nuclear exchange symmetry restrictions in the $^1\Delta/^3\Sigma$ curve crossing. Since these restrictions are absent for the heteronuclear O_2 isotopes, an isotope-dependent $^1\Delta/^3\Sigma$ branching ratio results. This isotopic selectivity might be responsible for the slight ^{18}O enrichment of ozone seen in the stratosphere by Rinsland *et al.*[47]

3.2.e. Vacuum Ultraviolet Absorption, Photoionization and Photoelectron Spectra

Vacuum ultraviolet photoabsorption studies of ozone were conducted by Tanaka *et al.*[141] in the 220–105 nm region, and Ogawa and Cook,[142] who extended the region down to 52 nm. The spectrum is continuous with various broad maxima, with a number of superimposed peaks starting around 8 eV. Theoretical aspects are discussed by Thunemann *et al.*,[73] whose calculated vertical excitation energies and assignments agree well with the experimental features.

In a measurement of neutral photodissociation product yields in the vacuum ultraviolet, Taherian and Slanger[143] inferred quantum yields of 1.5 for $O(^3P)$, 0.55 for $O(^1D)$ and a minimum of 0.5 for $O_2(b\,^1\Sigma_g^+)$ for photolysis at 157.6 nm.

Photoionization and photoelectron spectra of ozone have been obtained by a number of workers, including Brundle,[144] Dyke *et al.*,[145] Frost *et al.*,[146] Weiss *et al.*,[147] Moseley *et al.*,[148] and Katsumata *et al.*[149] There is some debate on the exact value of the adiabatic ionization potential, which is given as 12.52 ± 0.004 eV by Weiss *et al.* and Moseley *et al.*, but as 12.43 eV if one uses the first, very weak vibrational band in the photoelectron spectrum of Katsumata *et al.* and Dyke *et al.* We tentatively accept the recommendation of Weiss and Moseley, and assign the 12.43 feature as an O_3 ν_2 hot band. The first three vertical ionization transitions consist of vibrational progressions centered at approximately 12.73, 13.00, and 13.54 eV from Katsumata *et al.*, who assigned these transitions to the 1^2A_1, 1^2B_2, and 1^2A_2 states of O_3^+ using photoelectron angular distribution measurements. Vibrational frequencies are approximately 640, 1350, and 900 cm^{-1} in these respective transitions.

Weiss *et al.* measured product branching ratios in ozone photoionization down to 60 nm, finding the major process to be the production of O_3^+. A weak onset for O_2^+ production appears at 13.08 eV, followed by more intense production at 13.43 eV. The onset for O^+ formation appears at 15.21 eV. When corrected for internal thermal energy of 0.043 eV, the O_2^+ production threshold yields an ozone dissociation energy of 1.066 ± 0.004 eV, in close agreement with calorimetric measurements[150] which yield 1.05 ± 0.02 eV. For data on electron-impact ionization, see Sec. 4.1.m.

Hiller and Vestal's studies of photodissociation of O_3^+ (Ref. 151) and O_3 (Ref. 152) yield threshold energies which are approximately 0.3 eV lower than expected based on both the ionization potential of 12.52 eV and the electron affinity of 2.1028 ± 0.0025 eV measured via photoelectron and photodetachment spectroscopy.[153] Hiller and Vestal rationalized this discrepancy by proposing that the measured ionization potential and electron affinity are both too low

due to the inadvertent preparation of electronically excited ozone in the photoelectron and photoionization work. We can find no support for this contention, particularly in the light of Katsumata *et al.*'s explanation of the photoelectron spectrum, which refutes Hiller and Vestal's proposed reassignment. Instead, we concur with Moseley *et al.*'s hypothesis that internal excitation of the ozone ions was responsible for Hiller and Vestal's unexpected results.

3.3. Spectroscopy of Vibrationally and Electronically Excited Ozone

The previous sections dealt with transitions involving the ground vibrational, ground electronic state of ozone, and, in addition, vibrational and rotational hot bands (Sec. 3.1) and fluorescence/resonance Raman emission from dissociative states (Sec. 3.2). This section deals with the remaining possibilities, i.e., spectra associated with a single, metastable electronic state (vibrational or rotational bands) in addition to electronic (near-infrared through ultraviolet) spectra of vibrationally excited states or metastable electronic states.

The ultraviolet spectrum (Hartley continuum) of excited vibrational states is now reasonably well understood. On the other hand, almost nothing is known about the spectroscopy of the metastable electronic states of ozone. Despite convincing theoretical predictions that one or more electronic states (particularly 1^3B_2) are metastable, and indirect experimental evidence (see Sec. 4.1.a of this review) that they are formed in recombination, there have been no unambiguous spectral observations of metastable electronic states as of the present time.

3.3.a. Emission Spectra of Excited Electronic States

We are aware of only a single observation, by von Rosenberg and Trainor,[156] of vibrational features ascribed to electronically excited ozone. They reported emission in the vicinity of 8 and 6.6 μm accompanying the recombination of ozone following flash photolysis of ozone–oxygen mixtures. They tentatively ascribed these signals to respectively vibrational (ν_3) and electronic emission from the 1^3B_3 state of ozone formed along with the ground state ($^1A_1$).

The above interpretations present several difficulties. One is that vibrational frequencies tend to decrease with the binding energy, consistent with Hay and Dunning's *ab initio* study[74] which tabulated ν_1 and ν_2 for a number of excited electronic states including 1^3B_2. If this is the case, all three fundamental modes of 1^3B_2 would be at wavelengths beyond 9 μm. Unfortunately, Wilson and Hopper[75] do not report vibrational frequencies in their latest *ab initio* work. The difficulty with von Rosenberg and Trainor's interpretation of the 6.6-μm feature is that triplet emission to the ground state is expected to be too weak to be observable ($f \sim 10^{-9}$).

A more recent study by Rawlins *et al.*[9,10] of infrared emission following ozone recombination found no unusual vibrational features [see Sec. 4.1.a.2.].

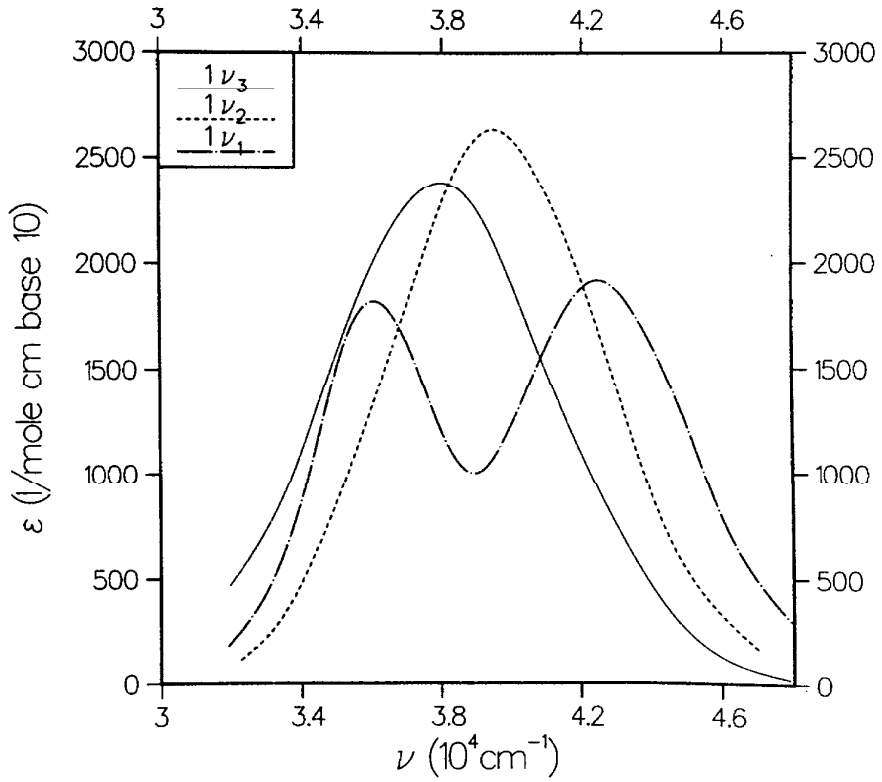

FIG. 2. Hartley continuum of vibrationally excited states.

3.3.b. Ultraviolet Absorption Spectra of Excited Electronic States

Several workers studying ozone recombination and radiolysis (e.g., Hochanadel *et al.*,[157] Riley and Cahill[158]) have reported absorption features in the vicinity of the Hartley continuum which might be attributable to electronically excited ozone. Indeed, Wilson and Hopper[75] predict a strong $^3B_2$–$^3A_1$ transition in the Hartley region. However, more recent interpretations and measurements by Bair and coworkers (Kleindienst *et al.*[159] and Joens *et al.*[160]) explain the observations as the Hartley continuum of vibrationally excited ozone, discussed in the following subsection.

McGrath *et al.*[95,96] reported a long-lived absorption transient at 320 nm following ozone irradiation in the Chappuis band. They ascribe this feature to the $^1A_2$ state, associated with the nearby Wulf bands. However, the diffuseness of the Wulf and Chappuis bands would seem to argue against direct photoproduction of stable $^1A_1$ ozone.

Although *ab initio* calculations (Sec. 3.2) can predict energies and intensities for electronic transitions between excited states of ozone, none have been published to our knowledge. This is clearly an important area for further research.

3.3.c. Ultraviolet Absorption Spectra of Vibrationally Excited States

Of the observed electronic transitions in ozone the Huggins and Hartley bands display distinct components due to excited vibrational states. Huggins hot bands are readily identifiable in high-resolution spectra, referred to in Sec. 3.2, and are particularly noticeable in the figures of Simons *et al.*[105] and of Katayama,[77] who provides vibrational assignments. The rather strong temperature dependence in the Huggins region results from these hot bands, as well as from changes in the rotational contours of the cold bands.

The shapes of excited vibrational components of the Hartley continuum are of critical importance for the interpretation of ultraviolet absorption of ozone recombination (see the previous section). These components are now fairly well characterized for the single-quantum vibrational levels. There is reasonable consistency among theoretical predictions (Adler-Golden,[107] Sheppard and Walker[79] and Atabek *et al.*[108]) and measurements based on laser irradiation (Adler-Golden *et al.*[130] and McDade and McGrath[161]), recombination (Bair and co-workers[159,160]) and thermal excitation (Simons *et al.*[105] and Astholz *et al.*[162]). Excitation in ν_2 produces only a slight change in the spectrum (mainly a red shift), while excitation in ν_1 yields a bimodal shape, and excitation in ν_3 both broadens and red-shifts the spectrum, as seen in Fig. 2 (from Adler-Golden's calculation[107]). The combined ν_1 and ν_3 components in this figure show particularly good agreement with laser excitation data. The ν_2 component appears to have a red shift relative to the (0 0 0) components of around 600 cm^{-1} (Bair and coworkers[105,159,160]) somewhat greater than predicted by theory (Adler-Golden[107] and Joens [163]).

4. Survey of Reaction Kinetics Data

In this section, kinetic data for reactions of ozone with each of the species enumerated in the Introduction are presented. For each reaction system considered, the value of the overall rate coefficient as recommended in previous surveys[1–5] is given, unless there is clear evidence that this value needs to be revised. The enthalpy changes (ΔH^0_{298}) from Refs. 1–3, augmented with spectroscopic and electron-affinity measurements, are included for convenience. Where data are available over a range of temperatures, the measurements are presented as an Arrhenius plot; the plots have been extended to cover the temperature range 170–400 K, of interest in upper-atmosphere processes. In each instance, the new information which is presented concerns reactant state selectivity and product state specificity for each of these reactions.

4.1. Reaction Rate Coefficients

4.1.a. Ozone Formation by Three-Body Recombination

$$O + O_2 + M \rightarrow O_3 + M, \quad \Delta H^0 = -106.3 \text{ kJ/mol.}$$

The three-body recombination of $O + O_2$ is the principal ozone-forming reaction at nearly all altitudes in the atmosphere. (See Sec. 4.1.b., immediately following, for a discussion of possible additional ozone-forming reactions that may be of importance in the upper atmosphere.) The principal questions concerning this reaction are (1) the value of the rate coefficient for various third bodies, and (2) the distribution of product vibrational (and possibly electronic) states.

4.1.a.1. Termolecular Rate Coefficient

M=O₂: The recommended value[3] over the range 200–300 K is $6.2\times10^{-34}\,(T/300)^{-2.0}$ cm^6 $molecule^{-2}$ s^{-1} (see Fig. 3); the value at 298 K is 6.3×10^{-34}.

M=N₂: The recommended value[3] over the range 200–300 K is $5.7\times10^{-34}\,(T/300)^{-2.8}$ cm^6 $molecule^{-2}$ s^{-1} (see Fig. 3); the value at 298 K is 5.8×10^{-34}.

M=Ar: The recommended value[2] over the range 200–300 K is $3.9\times10^{-34}\,(T/300)^{-1.9}$ cm^6 $molecule^{-2}$ s^{-1} (see Fig. 3); the value at 298 K is 3.95×10^{-34}.

Recent infrared chemiluminescence measurements[10] have provided values of the rate coefficient between 80 and 170 K which can be fit by the expression $k = 8\times10^{-33}\,(T/100)^{-3.2}$ cm^6 $molecule^{-2}$ s^{-1}; these values are shown in Fig. 4.

M=He: The efficiency of He is stated to be ~60% that of O_2 or N_2.[3,164,165] This would give k (M = He, $T = 298$ K) $= 3.4\times10^{-34}$ cm^6 $molecule^{-2}$ s^{-1}. A temperature dependence for M = He recombination has not been reported.

M=O₃: The efficiency of O_3 is stated to be 2.27× that of O_2,[164] which would give a value of $k = 1.43\times10^{-33}\,(T/300)^{-2.0}$ cm^6 $molecule^{-2}$ s^{-1}. Benson and Axworthy[166] give the same relative efficiency, but give a different expression for k, $1.65\times10^{-34}\exp(300/T)$ cm^6 $molecule^{-2}$ s^{-1}. These expressions are shown in Fig. 5.

M=O: Two sets of values for the rate coefficient with O atom as the third body have been reported, viz.:

$k = 2.15\times10^{-34}\exp(345/T)$ cm^6 $molecule^{-2}$ s^{-1}

(Refs. 1 and 167);

$k = 2.52\times10^{-36}\exp(1057/T)$ cm^6 $molecule^{-2}$ s^{-1}

(Refs. 167 and 193). These are shown in Fig. 6.

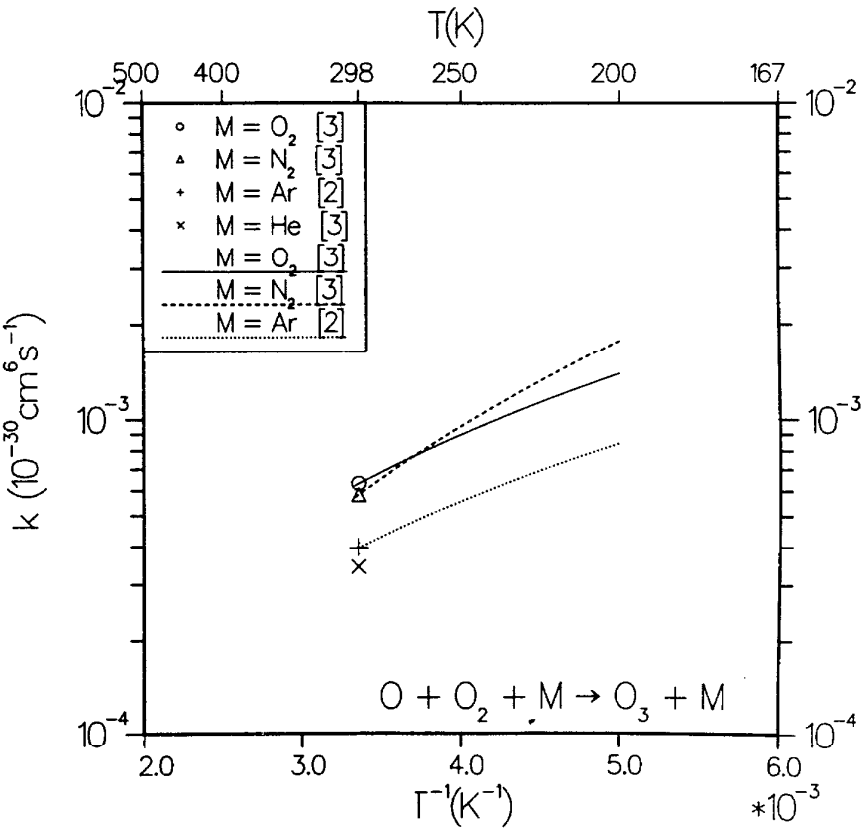

FIG. 3.Three-body recombination rate coefficients for $O + O_2 + M \rightarrow O_3 + M$ ($M = O_2$, N_2, Ar, He).

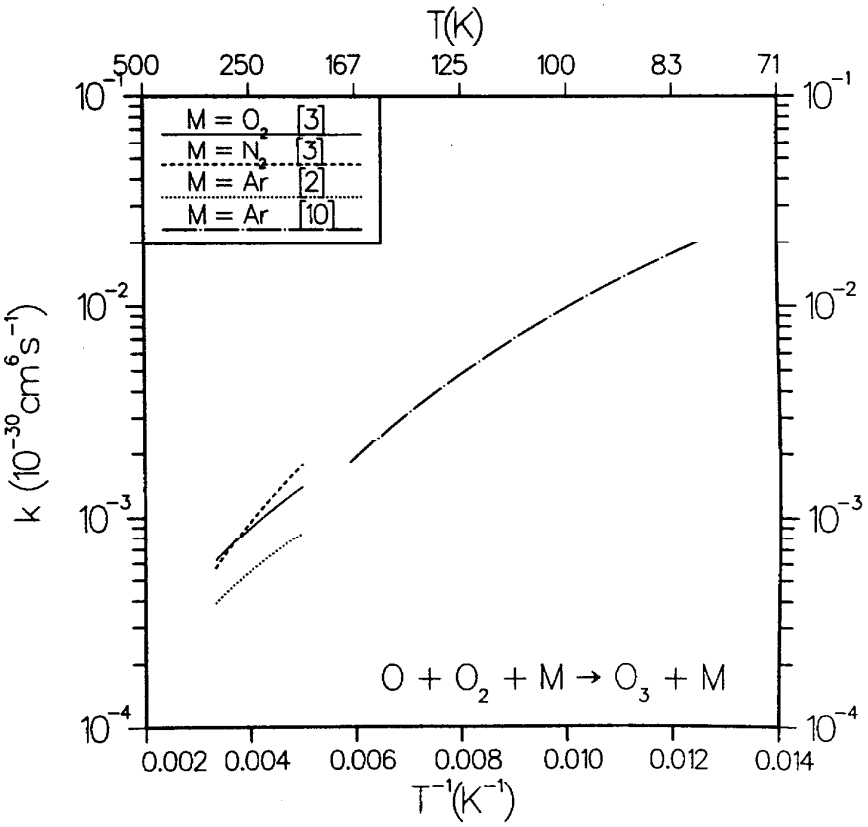

FIG. 4.Three-body recombination rate coefficients for $O + O_2 + M \rightarrow O_3 + M$, including low-temperature data of Rawlins *et al.*, Ref. 10, for M = Ar.

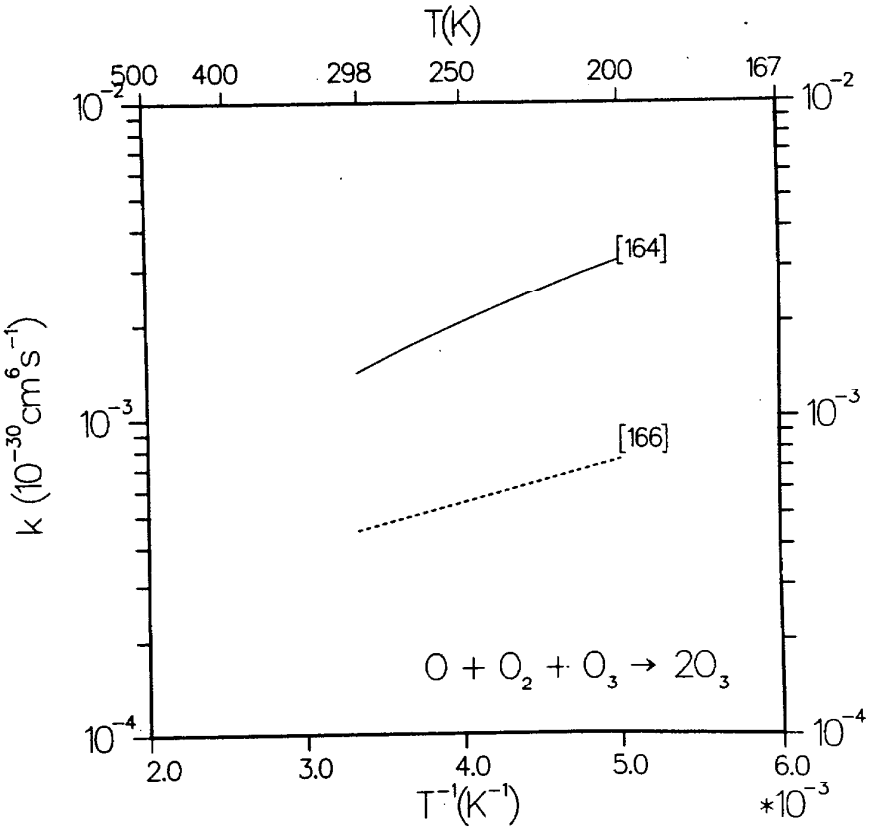

FIG. 5.Three-body recombination rate coefficient for $O + O_2 + O_3 \rightarrow 2O_3$. Refs. 164 and 166.

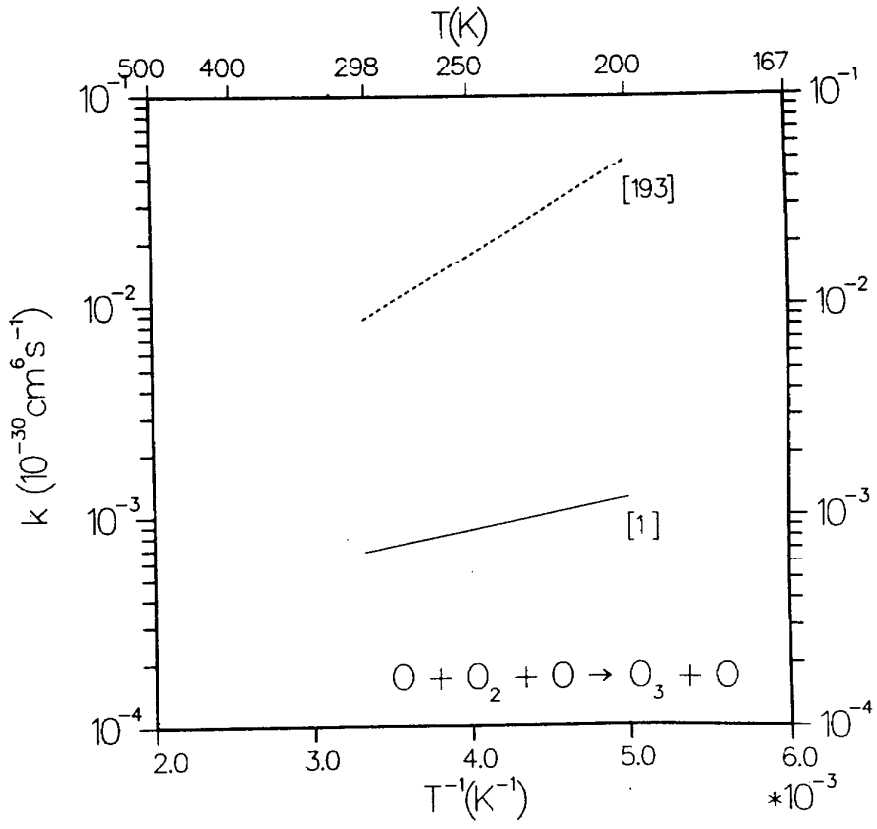

FIG. 6.Three-body recombination rate coefficient for $O_2 + 2O \rightarrow O_3 + O$, Refs. 1 and 193.

4.1.a.2. Product State Distributions

A substantial fraction of the exothermicity of the recombination process appears as vibrational excitation of the product ozone molecule; this is a major source of the ozone infrared luminescence from the upper atmosphere. Attempts to measure this distribution in the laboratory have employed both infrared chemiluminescence and transient UV absorption spectroscopy to observe the virationally excited molecules.

Von Rosenberg and Trainor[156,168,169] were the first to observe infrared chemiluminescence from vibrationally excited ozone molecules. However, since their experiments were carried out a high pressures (100–400 Torr O_2), the ozone molecules underwent extensive relaxation before they could be observed. Rawlins *et al.*[8–10,170] carried out experiments at lower pressures and temperatures in the COCHISE facility at the Air Force Geophysics Laboratory. Since, even in this apparatus, the ozone molecules still undergo $\sim 10^4$ collisions with argon atoms before they radiate, it is not possible to observe a pure nascent distribution. The most recent COCHISE results[10] show ozone with population in $(0, 0, v_3)$ and $(1, 0, v_3 - 1)$ vibrational levels with up to $v_3 - 5$ quanta in the asymmetric stretching mode. The distribution within the v_3 manifold appears to be equilibrated (presumably by efficient collisional relaxation), with an effective vibrational temperature $T_v \simeq 2000$ K.

An alternative technique for monitoring vibrational excitation in the ozone molecule, employed by Bair and coworkers,[159,171,172] is observation of transient UV absorption in the Hartley band. Both this technique and that of infrared chemiluminescence depend on knowledge of vibrational-excited-state spectroscopy for proper interpretation. The IR chemiluminescence technique requires knowledge of infrared band intensities (see Sec. 3.1.b), while the transient UV absorption technique requires knowledge of the UV absorption spectra of the vibrationally excited states (see Sec. 3.3.c). In addition, both techniques follow changes in spectra as the initially formed molecules relax, and thus require a vibrational deactivation model for proper interpretation (see Sec. 4.1.c).

The possibility that recombination occurs to a metastable electronic state of ozone, as an alternative to high vibrational levels of the ground electronic state, has been suggested several times. Von Rosenberg and Trainor[169] observed infrared emission at 6.6 μm, which they tentatively assigned to emission from $^3B_2$; however, this emission was *not* observed by Rawlins *et al.*[10] Wraight[173] suggested a similar possibility, but proposed the $^1A_2$ state, lying ~ 1.0 eV above the ground state, as the one being formed. Perhaps the most convincing evidence for formation of the $^3B_2$ state is the measurement of the rate of formation of ozone using transient UV absorption[172,174] or IR emission techniques.[156] These studies conclude that as much as 60% of the available oxygen atoms may react to form triplet ozone. Additional experiments by Locker *et al.*[175] provide further corroboration. In that work, Locker *et al.* also determine effective rate coefficients for quenching of $O_3(^3B_2)$:

$$\begin{aligned} M = O_2 \quad & k_Q = (2.9 \pm 0.5) \times 10^{-15} \text{ cm}^3 \text{ molecule}^{-1} \text{ s}^{-1} \\ = N_2 \quad & = (1.0 \pm 0.4) \times 10^{-15} \text{ cm}^3 \text{ molecule}^{-1} \text{ s}^{-1} \\ = Ar \quad & = (1.3 \pm 0.4) \times 10^{-15} \text{ cm}^3 \text{ molecule}^{-1} \text{ s}^{-1}. \end{aligned}$$

The reaction $O + 2O_2 \rightarrow O_3 + O_2(a^1\Delta_g)$ would be approximately 10.5 kJ/mol exothermic. Popovich *et al.*[176] considered the possibility that $O_2(^1\Delta)$ is formed in the recombination reaction by using detailed balancing to calculate the rate coefficient from the known rate for the reverse reaction (see Sec. 4.1.e.). They found $k = 5 \times 10^{-37} \exp(-2940/T)$ cm^6 molecule^{-2} s^{-1}, which would make no significant contribution in the temperature range we are considering.

4.1.a.3. Dissociation of Ozone

$$O_3 + M \rightarrow O_2 + O + M, \quad \Delta H^0 = +106.3 \text{ kJ/mol}.$$

While the thermal unimolecular decomposition of ozone will not make any contribution to kinetics at atmospheric temperature, a knowledge of its rate coefficient serves as a valuable check on the three-body recombination rate coefficient, since the two are related by detailed balancing[177]:

$$\frac{k(\text{recombination})}{k(\text{dissociation})} = K_{eq}(T).$$

The decomposition rates have been reviewed by several authors with the following results:

M=O$_3$: $k_d = 1.65 \times 10^{-9} \exp(-11\,435/T)$ cm^3 molecule^{-1} s^{-1} for $T = 200$ to 1000 K[178]; $k_d = 7.15 \times 10^{-10} \exp(-11\,195/T)$ cm^3 molecule^{-1} s^{-1} for $T = 300$ to 3000 K.[179]

M=O$_2$: As for the recombination process, O_2 is (1/2.27)× as effective as ozone, so $k_d = 7.26 \times 10^{-10} \exp(-11\,435/T)$ cm^3 molecule^{-1} s^{-1} for $T = 200$ to 1000 K.[167,178]

In summary, the recombination and thermal dissociation data are mutually consistent.

4.1.b. Additional Sources of Ozone in the Upper Atmosphere

While the three-body recombination process discussed in the preceding section is certainly the major source of atmospheric ozone, and probably the only significant source in the stratosphere, the possibilities of additional reactions producing ozone have been suggested a number of times. In particular, Allen[180] has recently noted that ozone concentrations observed in the lower thermosphere (90–110 km) are significantly in excess of model predictions, and suggests a bimolecular process involving electronically excited oxygen molecules as a possible source of the discrepancy. We consider this process below, along with several ionic processes that may also contribute to ozone formation.

(i) $O_2^* + O_2 \rightarrow O_3 + O$

The molecular oxygen excitation energy must be in excess of 392 kJ/mol in order for reaction (i) to proceed. The metastable $O_2 A(^3\Sigma_u^+)$, $A'(^3\Delta_u)$, and $c(^1\Sigma_u^-)$ states are sufficiently energetic to be candidates for the reactive O_2^* species. Reaction (i) has been proposed by Benson[181] and Sugi-

mitsu and co-workers[182,183] in order to account for net ozone production rates in electric-discharge ozonizers. Popovich *et al.*[184] pointed out that a reaction similar to (i), involving thermally excited ground-state oxygen molecules, must occur by virtue of detailed balancing, with an activation energy of ~414 kJ/mol. Kenner and Ogryzlo[185] attributed the appearance of the NO_2^* continuum chemiluminescence spectrum in their experiments to reaction of NO with vibrationally excited ozone, which they suggested may be formed in reaction (i) (see Sec. 4.1.k). Kolb *et al.*[186] proposed that reaction (i) may be significant for interpretation of EXCEDE experiments (infrared emission from electron-beam-pumped atmospheric mixtures). Rawlins *et al.*[10] considered the bimolecular process but found it did not account for the COCHISE data, since all the data followed the $T^{-3.2}$ temperature dependence noted above. However, this type of reaction may be implicated in the HIRIS auroral data.[187–189]

Despite these numerous citations of reaction (i), in a variety of experimental contexts, essentially no rate data are available for this process. Sugimitsu and Okazaki[182] inferred a value of $k(\text{i}) = 4.8\times10^{-15}$ cm^3 molecule^{-1} s^{-1} from modeling ozone formation in a pulsed electrical discharge. Kenner and Ogryzlo[185] and Kolb *et al.*[186] suggested that a substantial fraction of the O_2^* (A, A′) quenching rate (approximately 10^{-12}~10^{-14} cm^3 molecule^{-1} s^{-1}) may proceed via the reactive pathway (i). We have been unable to find any direct measurement of k(i) in the literature.

(ii) $O^- + O_2 \rightarrow O_3 + e^-$

Although reaction (ii) is approximately 42 kJ/mol endothermic[181] it may be promoted by accelerated O^- ions or vibrationally excited O_2 [also see reaction (iii)]. A rate coefficient $k(\text{ii}) = 5\times10^{-15}$ cm^3 molecule^{-1} s^{-1} has been estimated by Niles,[190] Eliasson,[167] and Zalepukhin *et al.*[191]

(iii) $O^- + O_2(^1\Delta_g) \rightarrow O_3 + e^-$

Excitation of the O_2 to the metastable $a^1\Delta_g$ state makes reaction (iii) approximately 52.3 kJ/mol exothermic. A rate coefficient $k(\text{iii}) = 3\times10^{-10}$ cm^3 molecule^{-1} s^{-1} has been estimated by Sabadil and co-workers,[192,193] Phelps,[194] Fehsenfeld *et al.*,[195] and Ferguson *et al.*[196]; $k(\text{iii}) = 1.0\times10^{-10}$ (Niles[190]).

(iv) $O^- + O_2 + M \rightarrow O_3^- + M$

The rate coefficient for the associative recombination process (iv), with M = O_2, has been variously estimated as 1.0×10^{-29} (Ref. 190), 1.1×10^{-30} (Refs. 167, 191, and 196), and 1.4×10^{-30} (Ref. 197) cm^6 molecule^{-2} s^{-1}. Data on k(iv) for several values of gas density and E/N have been obtained by Harrison and Moruzzi,[198] and are shown in Fig. 7; the values fall between (0.5 and 1.0)$\times10^{-30}$.

(v) $O^- + O_2 \rightarrow O_3^- + h\nu$

A rate coefficient for the radiative ion-association process (v) has been estimated as $k(\text{v}) = 1.0\times10^{-17}$ cm^3 molecule^{-1} s^{-1}.[190,199]

(vi) $O_2^- + O \rightarrow O_3 + e^-$

Estimates of the rate coefficient for the associative detachment process (vi) are 3.0×10^{-10} (Ref. 200), $(3.0\pm0.5)\times10^{-10}$ (Ref. 194), 1.5×10^{-10} (Ref. 196), 2.5×10^{-10} (Ref. 190), and 3.5×10^{-10} cm^3 molecule^{-1} s^{-1}.[191] The most reliable appears to be the measure-

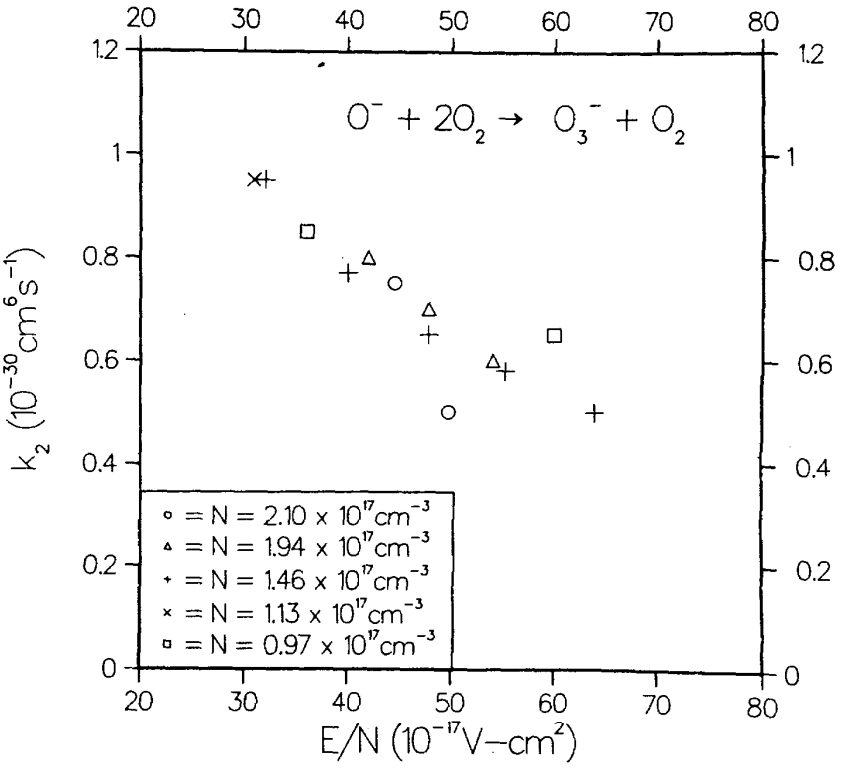

FIG. 7. Three-body recombination rate coefficient for $O^- + 2O_2 \rightarrow O_3^- + O_2$, Ref. 198.

ment of $k = 1.5\times10^{-10}$ cm^3 molecule^1 s^{-1} by Ferguson *et al.*,[196] although this value is a factor of 2 smaller than the average of the other estimates.

(vii) Charge-Neutralization Processes

A rate coefficient for the three-body charge-neutralization process

$$O^- + O_2^+ + M \rightarrow O_3 + M$$

has been estimated as 2.0×10^{-25} cm^6 molecule^{-2} s^{-1}.[167,190] However, because of the large amount of energy released ($\sim$1000 kJ/mol), the product is surely unstable to $O_2 + O$, so that the net result is an electron transfer

$$O^- + O_2^+ \rightarrow O_2 + O.$$

Rates have also been estimated for other charge-neutralization processes that would be required to produce neutral ozone from the O_3^- ions formed in reactions (iv) and (v). These include the following:

(a) $O_3^- + O^+ \rightarrow O_3 + O$,

$k(a) = 1\times10^{-7}(300/T)^{1/2}$ cm^3 molecule^{-1} s^{-1}, Ref. 167,

$k(a) = 2\times10^{-7}$ cm^3 molecule^{-1} s^{-1} at 300 K, Ref. 190,

and (b) $O_3^- + O_2^+ \rightarrow O_3 + O_2$

$k(b) = 2\times10^{-7}(300/T)^{1/2}$ cm^3 molecule^{-1} s^{-1}, Ref. 167,

$k(b) = 2\times10^{-7}$ cm^3 molecule^{-1} s^{-1} at 300 K, Refs. 190 and 199.

It should be noted that reactions (vii.a) and (vii.b) are also highly exothermic, on the order of 800 kJ/mol exothermic. This would be sufficient to dissociate the newly formed ozone, yielding $2O + O_2$ and $2O_2 + O$, respectively, or alternatively to produce highly vibrationally excited ozone, $O_3^\ddagger$.

(viii) Other Reactions

Several other possible reactions may be mentioned briefly, for which no data are available at present. Three-body electron attachment

$$O_2 + O_2 + e^- \rightarrow O_3 + O^-$$

is $\sim$250 kJ/mol endothermic[181] and is not likely to occur. Similarly, the reaction $O_2^- + O_2 \rightarrow O_3^- + O$ has a threshold in excess of 5 eV.[201] Radiative recombination

$$O_2^* + O \rightarrow O_3 + h\nu$$

is not known for neutrals, although the ionic process (v) has been noted above. A negative ion cluster reaction

$$O_4^- + O \rightarrow O_3^- + O_2, \quad k = 4\times10^{-10} \text{ cm}^3 \text{ molecule}^{-1} \text{ s}^{-1}$$

has been noted by Ferguson *et al.*[196]; the corresponding positive ion cluster reaction

$$O_4^+ + O \rightarrow O_3 + O_2^+ \text{ (or } O_3^+ + O_2)$$

is an important atmospheric reaction. Its rate has been measured[202] as $k = (3\pm2)\times10^{-10}$ cm^3 molecule^{-1} s^{-1}.

4.1.c. Energy Transfer Processes Involving Vibrationally Excited Ozone

As a result of the low ambient pressures in the upper atmosphere, molecules may exist in a nonequilibrium distribution of vibrational and rotational states, and relaxation rates may compete with chemical reaction rates. In this section, we summarize the available data on vibrational and rotational relaxation of ozone.

4.1.c.1. Vibrational Relaxation

Vibrationally excited ozone has been produced in the laboratory using either of two techniques: as the product of the $O + O_2 + M$ recombination reaction (Sec. 4.1.a) or by infrared laser pumping (Sec. 4.2.a). In the former instance, a broad distribution of vibrational states is produced; in the latter, a well-defined initial vibrational distribution is obtained, but it has not been possible to excite the ozone molecule beyond one or two quanta of excitation in the stretching modes.

Several techniques are available for detection of the vibrationally excited molecules. Transient ultraviolet absorption of newly formed ozone molecules has been employed by Bair and co-workers.[159,160,164,171,172] Infrared chemiluminescence has been used by von Rosenberg and Trainor[156,168,169] and at the COCHISE facility at the Air Force Geophysics Laboratory.[8–10,170] Both of these techniques require knowledge of state-dependent spectroscopic parameters: either the dependence of the UV absorption cross section on vibrational state (Sec. 3.3.c), or of the vibrational transition moment on vibrational state (Sec. 3.1.c).

Analogous techniques have been used to monitor populations produced by infrared (mainly CO_2) laser pumping. IR–UV double resonance absorption has been used by McDade and McGrath[203] and by Adler-Golden *et al.*[130,204] IR fluorescence has been used by Cool and co-workers[205–209] and West *et al.*[210] An additional technique for monitoring vibrationally excited ozone depends on the enhancement of the NO_2^* chemiluminescence in the $O_3 + NO \rightarrow NO_2 + O_2$ reaction due to reactant vibrational excitation (see Sec. 4.1.k); this technique has been used by Kurylo *et al.*,[211–213] Gordon and co-workers,[214–218] and Cool *et al.*[219] While the deactivation rate coefficient obtained from the NO chemiluminescence technique is difficult to interpret in terms of state-to-state kinetics, the data obtained using this technique are so extensive that the results are included in this survey.

Vibrational deactivation measurements on ozone are summarized in Table 19. Typically, the asymmetric stretching state (001) is populated by a CO_2 laser, and vibrational relaxation proceeds via the mechanism identified by Rosen and Cool,[205] as follows. The stretching states (001) and

(100) equilibrate with each other very rapidly, with a nearly gas-kinetic rate coefficient, and subsequently relax into the bending state (010) with a slower V–V rate constant k_1. Finally, V–T relaxation deactivates (010) with rate constant k_2 to yield ground state ozone. This mechanism is generalized to higher vibrational levels by presuming that stretching quanta equilibrate rapidly among themselves and then relax into bending quanta, which in turn are removed via V–T. An exception to this mechanism occurs with a quencher molecule (e.g., SF_6) which has a vibrational frequency close to ozone's stretching modes, and which therefore could remove stretching quanta via V–V transfer.

According to Rosen and Cool's model the vibrational level populations follow two characteristic decay constants, λ_1/p and λ_2/p, from which k_1 and k_2 can be computed. However, in only a few cases (O, O_2, O_3, and Ar quenchers) have both decay constants been reported. The ratio k_1/k_2 is less than unity for Ar (and, according to theory,[226] for He as well) but greater than unity for O, O_2, and O_3. The claim by Jocns *et al.*[160] of a less-than-unity ratio for O_2 was based on rather hazardous analysis of a complex system (ozone recombination studied by ultraviolet absorption) and a faulty interpretation of previous data.[204] Based on three independent studies[156,204,210] the ratio for O_2 is 1.7 ± 0.1.

There are essentially no direct measurements of state-to-state relaxation rates for the higher-lying vibrational levels. Endo *et al.*[224] analyzed shock-tube data on thermal dissociation of ozone to obtain $\langle \Delta E \rangle$, the average amount of energy transferred per collision, for a variety of bath gases at 600–1100 K. The values obtained range from 0.16 kJ/mol (for argon) to 2.7 kJ/mol (for SF_6). These are still highly averaged quantities, however, and do not yield state-specific information.

4.1.c.2. Rotational Relaxation

There are no data available on rotational energy transfer rates in ozone. Ensemble-averaged rates can be extracted from the spectroscopic pressure-broadening coefficients discussed in Sec. 3.1.d.

Table 19

Energy transfer processes in ozone

O_3 initial state	O_3 final state	Process	Collision Partner	T/K	Technique	Rate coefficients cm^3 molecule^{-1} s^{-1}		±	Reference	Comments
100,001	010	V-V	O_3	298	IR fluorescence	k_1	1.7(-13)	30%	206	preferred value
010	000	V-T	O_3	298	IR fluorescence	k_2	8.8(-14)	20%	206	preferred value
100,001	010	V-V	O atom	298	IR fluorescence	k_1	9(-12)	+100%, -50%	210	
010	000	V-T	O atom	298	IR fluorescence	k_2	3(-12)	+100%, -50%	210	
100,010,001		V-V,V-T	O_2	298	IR fluorescence	k_2/p	1.9(-14)	20%	205	
100,001	010	V-V	O_2	298	IR-UV DR	k_1	5.2(-14)	20%	204	preferred value
010	000	V-T	O_2	298	IR-UV DR	k_2	3.0(-14)	12%	204	preferred value
100,001	010	V-V	O_2	298	transient UV	k_1	9.4(-15)	16%	160	
010	000	V-T	O_2	298	transient UV	k_2	2.27(-14)	20%	160	
100,010,001	000	V-T	O_2	298	NO reaction	k	1.3(-14)	10%	211, 212	(a)
100,001	010	V-V	O_2	298	IR fluorescence	k_1	3.7(-14)	50%	210	
010	000	V-T	O_2	298	IR fluorescence	k_2	2.0(-14)	30%	210	
000	005	E-V	$O_2^*(b^1\Sigma_g^+)$	80-170	IR chemiluminescence				10	(f)
100,010,001		V-V,V-T	H_2	298	IR fluorescence	k_2/p	7.1(-13)	15%	205	
100,010,001	000	V-T	H_2	298	NO reaction	k	1.18(-12)	10%	211, 212	(a)
100,010,001	000	V-T	H_2	424	NO reaction	k	2.14(-12)	10-20%	214, 221	(b)
				408			1.94	10-20%		
				407			1.84	10-20%		
				365			1.48	10-20%		
				362			1.51	10-20%		
				321			1.36	10-20%		
				308			1.03	10-20%		
				298			1.10	10-20%		
				284			1.01	10-20%		
				249			1.08	10-20%		
				224			0.58	10-20%		
				200			0.70	10-20%		
				181			0.66	10-20%		
				167			0.80			
		10-20%								
100,010,001	000	V-T	para-H_2	425	No reaction	k	9.6(-13)	10-20%	214, 221	(b)
				408			10.5	10-20%		
				405			11.8	10-20%		
				390			13.9	10-20%		
				383			12.1	10-20%		
				365			11.3	10-20%		
				348			9.3	10-20%		
				333			9.8	10-20%		

Table 19 (cont'd.)

O_3 initial state	O_3 final state	Process	Collision Partner	T/K	Technique	Rate coefficients cm^3 molecule$^{-1}s^{-1}$		±	Reference	Comments
				320			8.3	10-20%	214, 221	(b)
				304			9.8	10-20%		
				301			6.8	10-20%		
				278			7.8	10-20%		
				261			7.5	10-20%		
				239			6.3	10-20%		
				224			6.0	10-20%		
				206			5.8	10-20%		
100,010,001		V-V,V-T	D_2	298	IR fluorescence	λ_2/p	1.5(-13)	10%	205	
100,010,001	000	V-T	D_2	413	NO reaction	k	2.44(-13)	10-20%	214	(b)
				372			2.37	10-20%		
				326			1.41	10-20%		
				298			1.30	10-20%		
				297			1.13	10-20%		
				266			1.21	10-20%		
				221			0.80	10-20%		
				200			0.98	10-20%		
				182			0.85	10-20%		
				165			1.58	10-20%		
				165			1.11	10-20%		
100,010,001		V-V,V-T	CH_4	298	IR fluorescence	λ_1/p	4.0(-13)	25%	208	
						λ_2/p	2.87(-14)	25%	205, 208	
100,010,001	000	V-T	CH_4	298	NO reaction	k	4.8(-13)	10%	211, 212	(a)
100,010,001		V-V,V-T	N_2	298	IR fluorescence	λ_2/p	2.0(-14)	15%	205	
100,010,001	000	V-T	N_2	298	NO reaction	k	1.94(-14)	10%	211, 212	(a)
100,010,001		V-V,V-T	He	298	IR fluorescence	λ_2/p	6.5(-14)	12%	205	
100,010,001	000	V-T	He	298	NO reaction	k	6.0(-14)	5%	211, 212	(a)
100,010,001	000	V-T	He	444	NO reaction	k	2.3(-13)	10-20%	214	(b)
				406			1.78(-13)	10-20%		
				298			7.0(-14)	10-20%		
				284			5.54	10-20%		
				246			3.65	10-20%		
				223			3.5	10-20%		
				198			2.16	10-20%		
				177			2.82	10-20%		
				164			1.66	10-20%		
100,001	010	V-V	Ar	298	IR fluorescence	k_1	5.6(-15)	30%	206	preferred value
010	000	V-T	Ar	298	IR fluorescence	k_2	7.4(-15)	30%	206	preferred value
100,010,001		V-V,V-T	Ar	298	IR fluorescence	λ_2/p	6.2(-15)	50%	205	
100,010,001	000	V-T	Ar	298	NO reaction	k	7.3(-15)	25%	211, 212	(a)
000		E→(V,E?)	$Ar_2^*(^3\lambda_u^+)$	298	pulsed e-beam	k	4.6(-9)	15%	222	

Table 19 (cont'd.)

O_3 initial state	O_3 final state	Process	Collision Partner	T/K	Technique	Rate coefficient cm^3 molecule^{-1} s^{-1}		±	Reference	Comments
100,010,001		V-V,V-T	CO_2	298	IR fluorescence	λ_2/p	9.7(-14)	5%	205	
100,010,001	000	V-T	CO_2	298	NO reaction	k	1.06(-13)	10%	211, 212	(a)
000	100,001	V-V	$CO_2(v_3=1)$	298	IR fluorescence	k	7.6(-13)	20%	208, 209	
100,010,001	000	V-T	SO_2	298	NO reaction	k	2.35(-13)	5%	211, 212	(a)
100,010,001		V-V,V-T	SF_6	298	IR fluorescence	λ_2/p	2.7(-12)	20%	206	
100,010,001	000	V-T	SF_6	298	NO reaction	k	1.9(-12)	10%	211, 212	(a)
000		V-V	$SF_6(v_3=1)$	298	NO reaction				218	(e)
100,010,001	000	V-V	SiF_4	298	NO reaction	k	3.8(-11)	15%	212, 213	
100,010,001	000	V-T	H_2O	298	NO reaction	k	3.5(-12)	10%	211, 212	(a)
100,010,001	000	V-R,T	H_2O	295	NO reaction	k	3.3(-12)	10-20%	215	
				360			2.2	10-20%		
				380			1.6	10-20%		
				395			1.8	10-20%		
				410			1.7	10-20%		
100,010,001	000	V-R,T	D_2O	300	NO reaction	k	1.59(-11)	10-20%	215	
				303			2.11	10-20%		
				333			1.15	10-20%		
				377			0.91	10-20%		
				473			0.78	10-20%		
100,010,001	000	V-T	HCℓ	173-419	NO reaction	k (graph)		~20%	210	
100,001	010	V-V	NO	350	NO reaction	k	4.8(-13)	20%	217	(c)
100,001	010	V-V	NO	308	NO reaction	k	3.6(-13)	50%	219	
		V-T	NO_2	298	NO reaction	k	1.8(-13)	15%	223	(d)
		V-T	OCS	298	IR fluorescence	k	2.7(-12)	45%	207	
		V-T,V-V	He,Ne,Ar, Kr,Xe,N_2,O_2, CO_2,CF_4,SF_6	600-1100	thermal dissociation (shock tube)	ΔE=0.16 - 2.7 kJ/mol depending on collision partner			224	
Theoretical Calculations										
		V-T	Xe	300-2500	classical trajectory calculations				225	
020,100,001,010,000		V-T	He	100- 450	BSIOS and VCCIOS calculations				226	
10-25 kcal/mole		V-V,V-T	Ar	250-2000	classical trajectory calculations				227	
		R-T	He,Ar,Xe	500,2500	CS and CIOS calculations				228	

J. Phys. Chem. Ref. Data, Vol. 16, No. 4, 1987

Comments to Table 19

(a) The rate coefficients determined by the NO chemiluminescence technique usually approximate the value of λ_2/p, except in the case of CH_4.

(b) As noted in the erratum to Ref. 214, there are two errors in Table II, p. 4218, of that reference. First, the k_5^M rate coefficients for M = He are all a factor of 10 too large as given. Second, the column labeled "Probability $\times 10^4$" is actually "Probability $\times 10^3$."

(c) Incorrect interpretation of $O_3^\dagger$ + NO reaction; reported value of $O_3^\dagger$ — He relaxation rate is a factor of ~3 too high.

(d) Incorrect interpretation of $O_3^\dagger$ + NO reaction; appear to have observed slow relaxation rate λ_2/p, on the basis of $O_3^\dagger - O_2$ result.[204,205]

(e) Efficient transfer from $SF_6^\dagger(v_3 = 1)$ to ozone observed.

(f) IR chemiluminescence results suggest 1/3 of $O_2^*(b)$ quenching by ozone ($k = 2.2 \times 10^{-11}$ cm^3 molecule^{-1} s^{-1}) may go by E–V transfer. V–V transfer from $O_2(v = 3)$ to produce $O_3(102)$ is also suggested.

4.1.c.3. Theoretical Calculations

Several theoretical calculations of energy transfer in ozone have been carried out. Stace and Murrell[225] carried out classical trajectory calculations on O_3 colliding with He, Ar, and Xe for temperatures in the range 300–2500 K, and compared their results with thermal unimolecular decomposition data. Additionally, Stace[229] determined the effect of anharmonicity on the value of the low-pressure rate coefficient for unimolecular decomposition. Clary[226] used breathing-sphere infinite-order-sudden (BSIOS) and vibrational-close-coupled infinite-order-sudden (VCCIOS) models to calculate the deactivation of O_3 (010) by He, and obtained good agreement with thermally averaged rate coefficient data[214] for $164 < T < 444$ K. In addition, V–V rate constants at 300 K were calculated for all combinations of levels (020), (100), (001), (010), and (000). Gelb[227] carried out classical trajectory calculations for ozone having initial total energy content of 42, 63, 84, and 105 kJ/mol, in collisions with Ar atoms at relative translational energies of 2.1, 4.2, 8.4, and 16.7 kJ/mol (corresponding to kinetic temperature of 250, 500, 1000, and 2000 K). He found that the direction of energy transfer (V–T as against T–V) is strongly influenced by the rotational angular momentum of the ozone molecule. These results are not inconsistent with, but are not directly comparable to the shock-tube measurements of Endo *et al.*[224] on $\langle \Delta E \rangle$ in O_3–Ar mixtures. It would be of interest to compare the trajectory results with other models of energy transfer in atom + polyatomic systems, such as the biased random-walk model[230] or information theory.[231]

Other relevant calculations include O_3 + (He, Ar, Xe) rotational energy transfer using centrifugal sudden (CS)

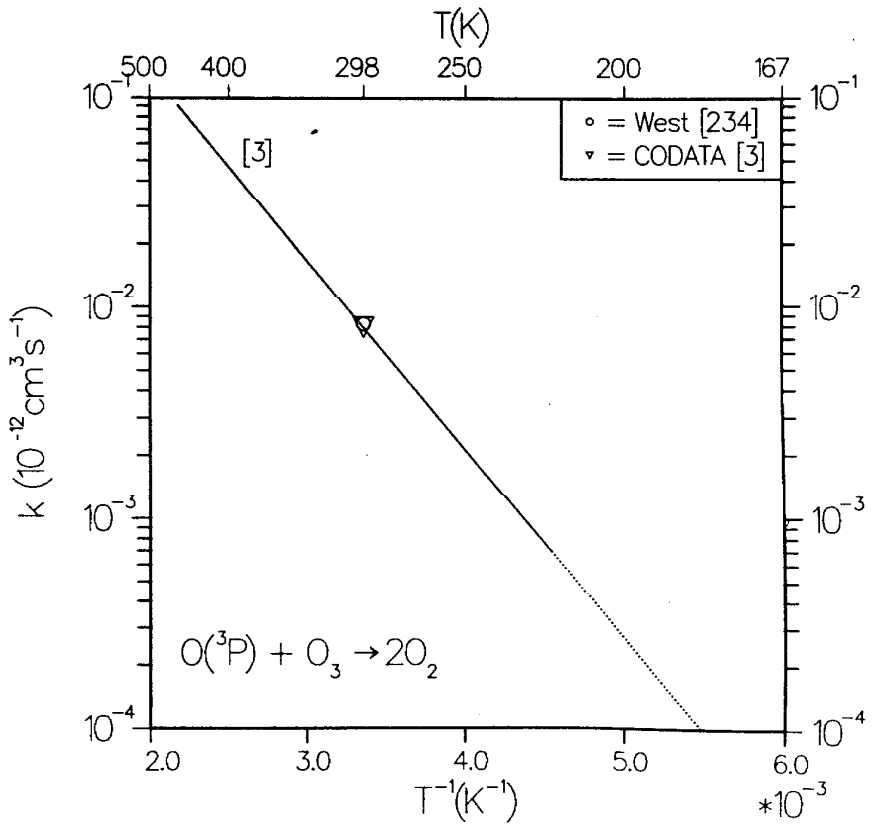

FIG. 8. Bimolecular rate coefficient for $O(^3P) + O_3 \rightarrow 2O_2$. In this and following figures, the dotted line indicates extrapolation of $k(T)$ beyond the temperature range recommended in Refs. 1–3.

and classical infinite-order-sudden (CIOS) approximations by Mulloney and Schatz,[228] and modeling the overall relaxation of ozone following CO_2 laser excitation of the (001) state, including all rotation–translation (R–T) vibration–vibration (V–V, V–V') and vibration–translation (V–T) terms.[232,233]

4.1.d. Reactions with Oxygen Atoms

	ΔH^0 (kJ/mol)
(i) $O(^3P) + O_3 \rightarrow 2O_2(^3\Sigma_u^-)$	−391.8
$\rightarrow O_2(^3\Sigma) + O_2(^1\Delta)$	−297.6
$\rightarrow O_2(^3\Sigma) + O_2(^1\Sigma)$	−234.8

The accepted value of the thermal rate coefficient[3]

$$8.0\times10^{-12}\exp(-2060/T)\ \text{cm}^3\ \text{molecule}^{-1}\ \text{s}^{-1}$$

is shown in Fig. 8. The value at 298 K is 8.0×10^{-15}.

Reactions of vibrationally excited ozone

West, Weston, and Flynn[234] measured the total removal rate of $O(^3P)$ atoms by O_3 (100,001), denoted $O_3^\ddagger$, excited by a CO_2 laser. The rate of $O_3^\ddagger$ deactivation is 1.5×10^{-11} cm^3 molecule^{-1} s^{-1}, but less than 30% can be attributed to the reactive channel, i.e., most of the deactivation proceeds via V–T inelastic collisions. Chekin *et al.*[235] (also see Ref. 236) reported a rate enhancement $k^\ddagger/k(0) = 3.4 \pm 0.5$, but their use of a cw CO_2 laser may have led to heating of the reaction mixute. Rawlins *et al.*[10] measured the following total rates for $O + O_3(v) \rightarrow O + O_3$, $O_2 + O_2$ at $T = 80$ to 170 K:

v	$k(v)$ (cm^3 molecule^{-1} s^{-1})
1	$\geqslant 0.8\times10^{-11}$
2	$\geqslant 1.4$
3	$\geqslant 2.0$
4	$\geqslant 2.7$
5	$\geqslant 3.6$

These rates are in good agreement with the measurement of West *et al.*[234] but the branching ratio between V–T deactivation and reaction has not been established.

Electronically excited molecular products

Washida *et al.*[237,238] have found that the rate of production of $O_2(^1\Delta)$ is less than 6% of the total reaction rate. Gauthier and Snelling[239] found that the rate of production of $O_2(^1\Delta)$ and $O_2(^1\Sigma)$ together are less than 3% of the total reaction rate. Thus, the reaction appears to give exclusively ground state O_2.

	ΔH^0(kJ/mol)
(ii) $O(^1D) + O_3 \xrightarrow{(a)} O_2 + 2O$	−83.3
$\xrightarrow{(b)} O(^3P) + O_3$	−189.6
$\xrightarrow{(c)} 2O_2(^1\Delta_g)$	393
$\xrightarrow{(d)} O_2(^1\Sigma_g^+) + O_2(^3\Sigma_g^-)$	−425
$\xrightarrow{(e)} 2O_2(^3\Sigma_g^-)$	−581

The recommended value for the rate coefficient[3] between 200 and 400 K is

$$2.5\times10^{-10}\ \text{cm}^3\ \text{molecule}^{-1}\ \text{s}^{-1};$$

no temperature dependence has been observed or reported.

The reaction proceeds mainly via channels (a) and (e), with roughly equal rates into each channel[3,240,241]; this is confirmed by the report of Klais *et al.*[242] that the rates of production of $O_2(^1\Delta)$ and $O_2(^1\Sigma_g^+)$ are much less than those of channels (a) and (e). The $O_2(^3\Sigma_g^-)$ is most likely produced with considerable vibrational excitation.[164,243] A theoretical calculation of the rate coefficient has been carried out by Tully[244]; it predicts very little temperature variation over the range 100–2100 K, but overestimates the absolute value by a factor of 2.

	ΔH^0(kJ/mol)
(iii) $O(^1S) + O_3 \rightarrow 2O_2(X^3\Sigma_g^-)$	−796
$\rightarrow 2O(^3P) + O_2$	−339.9
$\rightarrow O(^3P) + O(^1D) + O_2$	−108.4

The only reported measurement[245] is for removal of $O(^1S)$ by O_3:

$$(5.8 \pm 1.0)\times10^{-10}\ \text{cm}^3\ \text{molecule}^{-1}\ \text{s}^{-1}\ \text{at 298 K.}$$

No information is available on which of the product channels noted above may be followed by the reaction.

4.1.e. Reactions with Oxygen Molecules

	ΔH^0
(i) $O_2^\ddagger(^3\Sigma_g^-, v) + O_3 \rightarrow 2O_2 + O(^3P)$	see comments

The reaction as written is ~105 kJ/mol endothermic from the vibrational ground state of the molecules but may be enabled by reactant excitation. Arnold and Comes[240,241] found that vibrationally excited O_2 reacts with ozone with a rate:

$$(2.8 \pm 0.3)\times10^{-15}\ \text{cm}^3\ \text{molecule}^{-1}\ \text{s}^{-1}\ \text{at 298 K.}$$

No temperature dependence has been measured.

The bimolecular isotope exchange region

$$^{18}O_2 + {}^{16}O_3 \rightarrow {}^{18}O_2{}^{16}O + {}^{16}O_2$$

appears to proceed extremely slowly ($k < 2\times10^{-25}$ cm^3 molecule^{-1} s^{-1}) at 298 K, and therefore is not of significance in atmospheric chemistry.[246]

(ii) $O_2(^1\Delta_g) + O_3 \rightarrow 2O_2 + O(^3P)$,

$\Delta H^0 = +12.1$ kJ/mol.

The recommended value for the rate coefficient[2] between 280 and 360 K is

$$5.2\times10^{-11}\exp(-2840/T)\ \text{cm}^3\ \text{molecule}^{-1}\ \text{s}^{-1}$$

with $k = 3.8\times10^{-15}$ at 298 K. An additional measurement[240,241] of $k = (5.1 \pm 0.5)\times10^{-15}$ at 298 K is in reasonable agreement with the recommended value. Exciting the O_3 (initially to $v_3 = 1$) with a CO_2 laser increases the rate by a factor of 38 ± 20, to $(1\text{–}2)\times10^{-13}$ cm^3 molecule^{-1} s^{-1}.[247] With ozone excited to two or more quanta of the stretch mode, the rate of this essentially thermoneutral reaction may increase to $10^{-11}\sim10^{-10}$ cm^3 molecule^{-1} s^{-1}.[10]

Parker[248] has suggested the possibility of an alternative energy transfer (E–E) channel,

$$O_2(^1\Delta_g) + O_3(^1A_1) \rightarrow O_2(^3\Sigma_g^-) + O_3(^3B_2).$$

This process was also suggested by Kurylo *et al.*,[247] to explain their observed rate enhancement.

	ΔH^0(kJ/mol)
(iii) $O_2(^1\Sigma_g^+) + O_3 \xrightarrow{(a)} 2O_2 + O$	− 50.6
$\xrightarrow{(b)} O_2(^1\Delta_g) + O_3$	− 62.8
$\xrightarrow{(c)} O_2(^3\Sigma_g^-) + O_3$	− 157

The recommended value for the rate coefficient[3,249–251] at 298 K is

$(2.1 \pm 0.3) \times 10^{-11}$ cm^3 molecule^{-1} s^{-1};

no temperature dependence has been observed or reported.

Slanger and Black[250] report that the ratio $k(a)/k(\text{total})$, i.e., reaction to total quenching of $O_2(^1\Sigma)$, is $\simeq 0.7$. Rawlins *et al.*[10] postulate a $E \rightarrow V$ energy transfer process producing O_3 in $v_3 = 5$ with a rate of 7×10^{-12} cm^3 molecule^{-1} s^{-1} ($T = 80$ to 170 K); this would correspond approximately to the nonreactive part of the $O_2(^1\Sigma)$ deactivation rate.

4.1.f. Reactions with Hydrogen Atoms

	ΔH^0(kJ/mol)
$H + O_3 \xrightarrow{(a)} OH(v) + O_2(^3\Sigma)$	− 322
$\xrightarrow{(a')} OH(v) + O_2(^1\Delta)$	− 228.5
$\xrightarrow{(b)} HO_2 + O$	− 89.6

The recommended value for the rate coefficient[2] between 220 and 360 K is

$$1.4 \times 10^{-10} \exp(-480/T) \text{ cm}^3 \text{ molecule}^{-1} \text{ s}^{-1};$$

the value at 298 K is 2.8×10^{-11}, in reasonable agreement with a more recent determination[252] of 1.5×10^{-11}.

After some disagreement, the branching ratio to $HO_2 + O$ has been determined[253] as $k(b)/k(\text{total}) \leqslant 0.02$. The branching ratio to $O_2(^1\Delta)$ is $\leqslant 0.001 * k(\text{total})$.[237,254]

The only determination of $k(v)/k(\text{total})$, the branching ratio to OH vibrational states, is the infrared chemiluminescence data of Charters *et al.*[255] The recommended values given in Ref. 2 for $v \leqslant 6$ are incorrect, since they are derived from values of relative $N(v)$ versus pressure for which collisional relaxation is significant. We have applied a linear surprisal analysis[256,257] to the valid data reported by Charters *et al.*,[255] viz.:

$$\frac{k(8)}{k(9)} = 0.8, \quad \frac{k(7)}{k(9)} = 0.4, \quad \frac{k(6)}{k(9)} < 0.4.$$

Analysis of these data yields the following branching ratios:

$k(9) = 0.43$, $k(8) = 0.35$, $k(7) = 0.17$,

$k(6) = 0.04$ (uncertain).

$k(5)$ through $k(0)$ are not well determined, but in any case account for less than 1% of the $H + O_3$ reaction. This is a remarkable reaction, in which nearly all the reagent exothermicity is channeled into product vibration. A theoretical potential surface for this reaction has been calculated,[258] but does not predict this feature very well.

4.1.g. Reaction with Hydroxyl

	ΔH^0(kJ/mol)
$OH + O_3 \xrightarrow{(a)} HO_2 + O_2$	− 159

The recommended value for the thermally averaged rate coefficient[2] between 220 and 450 K is

$$1.9 \times 10^{-12} \exp(-1000/T) \text{ cm}^3 \text{ molecule}^{-1} \text{ s}^{-1};$$

the value at 298 K is 6.7×10^{-14}.

There have been several determinations of $OH(v)$ removal rate by ozone, which are summarized below:

v	Ref. 259	Ref. 260	Refs. 252,261
9	$(7.7 \pm 0.3) \times 10^{-12}$	$(11.0 \pm 0.4) \times 10^{-12}$	2.0×10^{-10}
8	$(6.7 \pm 0.5) \times 10^{-12}$	$(8.9 \pm 0.2) \times 10^{-12}$	
7	$(6.5 \pm 0.5) \times 10^{-12}$	$(8.5 \pm 0.2) \times 10^{-12}$	
6	$(5.3 \pm 0.6) \times 10^{-12}$	$(7.1 \pm 0.2) \times 10^{-12}$	
5	$(3.4 \pm 0.7) \times 10^{-12}$	$(4.5 \pm 0.1) \times 10^{-12}$	
4	$(2.8 \pm 0.8) \times 10^{-12}$	$(3.7 \pm 0.1) \times 10^{-12}$	
3	$(2.4 \pm 0.9) \times 10^{-12}$		
2	$(1.9 \pm 1.1) \times 10^{-12}$		

The first two data sets are plotted in Fig. 9. The extrapolation to $k(0) = 1.0 \times 10^{-12}$ cm^3 molecule^{-1} s^{-1}, suggested by Coltharp *et al.*,[259] is clearly incompatible with the thermal data. The data for higher vibrational levels [including the very large value for $k(9)$ reported by Greenblatt and Wiesenfeld[252]], are not inconsistent, since level populations in $v \geqslant 1$ are too small to make any contribution to the thermal rate coefficient at $T < 1000$ K.

The measurements *per se* do not distinguish between reaction (a), above, and simple vibrational deactivation. There are two additional reactive channels that are endothermic from $OH(v = 0)$, but become exothermic at higher v levels:

$$OH + O_3 \xrightarrow{(b)} H + 2O_2 \quad (v \geqslant 1),$$

$$OH + O_3 \xrightarrow{(c)} OH + O + O_2 \quad (v \geqslant 3).$$

Slanger and Huestis[261] conclude that the initial step leading to removal of OH is indeed energy transfer (V–V),

$$OH(v = 9) + O_3 \rightarrow OH + O_3^{\ddagger},$$

which is immediately followed by dissociation of $O_3^{\ddagger} \rightarrow O_2 + O$, so that the dominant overall reaction channel at high $OH(v)$ levels is (c).

4.1.h. Reactions with Hydroperoxyl

$$HO_2 + O_3 \rightarrow OH + 2O_2, \quad \Delta H^0 = -125 \text{ kJ/mol}.$$

The recommended rate coefficient[2] between 250 and 400 K,

$$1.4 \times 10^{-14} \exp(-600/T) \text{ cm}^3 \text{ molecule}^{-1} \text{ s}^{-1}$$

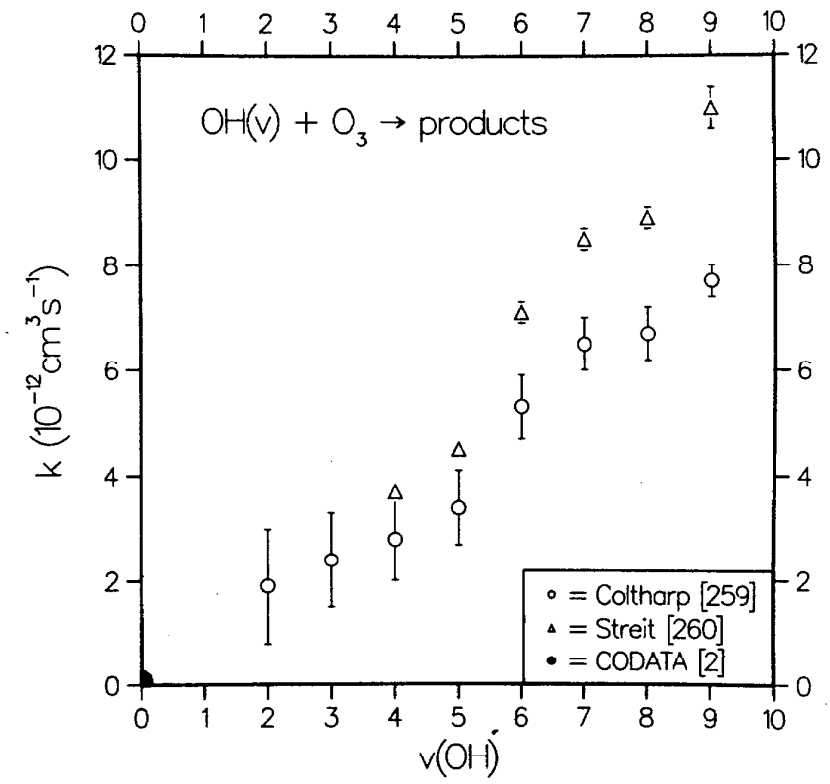

FIG. 9. Rate coefficient for $OH(v) + O_3 \rightarrow$ products reported by Coltharp (Ref. 259) and Streit *et al.* (Ref. 260). The thermal rate coefficient (Ref. 2) is shown at $v = 0$.

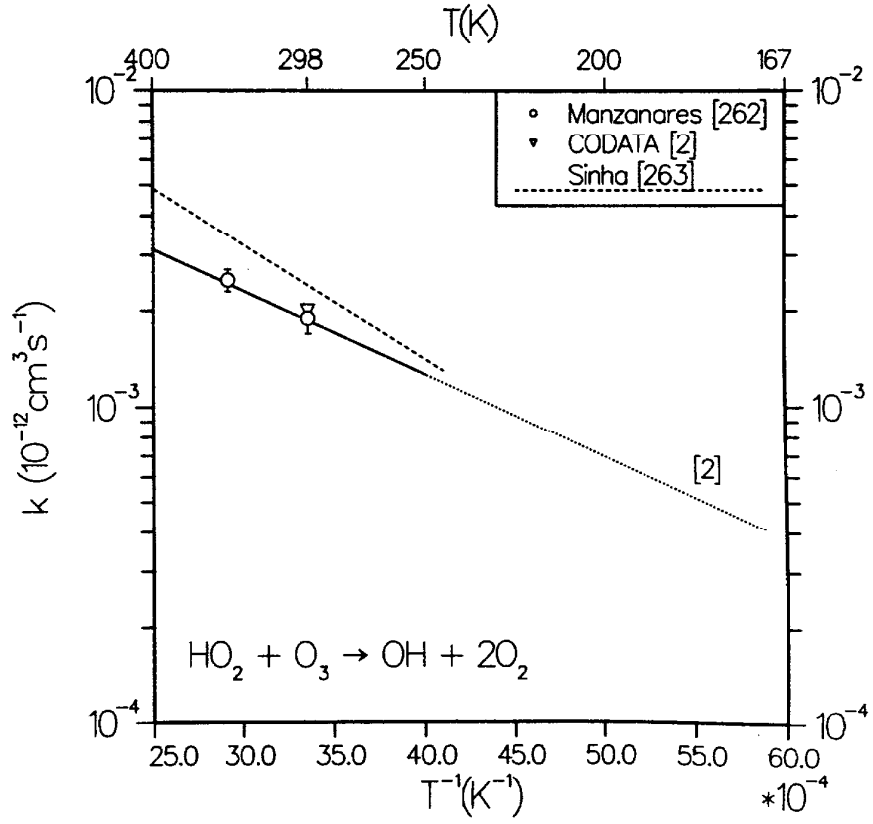

FIG. 10. Bimolecular rate coefficients for $HO_2 + O_3 \rightarrow OH + 2O_2$.

is shown in Fig. 10. The value at 298 K is 2.0×10^{-15}.

Manzanares *et al.*[262] have measured rate coefficients for this reaction, $k=(1.9\pm0.3)\times10^{-15}$ cm^3 molecule^{-1} s^{-1} at 298 K, $(2.5\pm0.2)\times10^{-15}$ at 343 K. Sinha *et al.*,[263] using isotopic labeling together with laser magnetic resonance detection, measured k over the range 243–413 K. Their value of the rate coefficient is

$$k=(3.84\pm2.4)\times10^{-14}\exp[(-825\pm91)/T].$$

These new data are also shown in Fig. 10. The more recent work, which appears to eliminate complications due to secondary reactions of the OH scavenger, suggests that a revision of the previously accepted[2] value of k is in order.

4.1.i. Reactions with Nitrogen Atoms

$$N(^4S)+O_3\rightarrow NO+O_2,\quad \Delta H^0=-525\text{ kJ/mol}.$$

The only measurement on this system[264] gives an upper limit for the rate at 298 K

$$k\leqslant5\times10^{-16}\text{ cm}^3\text{ molecule}^{-1}\text{ s}^{-1}.$$

Despite the large exothermicity, $N(^4S)$ is not very reactive to ozone. Unfortunately, several modeling calculations[265,266] have made use of an incorrect rate coefficient for this reaction.

4.1.j. Reactions with Nitrogen Molecules

$$N_2+O_3\rightarrow N_2O+O_2,\quad \Delta H^0=-60.7\text{ kJ/mol}$$

(from vibrationless reactants).

The reaction between N_2 and O_3, when both species are in their ground electronic and vibrational states, is extremely slow[267]:

$$k\simeq5\times10^{-28}\text{ cm}^3\text{ molecule}^{-1}\text{ s}^{-1}\text{ at 292 K}.$$

Prasad[268] conjectured that a rapid reaction may occur between $O_3^*(^3B_2)$ and N_2 at 77 K; no rate coefficient can be derived from his data. There is also a suggestion that vibrationally excited $N_2^{\ddagger}$ may react with ozone with a rate $\simeq10^{-12}$ cm^3 molecule^{-1} s^{-1}.[269,270] None of these kinetic processes have been directly observed, however.

4.1.k. Reactions with Nitric Oxide

$$NO+O_3\rightarrow NO_2+O_2,\quad \Delta H^{0\circ}=-199.2\text{ kJ/mol}.$$

The reaction between nitric oxide and ozone has been extensively studied. The recommended rate coefficient[3] between 195 and 304 K,

$$1.8\times10^{-12}\exp(-1370/T)\text{ cm}^3\text{ molecule}^{-1}\text{ s}^{-1},\quad(1)$$

is shown in Fig. 11. The value at 298 K is 1.8×10^{-14}.

Borders and Birks[271] carried out measurements over a wider temperature range (204–353 K), and found a nonlin-

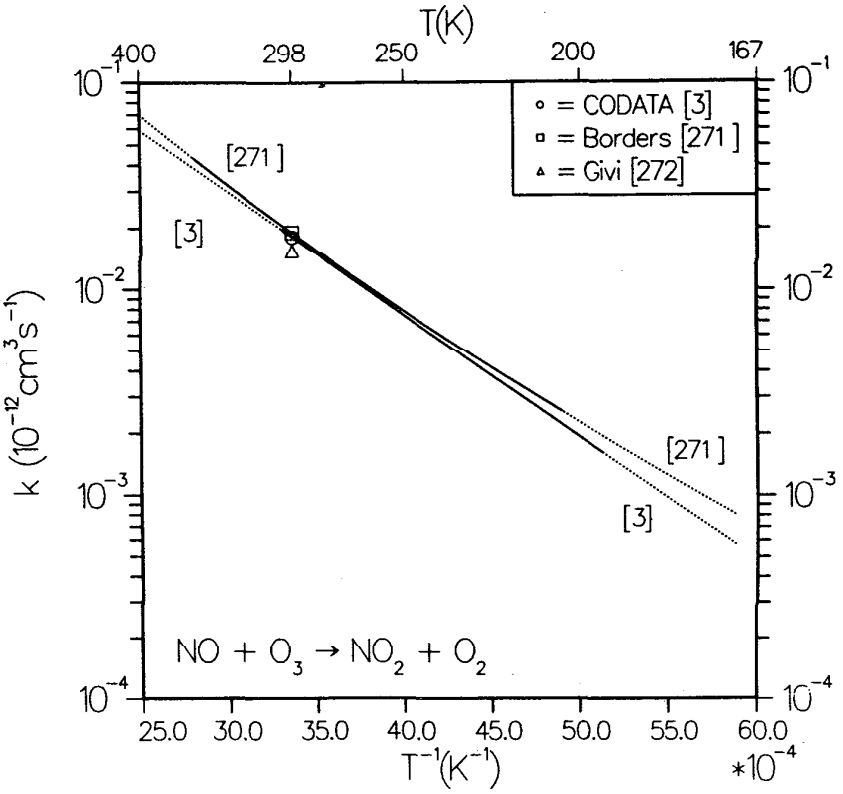

FIG. 11. Bimolecular rate coefficients for $NO+O_3\rightarrow NO_2+O_2$.

ear Arrhenius behavior that may be represented by

$$8.9\times10^{-19}\,T^{2.2}\exp(-765/T)\ \text{cm}^3\ \text{molecule}^{-1}\ \text{s}^{-1}. \quad (2)$$

Their value of $k(298)$ is 1.9×10^{-14}. Another recent determination[272] is $k(298) = 1.54\times10^{-14}$. We recommend the use of Eq. (2), since it is valid over a wider temperature range than Eq. (1). Note from Fig. 11 that Eqs. (1) and (2) give nearly identical numerical results over the temperature range 200–300 K, but diverge at higher and lower temperatures.

Visible chemiluminescence is observed in this reaction, and most analyses of the kinetics have assumed that the reaction takes place along two potential energy surfaces, as follows:

$$NO + O_3 \rightarrow NO_2(^2A_1) + O_2,$$

and

$$NO + O_3 \rightarrow NO_2^*(^2B_2) + O_2,$$
$$NO_2^* \rightarrow NO_2 + h\nu,$$

with different rate coefficients and activation energies for each pathway. Recently, however, Adler-Golden[273,274] has shown that the experimental data can be explained in terms of reaction on a single potential surface. Because of the extensive mixing between the $^2B_2$ state and high vibrational levels of the ground ($^2A_1$) state at energies above the origin of the $^2B_2$ state (approximately 10 000 cm^{-1}), a description in terms of Born–Oppenheimer eigenstates is not valid. Energy in the NO_2 product may be emitted as either vibrational (infrared) or electronic (visible to near-infrared) chemiluminescence. Because of the spectral dependence on NO_2 internal energy, the apparent rate coefficient, activation energy, etc., is a function of what portion of the emission is detected in the experiment. The branching ratio, ϕ^*, and activation energy, E_a^*, for the total chemiluminescence have recently been measured by Schurath *et al.*,[275] who obtained $\phi^* = 0.20$ and $E_a^*/R = 1950$ K. According to Adler-Golden,[273,274] these values are preferred to those of earlier studies.

A number of experiments have investigated the effect of initial reactant state on the reaction rate. These are summarized in Table 20. Nearly all of these have made use of the visible chemiluminescence to follow the reaction; only Hui and Cool[219] carried out additional measurements of the vibrational chemiluminescence with an infrared detector. Since nearly all measurements made use of the same red-sensitive photomultiplier (RCA C31034), the results are intercomparable; however, the results given in Table 20 are strictly valid only for that fraction of the reaction yielding NO_2^* that can emit radiation between the short wavelength cutoff of the continuum ($\sim$25 000 cm^{-1}) and the long wavelength cutoff of the photomultiplier tube ($\sim$15 000 cm^{-1}).

A number of these experiments investigated the effect of vibrational excitation in the ozone molecule, using a CO_2 laser to excite the $\nu_3 = 1$ stretching mode of O_3. All the results showed an increase in reaction rate upon excitation.[217,219,220,223,276,277] Since the two stretching modes (ν_1,ν_3) are equilibrated with each other, and partially with the ν_2 bending mode, on the timescale of the reaction, there can be no evidence for mode-specific enhancement.[219,276] Measurements of the enhancement of the infrared chemiluminescence[219] yield the same effective reduction in activation energy as for the visible chemiluminescence,[277] namely, -5.4 kJ/mol. The fact that the effective activation energies for both the visible (electronic) and infrared (vibrational) chemiluminescence are the same is fully consistent with the model of a single reactive potential surface.

Excitation of the NO($v = 1$) level by a CO laser produces a rate enhancement comparable in magnitude to that caused by excitation of the ozone.[278] It may also be noted that vibrational excitation of either O_3 or NO in low-temperature matrices (6–16 K) or cryogenic liquids also enhances the NO_2 formation rate.[279,280] Kenner and Ogryzlo[185] measured spectrally resolved chemiluminescence ascribed to a reaction between NO and vibrationally excited ozone, presumed to have been formed in a bimolecular reaction between O_2^* and O_2 (see Sec. 4.1.b.i.). The peak of the chemiluminescence is shifted to shorter wavelengths by approximately 4000 cm^{-1} ($\sim$50 kJ/mol).

Measurements have also been carried out of the dependence of reaction cross section on relative translational kinetic energy,[281,282] NO and O_3 rotational energy,[281,283] NO spin-orbit state,[283,284] and NO alignment and orientation.[284,285] These measurements were carried out with a supersonic beam of NO, interacting with either an effusive beam or static gas of O_3, using visible chemiluminescence detection. These results are also summarized in Table 20. In general, it appears that translational, rotational, and vibrational energy all contribute to the reaction, but that the cross section is independent of the NO spin-orbit state.

Several classical trajectory studies of the NO + O_3 reaction have appeared.[286,287] These models agree with the experimental finding that there is no mode specificity in the vibrational enhancement of the rate coefficient, but the potential energy surfaces are not sufficiently accurate to permit prediction of many of the details given in Table 20.

Table 20

State-dependent rates for O_3 + NO reaction

NO (initial)	O_3 (initial)	NO_2 (final)	O_2 (final)	Experimental details	Rate data	Reference
	001			invalid analysis, see Ref. 270		217
	001			visible CL, RCA C31034 T = 308 K	$k = (9 \pm 1) \times 10^{-14}/cm^3 s^{-1}$ $\frac{k(001)}{k(thermal)} = 5.4$ relative CL yield = 0.08, no change	276
	001			visible CL T = 298 K	k increases	223
	001			visible CL, RCA C31034 155 K < T < 303 K	$\frac{k(001)}{k(thermal)}$ vs. T $\Delta(E_{act}) = -5.4$ kJ/mol	277
	001			visible CL, "red-sensitive PMT" 158 K < T < 437 K	measured k(total) = k(reaction) + k(deactivation)	220
	(001+100+010)			visible CL, RCA 31034A IRCL, 3.4-4.0 μm 138 K < T < 410 K	T/K — 10^{13} k/cm^3 s^{-1} 400 — 2.13 333 — 1.07 286 — 0.75 250 — 0.64 222 — 0.62 200 — 0.68 182 — 0.74 167 — 0.83 154 — 0.97 143 — 1.13 $\Delta(E_{act}) = -5.4$ kJ/mol for both visible and IR emission	219
	E_{vib} = 9-14 kcal/mole			resolved CL, RCA 4832	emission maximum shifts ~4000 cm^{-1} higher energy	185
v=1				visible CL, RCA C31034	$\frac{k(NO^{\ddagger})}{k(thermal)} = 5.7(^{+2.6}_{-1.4})$	278
v=1				FTIR of products 6 K < T < 16 K (matrix)	$\frac{k(NO^{\ddagger})}{k(dark)} \propto$ (laser power)	279
	vib. exc. (CO_2 laser)			rate enhancement in "liquid cryosystem" (probably thermal)		280

Table 20 (cont'd.)

NO (initial)	O_3 (initial)	NO_2 (final)	O_2 (final)	Experimental details	Rate data	Reference
supersonic beam, 280-380 K	effusive beam, 300,181 K			crossed beam visible CL, RCA C31034	$\sigma_R(E) \propto \left[\frac{E}{9.6\ kJ/mol-1}\right]^{2.05}$	281
"	"			"	$\sigma_R(E_{rot}) \propto (E_{rot})^{1.5\pm0.3}$	268
supersonic beam, v_s = 551 ms^{-1}	effusive beam			crossed beam visible CL, RCA C31034	σ_R vs. E_{transl}	282
Ω = 1/2,3/2	"			"	$\frac{\sigma_R(\Omega=1/2)}{\sigma_R(\Omega=3/2)} \simeq 0.27$ (reinterpreted in 270, 278)	282
supersonic beam Ω = 1/2,3/2	effusive beam			"	$\frac{\sigma_R(\Omega=1/2)}{\sigma_R(\Omega=3/2)} = 0.9 \pm 0.2$	290
"	"			"	$\frac{\sigma_R(O_3+NO)}{\sigma_R(O_3+ON)} = 1.66 \pm 0.05$	290
supersonic beam Ω = 1/2,3/2	static cell, 298 K			"	$\frac{\sigma_R(\Omega=1/2)}{\sigma_R(\Omega=3/2)} \simeq 1$	283
"	"			"	$\sigma_R(E_{rot}) \propto (E_{rot})^{2.0\pm0.5}$	283
supersonic beam M = 3/2,1/2, -1/2,-3/2	static cell, 160 K			"	M: 3/2 → $\sigma_\ell/\bar{\sigma}$ = 1.192±0.009; 1/2 → 0.848±0.015; -1/2 → 1.177±0.015; -3/2 → 0.783±0.009	285
			$a(^1\Delta_g)$	PI-MS	$k(\rightarrow {}^1\Delta) < 0.002 * k(total)$	237, 238
			$a(^1\Delta_g)$	(resolved CL	$k(\rightarrow {}^1\Delta) < 0.003 * k(total)$	239
			$b(^1\Sigma_g)$	770-1240 nm)	$k(\rightarrow {}^1\Sigma) < 0.005 * k(total)$	
supersonic beam E_{COM} = 0.61 eV	supersonic beam			"universal detector" (total NO)	two mechanisms proposed (O_3 + NO, O_3 + ON?)	291

4.1.l. Reaction with Nitrogen Dioxide

$NO_2 + O_3 \rightarrow NO_3 + O_2$, $\Delta H^0 = -105$ kJ/mol.

The recommended rate coefficient[1] between 230 and 360 K,

$1.2\times10^{-13}\exp(-2450/T)$ cm^3 molecule^{-1} s^{-1},

is shown in Fig. 12. The value at 298 K is 3.2×10^{-17}. An additional determination at 296 K gives $(3.45\pm0.12)\times10^{-17}$, in good agreement with the foregoing.[288] Results on decomposition of ozone in the presence of nitrogen oxides are consistent with the recommended value.[289]

4.1.m. Electron and Ion Collision Processes

4.1.m.1. Interaction of Electrons with Ozone

(a) Electron affinity. Lifshitz *et al.*[201] surveyed determinations of $EA(O_3)$ and recommended a value of 2.26(+ 0.04, − 0.06) eV. More recently, Novick *et al.*[153] found a value of 2.103 eV using laser photoelectron, photodetachment, and photodestruction spectroscopy. We have taken a value of $EA = 2.10$ eV $= 202.6$ kJ/mol in this report.

(b) Elastic electron scattering. The only information available on elastic electron scattering is a theoretical calculation by Joshipura.[292] His results are the following:

Electron energy (eV)	Cross section ($cm^2\times10^{16}$)
100	18.5
200	9.8
400	5.1
700	2.8
1000	2.1

(c) Dissociative attachment reactions. The rate coefficient for

$O_3 + e^- \rightarrow O_2 + O^-$ $(\Delta H^0 = -42$kJ/mol$)$[175],

has been variously estimated as $9\times10^{-12}\,(T/300)^{1.5}$ cm^3 molecule^{-1} s^{-1} (Refs. 167 and 196), $(1\text{–}10)\times10^{-10}$ (Refs. 191 and 194), and 3×10^{-12} (Ref. 190). The rate coefficient for

$O_3 + e^- \rightarrow O_2^- + O$

is even less well established; estimates range from 1.3×10^{-30} (Ref. 167) to 3.8×10^{-22} cm^3 molecule^{-1} s^{-1} (Ref. 190). In any case, it seems to be of minor importance as compared with the preceding reaction. The rate for the electron-collision-dissociation of ozone,

$O_3 + e^- \rightarrow O_2 + O + e^-$

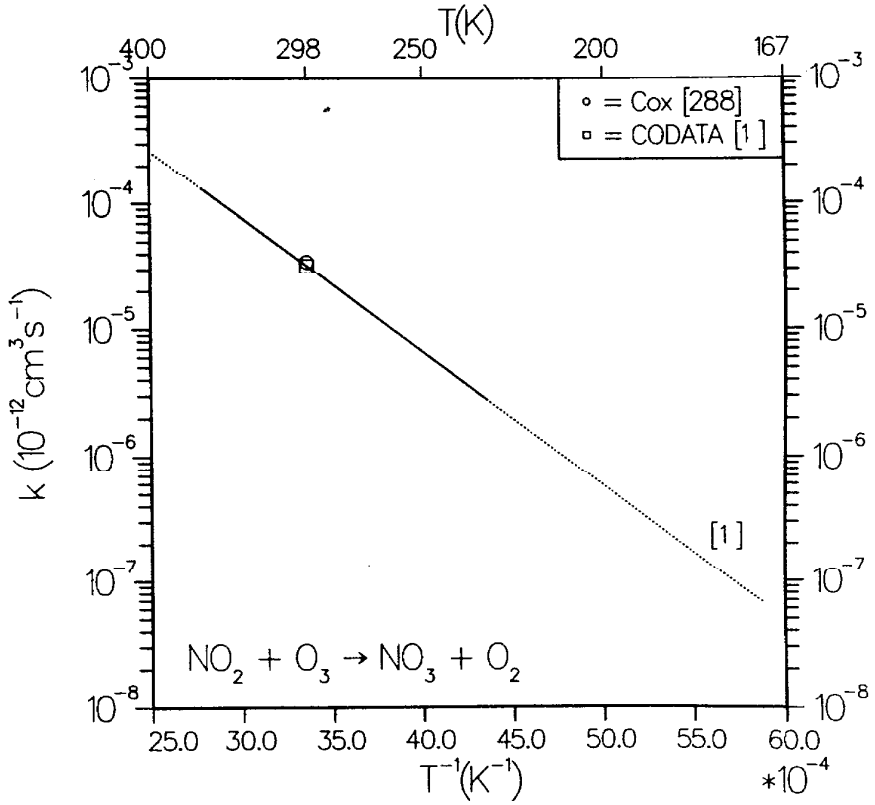

FIG. 12. Bimolecular rate coefficients for $NO_2 + O_3 \rightarrow NO_3 + O_2$.

has been estimated to be five times the corresponding rate for $O_2 + e^- \rightarrow 2O + e^-$[293]; the rate for the latter reaction has been multiplied by 5 to obtain the value for ozone, shown as a function of electron energy in Fig. 13.

(d) Electron attachment reactions. The three-body attachment reaction,

$$O_3 + e^- + M \rightarrow O_3^- + M \qquad (\Delta H^0 = -EA = -202.6 \text{ kJ/mol})$$

is estimated to proceed with a rate coefficient (for $M = O_2$) 4.6×10^{-28} cm^6 molecule^{-2} s^{-1}.[167] The rate coefficient for the radiative attachment process,

$$O_3 + e^- \rightarrow O_3^- + h\nu,$$

is estimated as 1×10^{-17} cm^3 molecule^{-1} s^{-1}.[190]

(e) Ionization processes. The electron impact ionization cross sections for the processes

$$O_3 + e^- \rightarrow O_3^+ + 2e^-$$
$$\rightarrow O_2^+ + O2e^-$$
$$\rightarrow O^+ + O^- + O + e^-$$

(first ionization potential = 12.52 eV, see Sec. 3.2.e) for electron energies in the range 10–100 eV have been reported by Siegel[294] and are shown in Fig. 14.

4.1.m.2. Ion–Molecule Reactions

(a) $O_3^- + O \rightarrow O_2^- + O_2$ $(\Delta H^0 = -241 \text{ kJ/mol})$.

The rate coefficient for this process has been estimated as $k = 1.1\times10^{-11}$ cm^3 molecule^{-1} s^{-1} (Ref. 161) and 2.5×10^{-10} (Ref. 295).

(b) $O_3^- + O \rightarrow O_2 + e^-$ $(\Delta H^0 = -197 \text{ kJ/mol})$,

$k = 1.1\times10^{-13}$ cm^3 molecule^{-1} s^{-1}, Ref. 167.

(c) $O_3^- + N_2 \rightarrow NO_2^- + NO$,

$k = 1.0\times10^{-20}$ cm^3 molecule^{-1} s^{-1} at 300 K,

Ref. 190.

(d) $O_3^- + NO_2 \rightarrow O_3 + NO_2^-$,

(e) $O_3^- + NO_2 \rightarrow O_2 + NO_3^-$

$(\Delta H^0 = -280 \text{ kJ/mol})$.

Rate coefficients for reaction (e) are estimated as 2.8×10^{-10} cm^3 molecule^{-1} s^{-1} at $T = 300$ K[296] and 1.2×10^{-11} cm^3 molecule^{-1} s^{-1} at laboratory ion energy (E_{LAB}) = 0.3 eV.[201] Rate coefficients for both the charge-exchange (d) and particle-transfer processes (e) are given as a function of center-of-mass ion energy (E_{COM}) by Lifshitz *et al.*[201]; the rate coefficient for (e) is about an order of magnitude less than that for (d) over the entire energy range E_{COM} = 0–5 eV (see Fig. 15). Rutherford *et al.*[297] give the charge-exchange cross-section $\sigma(E)$ vs E_{COM} for E_{COM} = 1–200 eV (Fig. 16).

(f) $NO_2^- + O_3 \rightarrow NO_2 + O_3^-$,

(g) $NO_2^- + O_3 \rightarrow O_2 + NO_3^-$

$(\Delta H^0 = -261 \text{ kJ/mol})$.

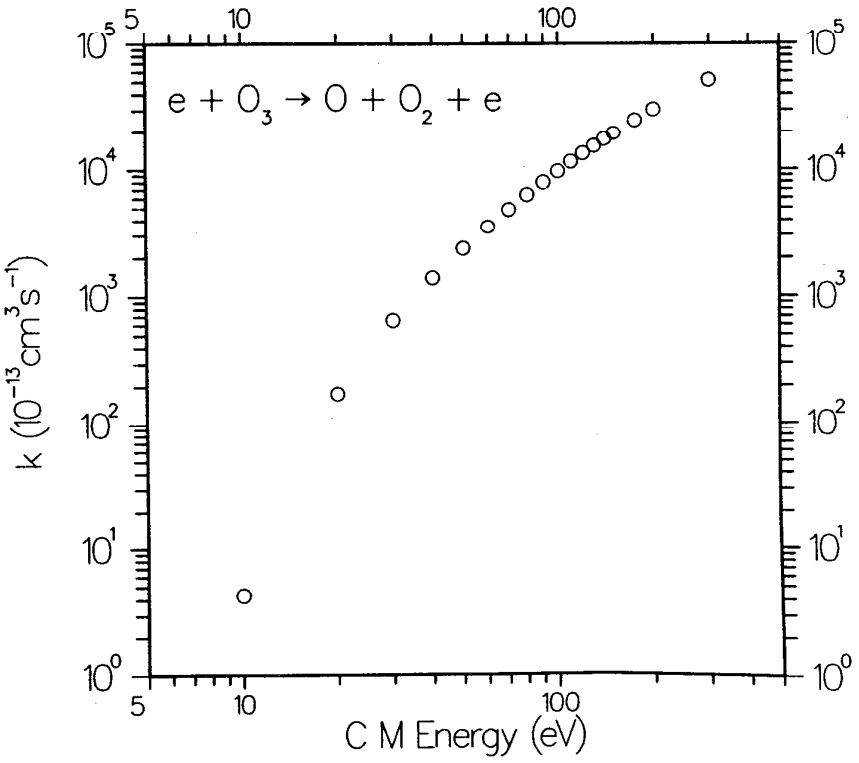

FIG. 13. Rate coefficients for electron-impact dissociation of ozone, estimated as 5×the rate for $e^- + O_2 + 2O + e^-$, Ref. 167.

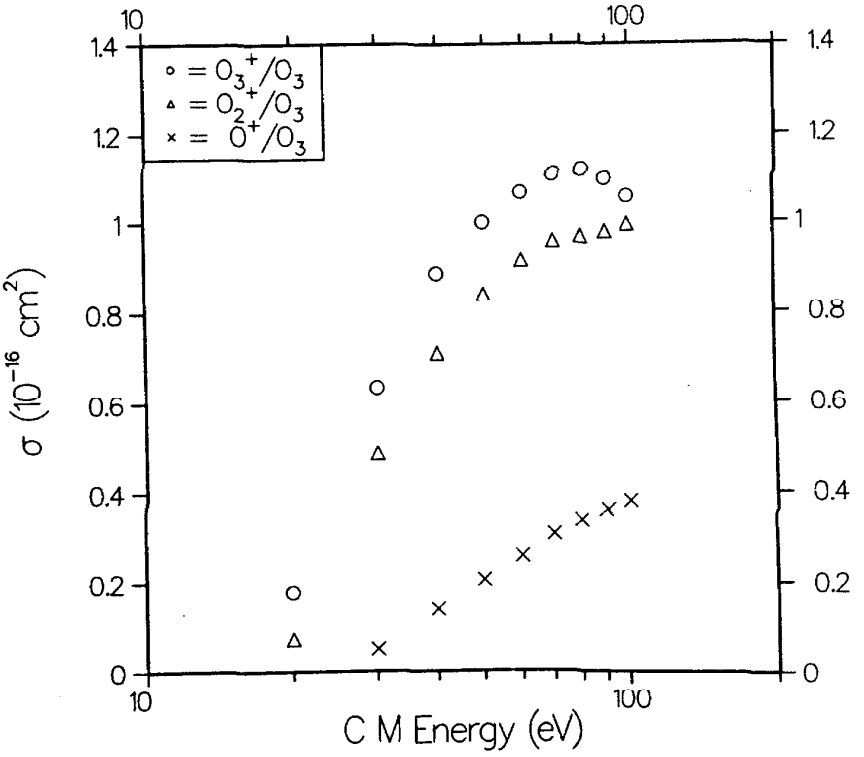

FIG. 14. Electron-impact ionization cross section for ozone, Ref. 294.

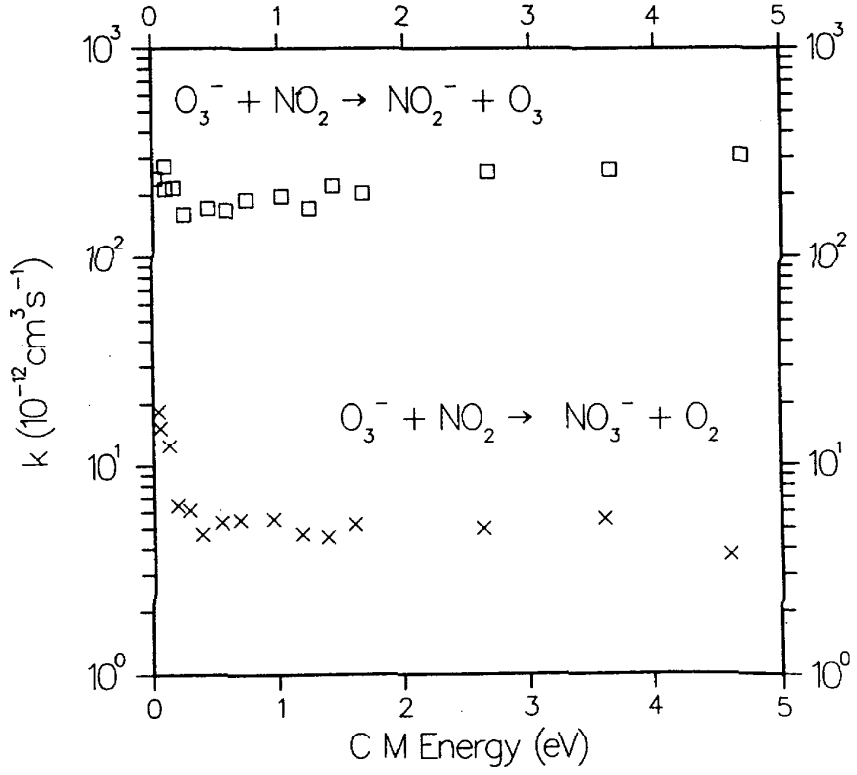

FIG. 15. Charge-transfer and atom-transfer rate for $O_3^- + NO_2$, Ref. 298.

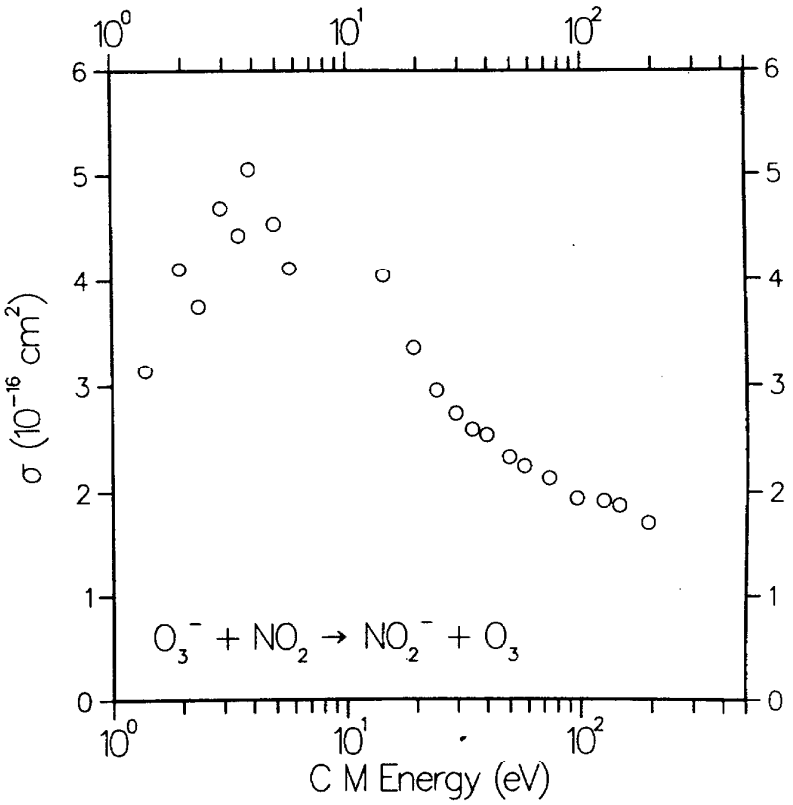

FIG. 16. Charge-transfer cross section for $O_3^- + NO_2$, Ref. 297.

Rate coefficients for reaction (g) are estimated as 9×10^{-11} cm^3 molecule^{-1} s^{-1} at $T = 300$ K (Ref. 295) and 4.4×10^{-12} cm^3 molecule^{-1} s^{-1} at $E_{LAB} = 0.3$ eV.[201] Cross sections for all four processes (d–g) vs laboratory ion energy (0–12 eV) have been given by Lifshitz *et al.*[201]

(h) $O^- + O_3 \rightarrow O_3^- + O$ ($\Delta H^0 = -59$ kJ/mol).

The rate coefficient for the charge-exchange process has been estimated as $(2\pm0.4)\times10^{-10}$ cm^3 molecule^{-1} s^{-1} at $E_{LAB} = 0.3$ eV,[201,298] 5.5×10^{-10} at $T = 300$ K.[167,190,191] Rutherford *et al.*[297] give the charge-exchange cross-section $\sigma(E)$ vs $E_{COM} = 0.03$–300 eV (Fig. 17).

(i) $O^- + O_3 \rightarrow O_2 + e^-$ ($\Delta H^0 = -255$ kJ/mol),

$k = (3\pm1)\times10^{-10}$ cm^3 molecule^{-1} s^{-1}

at $E_{LAB} = 0.3$ eV, Ref. 298.

(j) $O^- + O_3 \rightarrow O_2^- + O_2$ ($\Delta H^0 = -297$ kJ/mol),

$k = (0.1\pm0.05)\times10^{-10}$ cm^3 molecule^{-1} s^{-1}

at $E_{LAB} = 0.3$ eV, Ref. 298.

(k) $O_2^- + O_3 \rightarrow O_3^- + O_2$ ($\Delta H^0 = -155$ kJ/mol).

The rate coefficient for the charge-exchange process has been estimated as 3.2×10^{-10} (Refs. 191 and 299), 4×10^{-10} (Ref. 190), 6×10^{-10} cm^3 molecule^{-1} s^{-1} at 300 K.[295] Rutherford *et al.*[297] give the charge-exchange cross-section $\sigma(E)$ vs E_{COM} for $E_{COM} = 0.3$–300 eV (Fig. 18).

(l) $OH^- + O_3 \rightarrow O_2 + HO_2 + e^-$

($\Delta H^0 = +15.5$ kJ/mol),

$k < 10^{-12}$ cm^3 molecule^{-1} s^{-1}

at $E_{LAB} = 0.3$ eV, Ref. 298.

(m) $OH^- + O_3 \rightarrow OH + O_3^-$

($\Delta H^0 = -15.1$ kJ/mol),

$k = (5\pm0.2)\times10^{-10}$ cm^3 molecule^{-1} s^{-1}

at $E_{LAB} = 0.3$ eV, Ref. 298.

Also $\sigma(E)$ vs E_{COM} for $E_{COM} = 0.03$–300 eV[297] (Fig. 19).

(n) $OH^- + O_3 \rightarrow HO_2^- + O_2$,

$k = (0.3\pm0.1)\times10^{-10}$ cm^3 molecule^{-1} s^{-1}

at $E_{LAB} = 0.3$ eV, Ref. 298.

(o) $OH^- + O_3 \rightarrow O_2^- + HO_2$

($\Delta H^0 = -27.2$ kJ/mol),

$k = (0.1\pm0.05)\times10^{-10}$ cm^3 molecule^{-1} s^{-1}

at $E_{LAB} = 0.3$ eV, Ref. 298.

4.2 Miscellaneous Topics

4.2.a. IR Multiphoton Excitation

Resonant absorption of CO_2 laser photons by the ν_3 stretching mode of ozone has been used to produce vibrationally excited ozone for energy-transfer studies (see Sec.

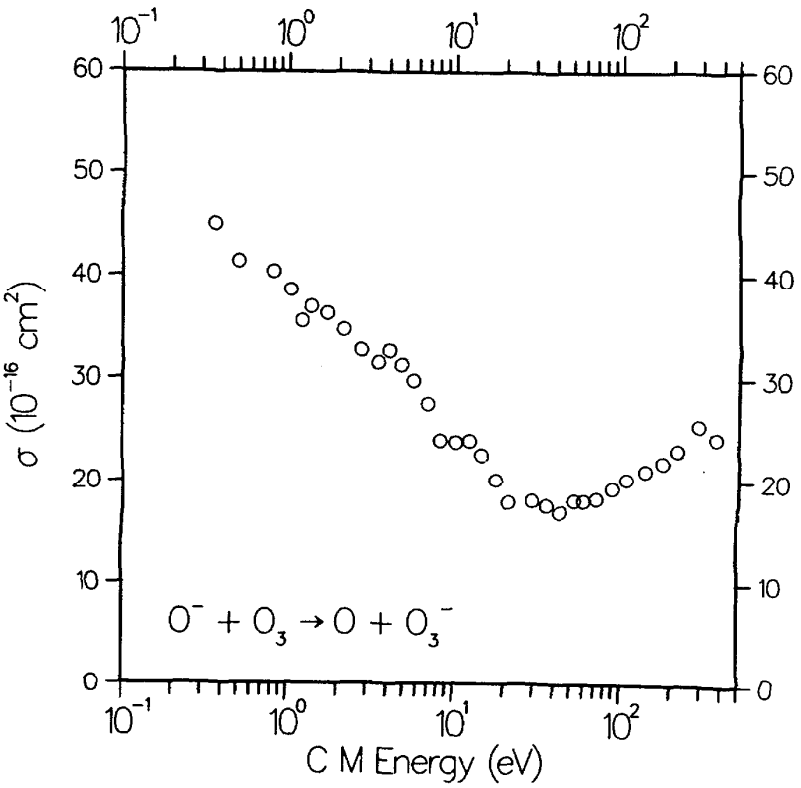

FIG. 17. Charge-transfer cross section for $O^- + O_3$, Ref. 297.

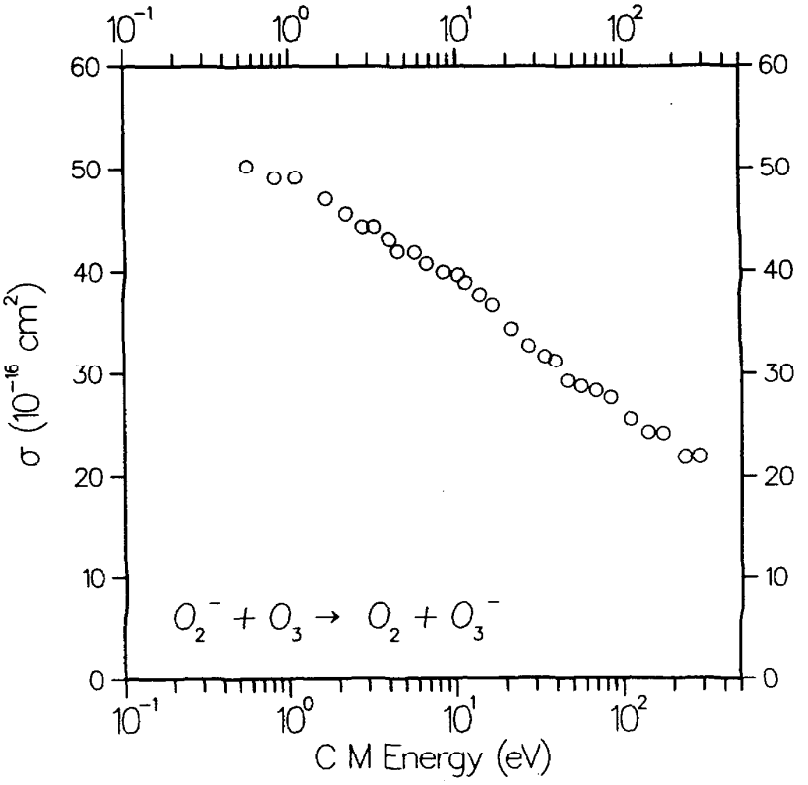

FIG. 18. Charge-transfer cross section for $O_2^- + O_3$, Ref. 297.

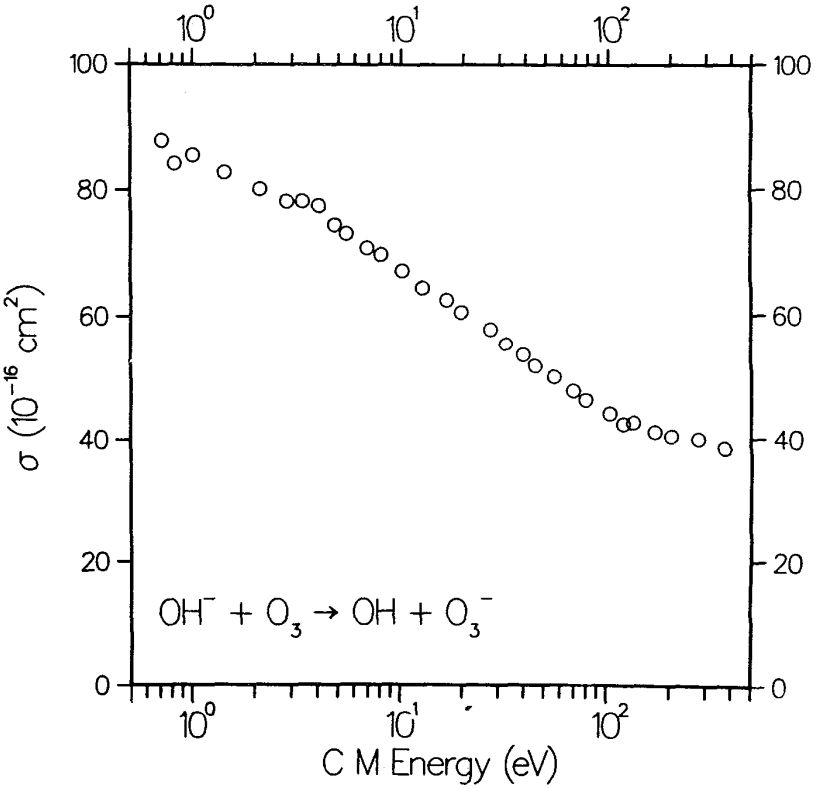

FIG. 19. Charge-transfer cross section for $OH^- + O_3$, Ref. 297.

4.1.c). In 1979, Proch and Schroder[300] reported the IR multiphoton decomposition of ozone, based on the observed decrease in ultraviolet absorbance following the CO_2 laser pulse (intensity $\sim 6\times 10^8$ W/cm^2). The decrease was not immediate, implying that dissociation of excited ozone involves collisions. Another complicating factor in this experiment is the change in Hartley band extinction coefficients as a result of vibrational excitation.[130] More recently, thermal decomposition of ozone and O_3/O_2 mixtures has been initiated by absorption of CO_2 laser energy.[301,302]

In studies of the vibrational state dependence of Hartley band absorption, Adler-Golden *et al.*[130] found no evidence of CO_2-laser excitation much beyond the $v_3 = 1$ level at moderate IR fluences (~ 1 MW/cm^2). The same result was obtained in CARS measurements on laser-pumped ozone.[102] However, Chugunov *et al.*[303] found evidence of two-photon processes at intensities of $\sim 10^9$ W/cm^2. Quack and Sutcliffe[304–306] analyzed the interaction of ozone with CO_2 laser radiation theoretically; they determined that collision-free multiphoton excitation should occur only at laser intensities above 40–100 GW/cm^2.

Another interesting recent observation[307] is that the Hartley band absorption can be saturated at the KrF laser wavelength (248 nm). The saturation fluence is approximately 0.1–0.5 J/cm^2, and is independent of buffer gas pressure.

4.2.b. Vapor Pressure Measurements

Hansen and Mauersberger[308,309] determined the vapor pressure of ozone by direct measurement over its condensed phases. Above the liquid [$T = 85$ to 95 K; $P(O_3) = 0.02$ to 0.25 Torr] the Clausius–Clapeyron equation for the vapor pressure derived from the data is

$$\log_{10}(P/\text{Torr}) = 8.544 \pm 0.013 - (867.6 \pm 1.2)/T.$$

Over the crystalline solid ($T = 66$ to 87 K) the equation is

$$\log_{10}(P/\text{Torr}) = 10.460 - 1021.6/T$$

with an estimated precision of $\pm 1\%$. Limited extrapolations of the first equation above 95 K, and of the second equation below 66 K, should be practicable.

5. Recommendations and Conclusions

While many of the reactions of mesospheric and thermospheric ozone are well characterized, additional information is still required regarding state-specific reaction rate coefficients. In particular, the following data should be obtained:

(1) The formation of metastable ($^3B_2$) ozone in three-body recombination should be further investigated; the spectroscopy and reactivity of this state need to be characterized.

(2) Additional data on vibrational deactivation pro-

cesses are required, particularly on state-to-state V–V and V–T rate coefficients for $(v_1,v_3) > 1$ and on the temperature coefficients for atmospheric deactivation by species such as O_2 and N_2.

(3) Rates for additional ozone formation channels, particularly reaction of excited-state neutrals and ion–molecule processes, need to be determined more accurately.

(4) Rate coefficients for many reactions should be measured in the temperature range 180–250 K, characteristic of the thermosphere.

(5) For the reaction of $O(^3P)$ with vibrationally excited ozone, absolute rate coefficients need to be determined as a function of ozone vibrational state, along with their temperature dependence. The branching ratio between reactions to form two oxygen molecules, relative to vibrational deactivation of the ozone, needs to be determined.

(6) The problem of the OH vibrational state distribution in the reaction $H + O_3 \rightarrow OH(v) + O_2$ should be reinvestigated, as well as the v-state dependence of the reaction of $OH(v) + O_3 \rightarrow$ products.

(7) Rate and/or cross-section measurements should be undertaken for electron and ion collision processes involving ozone. Most of the values appearing in the literature appear to be simply cited from other data surveys and estimates.

(6) Estimates should be made of the relative contributions to overall atmospheric rates of the new and/or revised reactions and rate coefficients discussed in this report, using existing or modified atmospheric modeling codes.

An alphabetical listing of references is available in JILA Data Center Report No. 31.

6. Acknowledgments

The preparation of this survey was supported by the Air Force Geophysics Laboratory, Work Order GLH6-6016. We would like to thank Dr. R. Armstrong (Mission Research Corp.), Dr. W. Blumberg (AFGL), and Dr. J. Winnick (AFGL) for helpful discussions; Dr. A. Phelps (JILA) for providing references on ion and electron processes; Dr. G. Anderson (AFGL), Dr. S. M. Anderson (Aerodyne Research Inc.), Dr. W. T. Rawlins (Physical Sciences Inc.), Dr. E. E. Ferguson (Université de Paris-Sud, Orsay), and the referees for providing comments on previous drafts and P. Krog (JILA) for doing everything.

References

[1]D. L. Baulch, R. A. Cox, R.F. Hampson, Jr., J. A. Kerr, J. Troe, and R. T. Watson, J. Phys. Chem. Ref. Data **9**, 295 (1980).
[2]D. L. Baulch, R. A. Cox, P. J. Crutzen, R. F. Hampson, Jr., J. A. Kerr, J. Troe, and R. T. Watson, J. Phys. Chem. Ref. Data **11**, 327 (1982).
[3]D. L. Baulch, R. A. Cox, R. F. Hampson, Jr., J. A. Kerr, J. Troe, and R. T Watson, J. Phys. Chem. Ref. Data **13**, 1259 (1984).
[4]R. T. Watson (editor), World Meteorological Organization Report No. 16, Global Ozone Research and Monitoring Project, Geneva, 1985.
[5]W. B. DeMore, J. J. Margitan, M. J. Molina, R. T. Watson, D. M. Golden, R. F. Hampson, M. J. Kurylo, C. J. Howard, and A. R. Ravishankara, JPL Publication No. 85-37, Jet Propulsion Laboratory, California Institute of Technology, Pasadena, CA, 1985.
[6]A. T. Stair, Jr., J. C. Ulwick, D. J. Baker, C. L. Wyatt, and K. C. Baker, Geophys. Res. Lett. **1**, 117 (1974).
[7]A.T. Stair, Jr., J. C. Ulwick, K. D. Baker, and J. D. Baker, in *Atmospheres of the Earth and the Planets*, edited by B. M. McCormack (D. Reidel, Dordrecht, Holland, 1975), pp. 335–346.
[8]W. T. Rawlins, G. E. Caledonia, and J. P. Kennealy, J. Geophys. Res. **86**, 5247 (1981).
[9]W. T. Rawlins and R. A. Armstrong, J. Chem. Phys. **87**, 5202 (1987).
[10]W. T. Rawlins, G. E. Caledonia, and R. A. Armstrong, J. Chem. Phys. **87**, 5209 (1987).
[11]J. I. Steinfeld, J. Phys. Chem. Ref. Data **13**, 445 (1984).
[12]A. Barbe, C. Secroun, and P. Jouve, J. Mol. Spectrosc. **49**, 171 (1974).
[13]V. M. Devi, S. P. Reddy, K. N. Rao, J.-M. Flaud, and C. Camy-Peyret, J. Mol. Spectrosc. **77**, 156 (1979).
[14]S. M. Adler-Golden and R. A. Armstrong, Report AFGL-TR-82-0231, Optical Physics Division, Air Force Geophysics Laboratory, Hanscom AFB, Massachusetts, Environmental Research Paper No. 788, 1982.
[15]E. Damon, R. L. Hawkins, and J. H. Shaw, Report RF Project 761420/711626, Interim Technical Report, The Ohio State University Research Foundation, Columbus, OH, Grant No. NSG-7479, 1981.
[16]D. G. Imre, J. L. Kinsey, R. W. Field, and D. H. Katayama, J. Phys. Chem. **86**, 2564 (1982).
[17]I. Benjamin, R. D. Levine, and J. L. Kinsey, J. Phys. Chem. **87**, 727 (1983).
[18]I. Benjamin and R. D. Levine, J. Phys. Chem. **88**, 1047 (1984).
[19]K. K. Lehmann, J. Phys. Chem. **88**, 1047 (1984).
[20]D. G. Imre, "Reaction Dynamics Studied by Photoemission Spectroscopy," Ph.D. thesis, Massachusetts Institute of Technology, 1984.
[21]A. D. Bykov, Yu. S. Makushkin, and O. N. Ulenikov, [Opt. Spektrosk. **54**, 100 (1983)]; Opt. Spectrosc. (USSR) **54**, 57 (1893).
[22]A. D. Bykov, Yu. S. Makushkin, and O. N. Ulenikov, J. Mol. Spectrosc. **93**, 46 (1982).
[23]D. J. McCaa and J. H. Shaw, J. Mol. Spectrosc. **25**, 374 (1968).
[24]J.-M. Flaud, C. Camy-Peyret, and L. S. Rothman, Appl. Opt. **19**, 655 (1980).
[25]S. A. Clough and F. X. Kneizys, J. Chem. Phys. **44**, 1855 (1966).
[26]H. M. Pickett, E. A. Cohen, and J. S. Margolis, J. Mol. Spectrosc. **110**, 186 (1985).
[27]S. M. Adler-Golden, S. R. Langhoff, C. W. Bauschlicher, Jr., and G. D. Carney, J. Chem. Phys. **83**, 255 (1985).
[28]A. Goldman, J. R. Gillis, D. G. Murcray, A. Barbe, and C. Secroun, J. Mol. Spectrosc. **96**, 279 (1982).
[29]K. M. Mack and J. S. Muenter, J. Chem. Phys. **66**, 5278 (1977).
[30]W. L. Meerts, S. Stolte, and A. Dymanus, Chem. Phys. **19**, 467 (1977).
[31]G. D. Carney, S. Giorgianni, and K. N. Rao, J. Mol. Spectrosc. **80**, 158 (1980).
[32]O. K. Voitsekhovskaya, Yu. S. Makushkin, and O. N. Sulakshina, [Izv. Vyssh. Uchebn. Zaved. Fiz. **9**, 103 (1983)]; Sov. Phys. J. **26**, 866 (1983).
[33]R. R. Gamache, J. Mol. Spectrosc. **114**, 31 (1985).
[34]R. R. Gamache and R. W. Davies, J. Mol. Spectrosc. **109**, 283 (1985).
[35]R. R. Gamache and L. S. Rothman, Appl. Opt. **24**, 1651 (1985).
[36]J.-M. Flaud, C. Camy-Peyret, V. M. Devi, C. P. Rinsland, and M. A. H. Smith, J. Mol. Spectrosc. **118**, 334 (1986).
[37]C. Camy-Peyret, J.-M. Flaud, A. Perrin, V. M. Devi, C. P. Rinsland, and M. A. H. Smith, J. Mol. Spectrosc. **118**, 345 (1986).
[38]F. J. Lovas, J. Phys. Chem. Ref. Data 7, 1445 (1978).
[39]P. Hennig and G. Strey, Z. Naturforsch. Teil A **31**, 244 (1976).
[40]S. Carter, I. M. Mills, J. N. Murrell, and A. J. C. Varandas, Mol. Phys. **45**, 1053 (1982).
[41]A. J. C. Varandas and J. N. Murrell, Chem. Phys. Lett. **88**, 1 (1982).
[42]G. D. Carney, L. A. Curtiss, and S. R. Langhoff, J. Mol. Spectrosc. **61**, 371 (1976).
[43]A. Barbe, C. Secroun, P. Jouve, A. Goldman, and D. G. Murcray, J. Mol. Spectrosc. **86**, 286 (1981).
[44]A. Barbe, C. Secroun, P. Jouve, C. Camy-Peyret, and J. M. Flaud, J. Mol. Spectrosc. **75**, 103 (1979).
[45]J.-M. Flaud, C. Camy-Peyret, A. Barbe, C. Secroun, and P. Jouve, J. Mol. Spectrosc. **80**, 185 (1980).
[46]A. Barbe, C. Secroun, A. Goldman, and J. R. Gillis, J. Mol. Spectrosc. **100**, 377 (1983).
[47]C. P. Rinsland, V. M. Devi, J.-M. Flaud, C. Camy-Peyret, M. A. H. Smith, and G. M. Stokes, J. Geophys. Res. **90**, 10719 (1985).
[48]N. Monnanteuil, J. C. Depannemaecker, J. Bellet, A. Barbe, C. Secroun, P. Jouve, S. Giorgianni, Y.-S. Hoh, and K. N. Rao, J. Mol. Spectrosc. **71**, 399 (1978).
[49]M. Carlotti, G. Di Lonardo, L. Fusina, A. Trombetti, A. Bonetti, B. Carli, and F. Mencaraglia, J. Mol. Spectrosc. **107**, 84 (1984).
[50]C. Secroun, A. Barbe, P. Jouve, P. Arcas, and E. Arie, J. Mol. Spectrosc. **85**, 8 (1981).

[51]F. L. Bartman, W. R. Kuhn, and L. T. Loh, J. Opt. Soc. Am. **66**, 860 (1976).
[52]B. J. Connor and H. E. Radford, J. Mol. Spectrosc. **117**, 15 (1986).
[53]N. Monnanteuil and J. M. Colmont, J. Quant. Spectrosc. Radiat. Transfer **29**, 131 (1983).
[54]J. M. Colmont and N. Monnanteuil, J. Mol. Spectrosc. **104**, 122 (1984).
[55]J. S. Margolis, J. Quant. Spectrosc. Radiat. Transfer **29**, 539 (1983).
[56]A. Barbe, P. Marche, C. Meunier, and P. Jouve, J. Phys. (Paris). **44**, 1015 (1983).
[57]C. Meunier, P. Marche, and A. Barbe, J. Mol. Spectrosc. **95**, 271 (1982).
[58]S. Lundqvist, J. Margolis, and J. Reid, Appl. Opt. **21**, 3109 (1982).
[59]J. M. Hoell, C. N. Harward, C. H. Bair, and B. S. Williams, SPIE **288**, 376 (1981).
[60]J. M. Hoell, C. N. Harward, C. H. Bair, and B. S. Williams, Opt. Eng. **21**, 548 (1982).
[61]L. S. Rothman, R. R. Gamache, A. Barbe, A. Goldman, J. R. Gillis, L. R. Brown, R. A. Toth, J.-M. Flaud, and C. Camy-Peyret, Appl. Opt. **22**, 2247 (1983).
[62]L. S. Rothman, A. Goldman, J. R. Gillis, R. R. Gamache, H. M. Pickett, R. L. Poynter, N. Husson, and A. Chedin, Appl. Opt. **22**, 1616 (1983).
[63]R. L. Poynter and H. M. Pickett, JPL Publication 80-23, Rev. 2, NASA-CR-173899, 1984.
[64]N. Husson, *et al.*, Ann. Geophys., Ser. A **4**, 185 (1986).
[65]T. Kostiuk, J. J. Hillman, and J. L. Faris, J. Mol. Spectrosc. **89**, 397 (1981).
[66]J. M. Hoell, Jr., C. N. Harward, and W. Lo, Opt. Eng. **21**, 320 (1982).
[67]M. El-Sherbiny, E. A. Ballik, J. Shewchun, B. K. Garside, and J. Reid, Appl. Opt. **18**, 1198 (1979).
[68]A. Barbe, C. Secroun, P. Jouve, N. Monnanteuil, J. C. Depannemaecker, B. Duterage, J. Bellet, and P. Pinson, J. Mol. Spectrosc. **64**, 343 (1977).
[69]C. Chiu and E. A. Cohen, J. Mol. Spectrosc. **109**, 239 (1985).
[70]E. A. Cohen and H. M. Pickett, J. Mol. Struct. **97**, 97 (1983).
[71]J.-C. Depannemaecker and J. Bellet, J. Mol. Spectrosc. **66**, 106 (1977); **70**, 484 (1978).
[72]M. J. C. Depannemaecker, B. Duterage, and M. J. Bellet, J. Quant. Spectrosc. Radiat. Transfer **17**, 519 (1977).
[73]K.-H. Thunemann, S. D. Peyerimhoff, R. J. Buenker, J. Mol. Spectrosc. **70**, 432 (1978).
[74]P. J. Hay and T. H. Dunning, Jr., J. Chem. Phys. **67**, 2290 (1977).
[75]C. W. Wilson, Jr. and D. G. Hopper, J. Chem. Phys. **74**, 595 (1981).
[76]A. Sinha, D. Imre, J. H. Goble, Jr., and J. L. Kinsey, J. Chem. Phys. **84**, 6108 (1986).
[77]D. H. Katayama, J. Chem. Phys. **71**, 815 (1979).
[78]P. J. Hay, R. T. Pack, R. B. Walker, and E. J. Heller, J. Phys. Chem. **86**, 862 (1982).
[79]M. G. Sheppard and R. B. Walker, J. Chem. Phys. **78**, 7191 (1983).
[80]N. Swanson and R. J. Celotta, Phys. Rev. Lett. **35**, 783 (1975).
[81]R. J. Celotta, N. Swanson, M. Kurepa, in *ICPEAC X: Abstracts of Papers of the Xth International Conference on the Physics of Electronic and Atomic Collisions* (Paris, France, 21–27 July 1977), edited by G. Watel (Commissariat a l'Energie Atomique, Paris, 1977), Vol. 2, pp. 656–657.
[82]R. O. Jones, J. Chem. Phys. **82**, 325 (1985).
[83]P. G. Burton, J. Chem. Phys. **71**, 961 (1979).
[84]O. R. Wulf, Proc. Natl. Acad. Sci. **16**, 507 (1930).
[85]M. Griggs, J. Chem. Phys. **49**, 857 (1968).
[86]P. J. Hay and W. A. Goddard III, Chem. Phys. Lett. **14**, 46 (1972).
[87]E. C. Y. Inn and Y. Tanaka, J. Opt. Soc. Am. **43**, 870 (1953).
[88]E. C. Y. Inn and Y. Tanaka, Adv. Chem. Ser. **21**, 263 (1959).
[89]E. Vigroux, Ann. Phys. (Paris) **8**, 709 (1953).
[90]A. G. Hearn, Proc. Phys. Soc. London **78**, 932 (1961).
[91]G. E. Shaw, J. Appl. Meteorol. **18**, 1335 (1979).
[92]A. Vassy and E Vassy, J. Chem. Phys. **16**, 1163 (1948).
[93]E. Castellano and H. I. Schumacher, Z. Phys. Chem. **34**, 198 (1962).
[94]S. N. Tkachenko, V. E. Zhuravlev, M. P. Popovich, Yu. N. Zhitnev, and Yu. V. Filippov, [Zh. Fiz. Khim. **54**, 2289 (1980)]; Russ. J. Phys. Chem. **54**, 1304 (1980).
[95]W. D. McGrath, J. M. Maguire, A. Thompson, and J. Trocha-Grimshaw, Chem. Phys. Lett. **102**, 59 (1983).
[96]W. D. McGrath, A. Thompson, J. Trocha-Grimshaw, Planet. Space Sci. **34**, 1147 (1986).
[97]J. J. Valentini, D. S. Moore, and D. S. Bomse, Chem. Phys. Lett. **83**, 217 (1981).
[98]D. S. Moore, D. S. Bomse, and J. J. Valentini, J. Chem. Phys. **79**, 1745 (1983).
[99]C. E. Fairchild, E. J. Stone, and G. M. Lawrence, J. Chem. Phys. **69**, 3632 (1978).
[100]H. Selig and H. H. Claassen, Isr. J. Chem. **6**, 499 (1968).
[101]J. A. Cooney, Opt. Eng. **22**, 292 (1983).
[102]E. L. Schweitzer and J. I. Steinfeld, Chem. Phys. **108**, 343 (1986).
[103]D. H. Katayama, J. Chem. Phys. **85**, 6809 (1986).
[104]J. C. D. Brand, K. J. Cross, and A. R. Hoy, Can. J. Phys. **56**, 327 (1978).
[105]J. W. Simons, R. J. Paur, H. A. Webster III, and E. J. Bair, J. Chem. Phys. **59**, 1203 (1973).
[106]S. M. Adler-Golden (unpublished data).
[107]S. M. Adler-Golden, J. Quant. Spectrosc. Radiat. Transfer **30**, 175 (1983).
[108]O. Atabek, M. T. Bourgeois, and M. Jacon, J. Chem. Phys. **84**, 6699 (1986).
[109]A. Devaquet and J. Ryan, Chem. Phys. Lett. **22**, 269 (1973).
[110]A. M. Bass and R. J. Paur, in *Proceedings of the Quadrennial International Ozone Symposium*, edited by J. London (NCAR, Boulder, CO, 1981), Vol. 1, pp. 140–145.
[111]A. M. Bass and R. J. Paur, in *Atmospheric Ozone, Proceedings of the Quadrennial Ozone Symposium* (Halkidiki, Greece, 3–7 September 1984), edited by C. S. Zerefos and A. Ghazi (D. Reidel, Dordrecht, Holland, 1985), pp. 606–610.
[112]R. J. Paur and A. M. Bass, in Ref. 111, pp. 611–616.
[113]K. Mauersberger, J. Barnes, D. Hanson, and J. Morton, Geophys. Res. Lett. **13**, 671 (1986).
[114]L. T. Molina and M. J. Molina, J. Geophys. Res. **91**, 14 501 (1986).
[115]D. E. Freeman, K. Yoshino, J. R. Esmond, and W. H. Parkinson, Planet. Space Sci. **32**, 239 (1984).
[116]J. Brion, D. Daumont, and J. Malicet, J. Phys. (Paris) Lett. **45**, L57 (1984).
[117]J. Brion, D. Daumont, J. Malicet, and P. Marche, J. Phys. (Paris) Lett. **46**, L105 (1985).
[118]D. E. Freeman, K. Yoshino, J. R. Esmond, and W. H. Parkinson, in Ref. 111, pp. 622–624.
[119]G. K. Moortgat, in FAA Technical Report FAA-EE-80-20, Federal Aviation Administration, Office of Environment and Energy, Washington, DC, Proceedings of the NATO Advanced Study Institute on Atmospheric Ozone, AD A088889, pp. 599–645, 1980.
[120]S. T. Amimoto, A. P. Force, J. R. Wiesenfeld, and R. H. Young, J. Chem. Phys. **73**, 1244 (1980).
[121]P. H. Wine and A. R. Ravishankara, Chem. Phys. **69**, 365 (1982).
[122]G. D. Greenblatt and J. R. Wiesenfeld, J. Chem. Phys. **78**, 4924 (1983).
[123]C. Cobos, E. Castellano, and H. J. Schumacher, J. Photochem. **21**, 291 (1983).
[124]J. C. Brock and R. T. Watson, Chem. Phys. Lett. **71**, 371 (1980).
[125]J. E. Davenport, FAA Technical Report EE-80-44-REV, Federal Aviation Administration, Office of Environment and Energy, Washington, DC, AD A117 502, 1982.
[126]J. C. Brock and R. T. Watson, Chem. Phys. **46**, 477 (1980).
[127]G. K. Moortgat and P. Warneck, Z. Naturforsch. Teil A **30**, 835 (1975).
[128]I. Arnold, F. J. Comes, and G. K. Moortgat, Chem. Phys. **24**, 211 (1977).
[129]G. K. Moortgat, E. Kudszus, and P. Warneck, J. Chem. Soc. Faraday Trans. 2 **73**, 1216 (1977).
[130]S. M. Adler-Golden, E. L. Schweitzer, and J. I. Steinfeld, J. Chem. Phys. **76**, 2201 (1982).
[131]R. D. Hudson. in Ref. 110. pp. 146–152.
[132]D. Martin, J. Girman, and H. S. Johnston, in "Proceedings of the 167th ACS National Meeting," Los Angeles, CA, 1974.
[133]J. R. Wiesenfeld (private communication).
[134]P. F. Zittel and D. D. Little, J. Chem. Phys. **72**, 5900 (1980).
[135]C.-L. Lin and W. B. DeMore, J. Photochem. **2**, 161 (1973).
[136]G. K. Moortgat and E. Kudszus, Geophys. Res. Lett. **5**, 191 (1978).
[137]P. W. Fairchild and E. K. C. Lee, Chem. Phys. Lett. **60**, 36 (1978).
[138]R. K. Sparks, L. R. Carlson, K. Shobatake, M. L. Kowalczyk, and Y. T. Lee, J. Chem. Phys. **72**, 1401 (1980).
[139]J. J. Valentini, Chem. Phys. Lett. **96**, 395 (1983).
[140]J. J. Valentini, D. P. Gerrity, D. L. Phillips, J.-C. Nieh, and K. T. Tabor, J. Chem. Phys. **86**, 6745 (1987).
[141]Y. Tanaka, E. C. Y. Inn, and K. Watanabe, J. Chem. Phys. **21**, 1651 (1953).
[142]M. Ogawa and G. R. Cook, J. Chem. Phys. **28**, 173 (1958).
[143]M. R. Taherian and T. G. Slanger, J. Chem. Phys. **83**, 6246 (1985).
[144]C. R. Brundle, Chem. Phys. Lett. **26**, 25 (1974).

[145]J. M. Dyke, L. Golob, N. Jonathan, A. Morris, and M. Okuda, J. Chem. Soc. Faraday Trans. 2 **70**, 1828 (1974).
[146]D. C. Frost, S. T. Lee, and C. A. McDowell, Chem. Phys. Lett. **24**, 149 (1974).
[147]M. J. Weiss, J. Berkowitz, and E. H. Appelman, J. Chem. Phys. **66**, 2049 (1977).
[148]J. T. Moseley, J.-B. Ozenne, and P. C. Cosby, J. Chem. Phys. **74**, 337 (1981).
[149]S. Katsumata, H. Shiromaru, and T. Kimura, Bull. Chem. Soc. Jpn. **57**, 1784 (1984).
[150]D. R. Stull and H. Prophet, *et al.*, NSRDS-NBS 37, Office of Standard Reference Data, National Bureau of Standards, Washington, DC, Contract No. F04611-67-C-0009 (1971).
[151]J. F. Hiller and M. L. Vestal, J. Chem. Phys. **77**, 1248 (1982).
[152]J. F. Hiller and M. L. Vestal, J. Chem. Phys. **74**, 6096 (1981).
[153]S. E. Novick, P. C. Engleking, P. L. Jones, J. H. Futrell, and W.C. Lineberger, J. Chem. Phys. **70**, 2652 (1979).
[154]R. R. Lucchese and H. F. Schaefer III, J. Chem. Phys. **67**, 848 (1977).
[155]J. S. Wright, S. Shih, and R. J. Buenker, Chem. Phys. Lett. **75**, 513 (1980).
[156]C. W. Von Rosenberg, Jr. and D.W. Trainor, J. Chem. Phys. **61**, 2442 (1974).
[157]C. J. Hochanadel, J. A. Ghormley, and J. W. Boyle, J. Chem. Phys. **48**, 2416 (1968).
[158]J. F. Riley and R. W. Cahill, J. Chem. Phys. **52**, 3297 (1970).
[159]T. Kleindienst, J. B. Burkholder, and E. J. Bair, Chem. Phys. Lett. **70**, 117 (1980).
[160]J. A. Joens, J. B. Burkholder, and E. J. Bair, J. Chem. Phys. **76**, 5902 (1982).
[161]I. C. McDade and W. D. McGrath, Chem. Phys. Lett. **73**, 413 (1980).
[162]D. C. Astholz, A. E. Croce, and J. Troe, J. Phys. Chem. **86**, 696 (1982).
[163]J. A. Joens and E. J. Bair, J. Chem. Phys. **79**, 5780 (1983).
[164]V. D. Baiamonte, L. G. Hartshorn, and E. J. Bair, J. Chem. Phys. **55**, 3617 (1971).
[165]C. L. Lin and M. T. Leu, in "Abstracts of the 14th Informal Photochemistry Conference," 1980.
[166]S. W. Benson and A. E. Axworthy, Jr., Adv. Chem. Ser. **21**, 398 (1959).
[167]B. Eliasson, Report No. KLR 82-34B, Brown Boveri, Forschungszentrum, Baden, Switzerland, 1982.
[168]C. W. Von Rosenberg, Jr. and D. W. Trainor, J. Chem. Phys. **59**, 2142 (1973).
[169]C. W. Von Rosenberg, Jr. and D. W. Trainor, J. Chem. Phys. **63**, 5348 (1975).
[170]W. T. Rawlins, H. C. Murphy, G. E. Caledonia, J. P. Kennealy, F. X. Robert, A. Corman, and R. A. Armstrong, Appl. Opt. **23**, 3316 (1984).
[171]T. Kleindienst and E. J. Bair, Chem. Phys. Lett. **49**, 338 (1977).
[172]T. Kleindienst, J. R. Locker, and E. J. Bair, J. Photochem. **12**, 67 (1980).
[173]P. C. Wraight, Planet. Space Sci. **25**, 1177 (1977).
[174]J. E. Ramirez, R. K. Bera, and R. J. Hanrahan, Radiat. Phys. Chem. **23**, 685 (1984).
[175]J. R. Locker, J. A. Joens, and E. J. Bair, J. Photochem. **36**, 235 (1987).
[176]M. P. Popovich, Yu. V. Filippov, and S. N. Tkachenko, Vestn. Mosk. Univ. Khim. **38**, 546 (1983); Moscow Univ. Chem. Bull. **38**, 27 (1983).
[177]L. E. Khvorostovskaya and V. A. Yankovskii, Opt. Spektrosk. **37**, 26 (1974); Opt. Spectrosc. (USSR) **37**, 13 (1974).
[178]D. L. Baulch, D. D. Drysdale, J. Duxbury, and S. Grant, *Evaluated Kinetic Data for High Temperature Reactions* (Butterworths, London, 1976), Vol. 3.
[179]J. M. Heimerl and T. P. Coffee, Combust. Flame **35**, 117 (1979).
[180]M. Allen, J. Geophys. Res. **91**, 2844 (1986).
[181]S. W Benson, Adv. Chem. Ser. **21**, 405 (1959).
[182]H. Sugimitsu and S. Okazaki, J. Chim. Phys. Phys. Chim. Biol. **79**, 655 (1982).
[183]H. Sugimitsu, T. Moriwaki, and S. Okazaki, J. Chim. Phys. Phys. Chim. Biol. **81**, 423 (1984).
[184]M. P. Popovich, Yu. V. Filippov, G. V. Egorova, [Zh. Fiz. Khim. **55**, 222 (1981)]; Russ. J. Phys. Chem. **55**, 119 (1981).
[185]R. D. Kenner and E. A. Ogryzlo, J. Chem. Phys. **80**, 1 (1984).
[186]C. E. Kolb, M. S. Zahniser, R. B. Lyons, Report ARI-RR-403, Aerodyne Research, Inc., Billerica, Massachusetts, 1984.
[187]W. T. Rawlins, J. Geophys. Res. **90**, 12283 (1985).
[188]W. T. Rawlins, G. E. Caledonia, J. J. Gibson, and A. T. Stair, Jr., J. Geophys. Res. **90**, 2896 (1985).
[189]B. D. Green, W. T. Rawlins, R. M. Nadile, J. Geophys. Res. **91**, 311 (1986).
[190]F. E. Niles, J. Chem. Phys. **52**, 408 (1970).
[191]R. V. Zalepukhin, V. I. Gibalov, V. G. Samoilovich, Yu. V. Filippov, Vest. Mosk. Univ. Khim. **22**, 259 (1981); Moscow Univ. Chem. Bull. **22**, 37 (1981).
[192]H. Sabadil and S. Pfau, Plasma Chem. Plasma Process. **5**, 67 (1985).
[193]H. Sabadil, P. Bachmann, and H. Kastelewicz, Beitr. Plasmaphys. **20**, 283 (1980).
[194]A. V. Phelps, Can. J. Chem. **47**, 1783 (1969).
[195]F. C. Fehsenfeld, D. L. Albritton, J. A. Burt, and H. I. Schiff, Can J. Chem. **47**, 1793 (1969).
[196]E. E. Ferguson, F. C. Fehsenfeld, and D. L. Albritton, in *Gas Phase Ion Chemistry* (Academic, New York, 1979), Vol. 1, pp. 45–82.
[197]M. L. Huertas, J. Fontan, and J. Gonzalez, Atmos. Environ. **12**, 2351 (1978).
[198]L. Harrison and J. L. Moruzzi, J. Phys. D **5**, 1239 (1972).
[199]M. Bacal and H. J. Doucet, Vacuum **24**, 595 (1974).
[200]R. J. Hill and S. A. Bowhill, J. Atmos. Terr. Phys. **41**, 607 (1979).
[201]C. Lifshitz, R. L. C. Wu, T. O. Tiernan, and D. T. Terwilliger, J. Chem. Phys. **68**, 2476 (1978).
[202]F. C. Fehsenfeld and E. E. Ferguson, Radio Sci. **7**, 113 (1972).
[203]I. C. McDade and W. D. McGrath, Chem. Phys. Lett. **72**, 432 (1980).
[204]S. M. Adler-Golden and J. I. Steinfeld, Chem. Phys. Lett. **76**, 479 (1980).
[205]D. I. Rosen and T. A. Cool, J. Chem. Phys. **62**, 466 (1975).
[206]K.-K. Hui, D. I. Rosen, and T. A. Cool, Chem. Phys. Lett. **32**, 141 (1975).
[207]K.-K. Hui and T. A. Cool, J. Chem. Phys. **65**, 3536 (1976).
[208]D. I. Rosen and T. A. Cool, J. Chem. Phys. **59**, 6097 (1973).
[209]T. A. Cool and J. R. Airey, Chem. Phys. Lett. **20**, 67 (1973).
[210]G. A. West, R. E. Weston Jr., and G. W. Flynn, Chem. Phys. Lett. **42**, 488 (1976).
[211]M. J. Kurylo, W. Braun, and A. Kaldor, Chem. Phys. Lett. **27**, 249 (1974).
[212]A. Kaldor, W. Braun, and M. J. Kurylo, IEEE J. Quantum Electron. **11**, 697 (1975).
[213]W. Braun, M. J. Kurylo, and A. Kaldor, Chem. Phys. Lett. **28**, 440 (1974).
[214]J. Moy, C.-R. Mao, and R. J. Gordon, J. Chem. Phys. **72**, 4216 (1980); **73**, 4713 (E) (1980).
[215]Y. Vlahoyannis and R. J. Gordon, J. Chem. Phys. **74**, 1682 (1981).
[216]R. J. Gordon, P. Brutto, and J. Moy, J. Chem. Phys. **69**, 3439 (1978).
[217]R. J. Gordon and M. C. Lin, Chem. Phys. Lett. **22**, 262 (1973).
[218]E. Bar-Ziv and R. J. Gordon, Chem. Phys. Lett. **52**, 355 (1977).
[219]K.-K. Hui and T. A. Cool, J. Chem. Phys. **68**, 1022 (1978).
[220]E. Bar-Ziv, J. Moy, and R. J. Gordon, J. Chem. Phys. **68**, 1013 (1978).
[221]C.-R. Mao, J. Moy, and R. J. Gordon, Chem. Phys. Lett. **59**, 425 (1978).
[222]J. W. Keto, C. F. Hart, and C.-Y. Kuo, J. Chem. Phys. **74**, 4450 (1981).
[223]S. M. Freund and J. C. Stephenson, Chem. Phys. Lett. **41**, 157 (1976).
[224]H. Endo and J. Troe, J. Phys. Chem. **83**, 2083 (1979).
[225]A. J. Stace and J. N. Murrell, J. Chem. Phys. **68**, 3028 (1978).
[226]D. C. Clary, Chem Phys. Lett. **87**, 407 (1982).
[227]A. Gelb, J. Phys. Chem. **89**, 4189 (1985).
[228]T. Mulloney and G. C. Schatz, Chem. Phys. **45**, 213 (1980).
[229]A. J. Stace, J. Chem. Soc. Faraday Trans. 2 **78**, 959 (1982).
[230]R. G. Gilbert, J. Chem. Phys. **80**, 5501 (1984).
[231]C. C. Jensen, J.I. Steinfeld, and R. D. Levine, J. Chem. Phys. **69**, 1432 (1978).
[232]V. M. Gordienko, M. S. Dzhidzhoev, V. Ya. Panchenko, V. K. Popov, I. M. Sizova, *et al.* Kvantovaya Elektron. (Moscow) **9**, 2204 (1982); Sov. J. Quantum Electron. **12**, 1432 (1982).
[233]V. Ya. Panchenko, I. M. Sizova, A. P. Sukhorukov, [Zh. Prikl. Mekh. Tekh. Fiz. No. **4**, 17 (1981)]; J. Appl. Mech. Tech. Phys. (USSR) **22**, 452 (1981).
[234]G. A. West, R. E. Weston Jr., and G. W. Flynn, Chem. Phys. Lett. **56**, 429 (1978).
[235]S. K. Chekin, Yu. M. Gershenzon, A. V. Konoplyov, and V. B. Rozenshtein, Chem. Phys. Lett. **68**, 386 (1979).
[236]Yu. M. Gershezon and S. K. Chekin, Kinet. Katal. **18**, 1374 (1977).
[237]N. Washida, H. Akimoto, and M. Okuda, Bull. Chem. Soc. Jpn. **53**, 3496 (1980).
[238]N. Washida, H. Akimoto and M. Okuda, in *14th Kosoku Hanno Toronkai Koen Yokoshu* (Tokyo Daigaku Uchu Koku Kenkyusho, Tokyo, Japan, 1979), pp. 58–60.
[239]M. Gauthier and D. R. Snelling, J. Chem. Phys. **54**, 4317 (1971).
[240]I. Arnold and F. J. Comes, J. Mol. Struct. **61**, 223 (1980).
[241]I. Arnold and F. J. Comes, Chem. Phys. **47**, 125 (1980).

[242]O. Klais, A. H. Laufer, and M. J. Kurylo, J. Chem. Phys. **73**, 2696 (1980).
[243]D. W. McCullough and W. D. McGrath, Chem. Phys. Lett. **12**, 98 (1971).
[244]J. C. Tully, J. Chem. Phys. **62**, 1893 (1975).
[245]G. London, R. Gilpin, H. I. Schiff, and K. H. Welge, J. Chem. Phys. **54**, 4512 (1971).
[246]S. M. Anderson and K. Mauersberger, in "Abstracts of the XVIIth Information Conference on Photochemistry" (Boulder, CO, 22–26 June 1986) National Bureau of Standards, Boulder, CO 1986.
[247]M. J. Kurylo, W. Braun, A. Kaldor, S. M. Freund, R. P. Wayne, J. Photochem. **3**, 71 (1974).
[248]J. G. Parker, J. Chem. Phys. **67**, 5352 (1977).
[249]P. J. Ogren, T. J. Sworski, C. J. Hochanadel, and J. M. Cassel, J. Phys. Chem. **86**, 238 (1982).
[250]T. G. Slanger and G. Black, J. Chem. Phys. **70**, 3434 (1979).
[251]R. Gilpin, H. I. Schiff, and K. H. Welge, J. Chem. Phys. **55**, 1087 (1971).
[252]G. D. Greenblatt and J. R. Wiesenfeld, J. Geophys. Res. **87**, 11 145 (1982).
[253]B. J. Finlayson-Pitts, T. E. Kleindienst, M. J. Ezell, and D. W. Toohey, J. Chem. Phys. **74**, 4533 (1981).
[254]N. Washida, H. Akimoto, and M. Okuda, J. Chem. Phys. **72**, 5781 (1980).
[255]P. E. Charters, R. G. Macdonald, and J. C. Polanyi, Appl. Opt. **10**, 1747 (1971).
[256]F. Kaufman and R. D. Levine, Chem. Phys. Lett. **54**, 407 (1978).
[257]R. D. Levine and J. L. Kinsey, in *Atom-Molecule Collision Theory: A Guide for the Experimentalist*, edited by R. B. Bernstein (Plenum, New York, 1979), pp. 693–750.
[258]M. M. L. Chen, R. W. Wetmore, and H. F. Schaefer III, J. Chem. Phys. **74**, 2938 (1981).
[259]R. N. Coltharp, S. D. Worley, and A. E. Potter, Appl. Opt. **10**, 1786 (1971).
[260]G. E. Streit and H. S. Johnston, J. Chem. Phys. **64**, 95 (1976).
[261]T. G. Slanger and D. L. Huestis, Int. J. Chem. Kinet. **17**, 713 (1985).
[262]E. R. Manzanares, M. Suto, L. C. Lee, and D. Coffey Jr., J. Chem. Phys. **85**, 5027 (1986).
[263]A. Sinha, E. R. Lovejoy, and C. J. Howard, J. Chem. Phys. **87**, 2122 (1987).
[264]L. J. Stief, W. A. Payne, J. H. Lee, and J. V. Michael, J. Chem. Phys. **70**, 5241 (1979).
[265]S. Yagi, M. Tanaka, J. Phys. D **12**, 1509 (1979).
[266]A. A. Besshaposhnikov, V. I. Blokhin, V. B. Voronin, V. A. Myslin, S. V. Pashkin, *et al.* [Khim. Vys. Energ. **16**, 344 (1982)]; High Energy Chem. (USSR) **16**, 270 (1982).
[267]R. M. Goody and C. D. Walshaw, Q. J. R. Meteorol. Soc. **79**, 496 (1953).
[268]S. S. Prasad, Nature **289**, 386 (1981).
[269]J. E. Morgan, L. F. Phillips, and H. J. Schiff, Discuss. Faraday Soc. **3**, 118 (1962).
[270]V. G. Samoilovich, M. Vronski, V. I. Gibalov, and R. V. Zalepukhin, Zh. Fiz. Khim. **58**, 1406 (1984); Russ. J. Phys. Chem. **58**, 850 (1984).
[271]R. A. Borders and J. W. Birks, J. Phys. Chem. **86**, 3295 (1982).
[272]P. Givi, W. A. Sirignano and S. B. Pope, Combust. Sci. Technol. **37**, 59 (1984).
[273]S. Adler-Golden, J. Chem. Phys. (submitted)
[274]S. Adler-Golden, J. Chem. Phys. (submitted)
[275]U. Schurath, H. H. Lippmann, B. Jesser, Ber. Bunsenges. Phys. Chem. **85**, 807 (1981).
[276]R. J. Gordon and M. C. Lin, J. Chem. Phys. **64**, 1058 (1976).
[277]J. Moy, E. Bar-Ziv, and R. J. Gordon, J. Chem. Phys. **66**, 5439 (1977).
[278]J. C. Stephenson and S. M. Freund, J. Chem. Phys. **65**, 4303 (1976).
[279]H. Frei and G. C. Pimentel, J. Phys. Chem. **85**, 3355 (1981).
[280]V. V. Bertsev, M. O. Bulanin, and A. P. Burtsev [Opt. Spektrosk. **49**, 1203 (1980)]; Opt. Spectrosc. (USSR) **49**, 661 (1980).
[281]C. C. Kahler, E. Ansell, C. M. Upshur, and W. H. Green Jr., J. Chem. Phys. **80**, 3644 (1984).
[282]D. Van Den Ende and S. Stolte, Chem. Phys. **45**, 55 (1980).
[283]S. L. Anderson, P. R. Brooks, J. D. Fite, and On Van Nguyen, J. Chem. Phys. **72**, 6521 (1980).
[284]R. A. Cox, J. P. Burrows, and T. J. Wallington, Chem. Phys. Lett. **84**, 217 (1981).
[285]D. Van Den Ende and S. Stolte, Chem. Phys. **89**, 121 (1984).
[286]S. Chapman, J. Chem. Phys. **74**, 1001 (1981).
[287]R. Viswanathan and L. M. Raff, J. Phys. Chem. **87**, 3251 (1983).
[288]R. A. Cox and G. B. Coker, J. Atmos. Chem. **1**, 53 (1983).
[289]V. P. Afanasev, S. B. Dorofeev, and V. I. Sinitsyn, [Dokl. Akad. Nauk SSSR **248**, 1348 (1979)]; Dokl. Phys. Chem. **248**, 860 (1979).
[290]D. Van Den Ende and S. Stolte, Chem. Phys. Lett. **76**, 13 (1980).
[291]D. Van Den Ende, S. Stolte, J. B. Cross, G. H. Kwei, and J. J. Valentini, J. Chem. Phys. **77**, 2206 (1982).
[292]K. N. Joshipura, Indian J. Pure Appl. Phys. **22**, 167 (1984).
[293]V. G. Samiolovich, M. P. Popovich, Yu. M. Emelyanov, and Yu. V. Filippov, J. Phys. Chem. **40**, 287 (1966).
[294]M. W. Siegel, Int. J. Mass Spectrom. Ion Phys. **44**, 19 (1982).
[295]E. E. Ferguson, NATO Adv. Study Inst. Scr. Scr. B **B40**, 377 (1979).
[296]D. B. Dunkin, F. C. Fehsenfeld and E. E. Ferguson, Chem. Phys. Lett. **15**, 257 (1972).
[297]J. A. Rutherford, B. R. Turner, and D. A. Vroom, J. Chem. Phys. **58**, 5267 (1973).
[298]C. Lifshitz, R. L. C. Wu, J. C. Haartz, and T. O. Tiernan, J. Chem. Phys. **67**, 2381 (1977).
[299]C. Willis, A. W. Boyd, M. J. Young, and D. A. Armstrong, Can. J. Chem. **48**, 1505 (1970).
[300]D. Proch and H. Schroder, Chem. Phys. Lett. **61**, 426 (1979).
[301]B. Raffel, J. Warnatz, and J. Wolfrum, Appl. Phys. B **37**, 189 (1985).
[302]E. A. Tveritinova, V. I. Shishnyaev, and Yu. N. Zhitnev, Vestn. Mosk. Univ. Khim. **25**, 368 (1984).
[303]A. V. Chugunov, M. S. Djidjoev, S. V. Ivanov, and V. Ya. Panchenko, Opt. Lett. **10**, 615 (1985).
[304]M. Quack and E. Sutcliffe, Chem. Phys. Lett. **99**, 167 (1983).
[305]M. Quack and E. Sutcliffe, Chem. Phys. Lett. **105**, 147 (1984).
[306]M. Quack and E. Sutcliffe, Isr. J. Chem. **24**, 204 (1984).
[307]I. J. Bigio and S. J. Thomas, Appl. Phys. Lett. **49**, 989 (1986).
[308]D. Hanson and K. Mauersberger, J. Chem. Phys. **83**, 326 (1985).
[309]D. Hanson and K. Mauersberger, J. Chem. Phys. **85**, 4669 (1986).